(12) INTERNATIONAL APPLICATION PUBLISHED UNDER THE PATENT COOPERATION TREATY (PCT)

(19) World Intellectual Property Organization
International Bureau

(43) International Publication Date
28 September 2017 (28.09.2017)

WIPO | PCT

(10) International Publication Number
WO 2017/165199 A1

(51) International Patent Classification:
C12Q 1/68 (2006.01)

(21) International Application Number:
PCT/US2017/022848

(22) International Filing Date:
16 March 2017 (16.03.2017)

(25) Filing Language: English

(26) Publication Language: English

(30) Priority Data:
62/313,425 25 March 2016 (25.03.2016) US
62/458,535 13 February 2017 (13.02.2017) US

(71) Applicant: **THE TRUSTEES OF COLUMBIA UNIVERSITY IN THE CITY OF NEW YORK** [US/US]; 412 Low Memorial Library, 535 W. 116th Street, New York, New York 10027 (US).

(72) Inventors: **LIU, Liang**; 4022 College Point Blvd., 15M, Flushing, New York 11354 (US). **SHEN, Yao**; 1150 Saint Nicholas Avenue, Rm. 318, New York, New York 10032 (US).

(74) Agent: **HOOPER, Kevin C.**; BRYAN CAVE LLP, 1290 Avenue of the Americas, New York, New York 10104 (US).

(81) Designated States *(unless otherwise indicated, for every kind of national protection available)*: AE, AG, AL, AM, AO, AT, AU, AZ, BA, BB, BG, BH, BN, BR, BW, BY, BZ, CA, CH, CL, CN, CO, CR, CU, CZ, DE, DJ, DK, DM, DO, DZ, EC, EE, EG, ES, FI, GB, GD, GE, GH, GM, GT, HN, HR, HU, ID, IL, IN, IR, IS, JP, KE, KG, KH, KN, KP, KR, KW, KZ, LA, LC, LK, LR, LS, LU, LY, MA, MD, ME, MG, MK, MN, MW, MX, MY, MZ, NA, NG, NI, NO, NZ, OM, PA, PE, PG, PH, PL, PT, QA, RO, RS, RU, RW, SA, SC, SD, SE, SG, SK, SL, SM, ST, SV, SY, TH, TJ, TM, TN, TR, TT, TZ, UA, UG, US, UZ, VC, VN, ZA, ZM, ZW.

(84) Designated States *(unless otherwise indicated, for every kind of regional protection available)*: ARIPO (BW, GH, GM, KE, LR, LS, MW, MZ, NA, RW, SD, SL, ST, SZ, TZ, UG, ZM, ZW), Eurasian (AM, AZ, BY, KG, KZ, RU, TJ, TM), European (AL, AT, BE, BG, CH, CY, CZ, DE, DK, EE, ES, FI, FR, GB, GR, HR, HU, IE, IS, IT, LT, LU, LV, MC, MK, MT, NL, NO, PL, PT, RO, RS, SE, SI, SK, SM, TR), OAPI (BF, BJ, CF, CG, CI, CM, GA, GN, GQ, GW, KM, ML, MR, NE, SN, TD, TG).

Published:

— *with international search report (Art. 21(3))*

— *before the expiration of the time limit for amending the claims and to be republished in the event of receipt of amendments (Rule 48.2(h))*

WO 2017/165199 A1

(54) Title: NEXT-GENERATION BIOMARKERS TO DETECT SUN DAMAGE AND PREDICT SKIN CANCER RISK

(57) Abstract: The present invention provides methods of detecting ultraviolet radiation (UVR)-induced skin damage in a subject. The method includes the steps of: a) obtaining a skin sample from the subject; b) analyzing expression levels in the skin sample of UVR-induced differentially expressed genes (DEGs) listed in Table 8 or a subset thereof; and c) comparing the expression levels of the UVR-induced DEGs to a control skin sample; wherein, when the expression levels of the UVR-induced DEGs in the skin sample is above or below the level of each of the UVR-induced DEGs in the control sample, the subject is identified as likely being afflicted with UVR-induced skin damage. Also provided are methods for measuring the effectiveness of a test agent in reducing ultraviolet radiation (UVR)-induced damage.

NEXT-GENERATION BIOMARKERS TO DETECT SUN DAMAGE AND PREDICT SKIN CANCER RISK

CROSS-REFERENCE TO RELATED APPLICATIONS

[0001] The present application claims priority to U.S. Provisional Patent Application No. 62/313,425, filed filed on March 25, 2016, and U.S. Provisional Patent Application No. 62/458,535, filed on February 13, 2017. The entire contents of the aforementioned applications are incorporated by reference as if recited in full herein.

GOVERNMENT FUNDING

[0002] This invention was made with government support under grant no. AR064315, awarded by the National Institutes of Health. The government has certain rights in the invention.

BACKGROUND OF THE INVENTION

[0003] Skin cancer is the most prevalent cancer worldwide. (Guy 2015; Rogers 2015) Every year in the United States, nearly 5 million people are treated for skin cancer, at an estimated cost of $8.1 billion. (The surgeon General 2014) Solar ultraviolet radiation (UVR), especially the UVB spectrum of sunlight, is widely recognized as the major carcinogen that promotes skin cancer development; and interplay with genetic factors is also involved. (Wu 2014; Robinson 2005; Pleasance 2010) Most skin cancer cases are preventable through proper protection against harmful UVR exposure, and sunscreen is one of the commonly used sun protection strategies especially in skin-cancer susceptible populations. (Lautenschlger 2007)

However, there are controversies surrounding the efficacy of sunscreen products. (Osterwalder 2009; Bens 2014; Dennis 2003; Hacker 2013)

[0004] Despite recent efforts to address risk factors, skin cancer rates continue to rise, mainly due to unprotected UV exposure. More importantly, there are no sensitive biomarkers available for monitoring solar UVR damage and predicting skin cancer risk. The current method for monitoring sun damage relies on the use of minimal erythema dose (MED), which refers to the amount of UVR that produces visible skin redness within 24 hours following exposure. As an indicator of sun damage, MED is both insensitive and inadequate because significant molecular and cellular damage occurs at sub-erythema doses lower than one MED. (Seite 2010; Heckman 2013) The lack of sensitive biomarkers for accurate assessment of sun damage and to test the ability of sunscreens in preventing sun damage and reducing skin cancer risk remains the greatest unmet clinical need in skin cancer research.

[0005] Numerous studies in the past have attempted to identify UVR biomarkers focusing on UVR-induced changes in the activity of individual genes as biomarkers to detect skin damage and cancer risk. (Dawes 2014; da le Fuente 2009; Yang 2006; Rieger 2004; Dazard 2003; Takao 2002) Such individual markers are simple and easy to characterize, but it is difficult for them to produce consistent and reliable information on UVR damage and skin cancer risk due to the complex effects of UVR on multiple biological pathways leading to skin neoplastic growth in addition to the variations in skin type-dependent UVR sensitivity.

[0006] In view of the foregoing, there exists an ongoing need to provide new and improved methods for detecting sun damage and predicting skin cancer risk. The present disclosure is directed towards solving this and other needs.

SUMMARY OF THE INVENTION

[0007] Numerous studies in the past have attempted to identify UVR biomarkers focusing on UVR-induced changes in the activity of individual genes as biomarkers to detect skin damage and cancer risk. Such individual markers are simple and easy to characterize, but it is difficult for them to produce consistent and reliable information on UVR damage and skin cancer risk due to the complex effects of UVR on multiple biological pathways leading to skin neoplastic growth in addition to the variations in skin type-dependent UVR sensitivity. To obtain UVR biomarkers with better reliability and accuracy, a panel of UVR-responsive genes has been identified through comprehensive transcriptomic profiling studies. Functions of these carefully selected UVR biomarker genes span several biological pathways including inflammation, cell growth and proliferation, DNA repair, and cancer pathogenesis. This panel of genes has been subjected to rigorous validation by both bioinformatics and experimental approaches to confirm that their mRNA expressions are consistently responsive to UVR among different skin types. Furthermore, the UVR-induced mRNA expression changes in the biomarker genes persist long after UVR, highlighting their potential as reliable UVR biomarkers.

[0008] The UVR biomarker panel can serve to set a new industrial standard in testing UVR-protective effects of sunscreen products to prevent cancer-inducing sun damage. Such a panel may also be used in clinical diagnosis to assist health care providers with a sensitive tool in assessing excessive sun exposure and skin cancer risk. To facilitate its future industrial and clinical applications, a gene array system is being designed in a 384-well plate format to allow simultaneous detection of the expression of the UVR biomarker genes from multiple samples. Ultimately, we anticipate that our UVR biomarker panel together with the high capacity screening

assay system will revolutionize how we assess sun damage and predict skin cancer risk to achieve effective prevention and reduction of skin cancer-related illness, death, and health care costs.

[0009] The present invention provides methods of detecting ultraviolet radiation (UVR)-induced skin damage in a subject. In some embodiments, this method comprises the steps of: a) obtaining a skin sample from the subject; b) analyzing expression levels in the skin sample of UVR-induced differentially expressed genes (DEGs) listed in Table 8 or a subset thereof; and c) comparing the expression levels of the UVR-induced DEGs to a control skin sample; wherein, when the expression levels of the UVR-induced DEGs in the skin sample is above or below the level of each of the UVR-induced DEGs in the control sample, the subject is identified as likely being afflicted with UVR-induced skin damage.

[0010] The present invention also provides a method of identifying or monitoring skin cancer in a test subject. In some embodiments, this method comprises the steps of: a) analyzing expression levels in a biological sample obtained from the subject of UVR-induced differentially expressed genes (DEGs) listed in Table 8, or a subset thereof; b) comparing the expression levels of the UVR-induced DEGs in the biological sample with a predetermined reference standard for the genes; and c) identifying or monitoring skin cancer in the test subject based on the comparison in b).

[0011] The present invention also provides a kit for detecting ultraviolet radiation (UVR)-induced skin damage in a subject. In some embodiments, this kit comprises: a set of primers or probes that specifically bind to UVR-induced differentially expressed genes (DEGs) listed in Table 8 or a subset thereof, packaged together with instructions for its use.

[0012] The present invention also provides a kit for identifying or monitoring skin cancer in a subject. In some embodiments, this kit comprises: a set of primers or probes that specifically bind to UVR-induced differentially expressed genes (DEGs) listed in Table 8 or a subset thereof, packaged together with instructions for its use.

[0013] The present invention also provides a method for measuring the effectiveness of a test agent in reducing ultraviolet radiation (UVR)-induced damage. In some embodiments, this method comprises the steps of: a) irradiating a test skin sample, to which the test agent has been applied, with UV radiation; b) obtaining an expression profile of the UVR-induced differentially expressed genes (DEGs) listed in Table 8, or a subset thereof, in the test skin sample; and c) comparing the expression profile of the UVR-induced DEGs, or a subset thereof, from the test skin sample, with an expression profile of the same genes in a reference skin sample and a control skin sample, wherein the reference skin sample is irradiated in the absence of the test agent, and the normal, control skin sample is not irradiated; wherein if the gene expression profile of the test skin sample is the same or substantially similar to the gene expression profile of the normal, control skin sample, the test agent is effective at reducing UVR-induced damage, whereas if the gene expression profile of the test skin sample is the same or substantially similar to the gene expression profile of the reference skin sample, the test agent is not effective at reducing UVR-induced damage.

[0014] The present invention also provides a method for diagnosing UVR-induced skin damage in a subject by analyzing a sample from the subject for an expression profile of UVR-induced DEGs listed in Table or a subset thereof that is different from an expression profile of the same genes in a normal, control sample,

wherein the subject is diagnosed with UVR-induced skin damage if the expression profile of the subject differs from the expression profile from the normal, control sample.

[0015] The present invention also provides a method for diagnosing skin cancer in a subject by analyzing a sample from the subject for the presence or absence of squamous cell carcinoma or pre-cancerous skin lesion cells by analyzing a sample from the subject for an expression profile of UVR-induced DEGs listed in Table 8 or a subset thereof that is different from an expression profile of the same genes in a normal, control sample, wherein the subject is diagnosed with skin cancer if squamous cell carcinoma or pre-cancerous skin lesion cells are detected.

[0016] The present invention also provides a method for diagnosing and treating UVR-induced skin damage in a subject comprising: analyzing a sample from the subject for an expression profile of UVR-induced DEGs listed in Table 8 or a subset thereof that is different from an expression profile of the same genes in a normal, control sample, wherein the patient is diagnosed with UVR-induced skin damage if the expression profile of the subject differs from the expression profile from the normal, control sample; and administering a treatment for UVR-induced skin damage to the diagnosed subject.

[0017] The present invention also provides a method for treating skin cancer in a subject comprising: requesting a test providing the results of an analysis of whether the subject has an expression profile of UVR-induced DEGs listed in Table 8 or a subset thereof that is different from an expression profile of the same genes in a normal, control sample; and administering a treatment for skin cancer to the subject if the expression profile of the subject differs from the expression profile from the normal, control sample.

BRIEF DESCRIPTION OF THE DRAWINGS

[0018] The patent or application file contains at least one drawing executed in color. Copies of this patent or patent application publication with color drawing(s) will be provided by the Office upon request and payment of the necessary fee.

[0019] FIG. 1A shows PCA analysis demonstrating time-dependent clustering of UVR-responsive transcriptomic profiles in human keratinocytes. FIG. 1B shows functional annotation of differentially expressed genes by DAVID pathway analysis. The size of the pie chart is proportional to the number of genes in each pathway.

[0020] FIG. 2 shows graphs showing the time-dependent pattern of differential gene signatures by comparing Day 3 (yellow) and Day 1 (red). The y-axis shows the log2 fold change of gene expression between irradiated and non-irradiated control cells. The x-axis indicates the sample names. ADAMTSL4 and CST6 demonstrated time-dependent up-regulation, while UHRF1 and TRIP13 displayed time-dependent down-regulation in response to UVR.

[0021] FIG. 3 shows plots of dose-dependent down-regulation (upper two panels) and up-regulation (lower two panels) of UVR-induced differentially expressed genes. Each point represents a sample at the corresponding UVR dose. X-axis represents three different UVR doses; Y-axis represents the log2 fold change of gene expression between irradiated and non-irradiated control cells. N0-1d, N0-3d, N1-1d, N1-3d, N2-1d, and N2-3d were colored in red, orange, yellow, green, blue and cyan, respectively.

[0022] FIG. 4 shows protein-protein interaction network map illustrating hub genes as well as their interacting partners among UVR signature genes. Each vertice represents a gene and each edge indicates an interaction between the two

genes. Genes belong to different clusters are colored in different colors respectively. The sizes of the vertices are proportionally to their degrees (number of interacting genes).

[0023] FIG. 5A shows a gene set enrichment analysis of UVR signatures (red bars) against the gene set dysregulated in human SCCs. UVR transcriptomic signature genes were sorted from the highest (left) to the lowest (right) based on their UVR-induced fold change. The normalized enrichment score (NES) and p values are indicated; FIG. 5B shows gene set enrichment analysis of the human SCC signatures (red bars) against the UVR transcriptomic signature. SCC signature genes were sorted from the highest (left) to the lowest (right) based on the fold change between SCC and normal control tissues; FIG. 5C shows Venn diagram showing the overlapping genes between UVR transcriptomic signatures and DEGs at 21 days after UVR; FIG. 5D and FIG. 5E show Venn diagram illustrating the overlapping genes between UVR transcriptomic signature and DEGs in two different human SCC cases.

[0024] FIG. 6A shows differential gene expression plots demonstrating transcriptomic changes in human keratinocytes following UVR. Each red dot represents a DGE 4 h or 72 h following UVR. Each blue dot represents a DGE that also displays differential H3K27 acetylation following UVR; FIG. 6B shows UV induced progressive losses of H3K27ac in human keratinocytes at 4 h and 72 h after UVR. x/y-values are tag numbers in merged peak regions. Slope value < 1 indicates a net loss of H3K27ac; FIG. 6C shows Venn diagram showing that 75 SNVs are common between the 4 h and 72 h SNV sets; FIG. 6D shows a schematic illustration of genomic distributions of UV-induced SNVs at 4 h and 72 h after UVR; FIG. 6E shows GSEA analysis showing that genes containing intron mutations are

significantly enriched in the DGE gene set (left panel) or DHA gene set (right panel) as highlighted by the red dotted rectangles. GSEA was based on the Kolmogorov-Smirnov test. The p-values were estimated from permutation tests by randomly shuffing genes.

[0025] FIG. 7A shows SE profiles in control and UV-irradiated keratinocytes showing that UV decreased the total number of SEs marked by H3K27ac; FIG. 7B shows Venn diagram showing the number of common and distinctive Ses among control, UV-4h, and UV-72h; FIG. 7C shows Genome-wide H3K27ac signals in promoter regions showing a pronounced loss of 72 h following UVR; FIG. 7E shows gene tracks of H3K27ac ChIP-seq exemplifying that UVR increased H3K27ac at the PHACTR3 gene locus but reduced H3K27ac at the TMPRSS11B gene locus. PHACTR3: phosphatase and actin regulator 3; TMPRSS11B: transmembrane protease, serine 11B (HATL5).

[0026] FIG. 8A shows integrative analyses of the DGE and H3K27ac DHA gene sets at 4 h or 72 h after UVR. Correlations between gene expression and H3K27ac are considered significant if $p < 0.05$. P-values were obtained using Student's t-test by comparing the log2FC of the expression values of the genes from the three DHA groups; FIG. 8B shows representative genes showing concordant changes in gene expression and H3K27ac following UVR. Cutoff is set at Log2FC > 1 or < - 1 for both DGE and DHA; FIG. 8C shows a summary of the overall correlations between DGE and DHA changes among UV-responsive genes at 4 h or 72 h after UVR. Pink highlights positive correlations; green highlights inverse correlations between DGE and DHA; FIG. 8D shows parallel analysis of H3K27 DHA status of the DGEs that are enriched in top UV-responsive biological pathways.

[0027] Figure 4. (A) Motif analysis showing a significant enrichment of multiple TF motifs in UV-induced DHA regions in keratinocytes following UVR; (B) RNA-seq results showing mRNA expression changes of the TFs identified in Fig. 4A between UV-irradiated and control keratinocytes; (C) Loss of function of selected UV-responsive TFs is significantly more detrimental to skin cancer cells than non-skin cancer cells; (D) Loss of function of selected UV target genes in Fig. 3B (more than 2-fold increases in both DGE and DHA) is significantly more detrimental to skin cancer cells than non-skin cancer cells. P-values were obtained using the Wilcoxon test by comparing the gene depletion scores between the skin cancer cells versus the non-skin cancer cells; (E) Box plot illustrating the Log2FC in the expression of the genes shown in Fig. 4C and D among 5 pairs of SCC and normal skin tissues. SLAMF7, ARNTL, ETV1, and GPR115 show more consistent upregulation in SCCs.

[0028] Figure 5. (A) Box plot illustrating the Log2FC in the expression of selected UV target genes between the 5 matched pairs of SCC and normal skin tissues; (B) Gene tracks of H3K27ac profiles showing that UVR increased H3K27ac levels at CPY24A1, PTGS2, GJA5, and SLAMF7 chromatin regions 72 h after UVR, which are highlighted by red dotted lines under each gene track; (C) Immunofluorescence staining showing protein expression of selected UV target genes in UV-irradiated keratinocytes; (D) Immunofluorescence staining showing protein expression of selected UV target genes in matched human SCC tumors and adjacent normal skin tissues. Blue: DAPI staining. Basement membrane in the normal skin is highlighted by the white dotted line. The stratum corneum is separated by the yellow line. Scale bar = 20 μm.

DETAILED DESCRIPTION OF THE INVENTION

[0029] The present invention provides methods of detecting ultraviolet radiation (UVR)-induced skin damage in a subject. In some embodiments, this method comprises the steps of: a) obtaining a skin sample from the subject; b) analyzing expression levels in the skin sample of UVR-induced differentially expressed genes (DEGs) listed in Table 8 or a subset thereof; and c) comparing the expression levels of the UVR-induced DEGs to a control skin sample; wherein, when the expression levels of the UVR-induced DEGs in the skin sample is above or below the level of each of the UVR-induced DEGs in the control sample, the subject is identified as likely being afflicted with UVR-induced skin damage.

[0030] As used herein, “ultraviolet radiation (UVR)-induced skin damage” is any damage to the skin caused by exposure to UV radiation and includes, for example, photocarcinogenesis (e.g., melanoma), photoaging (e.g., wrinkles, loss of elasticity), immunosuppression, and oxidative stress. In some embodiments, the radiation is solar UV, comprising UVA, UVB, and/or UVC. In other embodiments, the UV radiation is generated by a lamp.

[0031] As used herein, a “subject” is a mammal, preferably, a human. In addition to humans, categories of mammals within the scope of the present invention include, for example, agricultural animals, domestic animals, laboratory animals, etc.

[0032] The phrase "skin sample" or “biological sample” as used herein, is intended to mean any sample comprising a skin cell or skin tissue in which expression of a gene or gene product can be detected. For example, skin cells or skin tissue may be taken from the dermis or epidermis, or a combination of both. The skin sample can be used either directly as obtained from the source or following a

pre-treatment to modify the character of the sample. The sample may be obtained by a variety of methods including, but not limited to, punch biopsy, surgical excision, and non-invasive or minimally invasive skin sampling methods such as a wet swabbing, tapelift, cotton tip swabbing, scraping of skin using a sterile surgical blade, scraping of skin using a wooden scraper, sticky surface of an adhesive pad (CapSure™ Clean-up Pad, Arcturus), film from LCM MacroCap™ (Arcturus), heated film from LCM MacroCap™ (Arcturus) and employing a small gauge needle (for example, 28 gauge), to collect micro-cores of skin tissue. These methods are well known in the art.

[0033] Alternatively, a skin sample may be a skin equivalent or a human or non-human cultured cell, for example, a keratinocyte, a melanocyte, a dermal fibroblast, a mast cell, an endothelial cell, a sebocyte, a hair papilla, or a matrix cell.

[0034] A "control" refers to a sample or standard used for comparison with an experimental sample, such as a skin sample obtained from a test subject exposed to UVR. In some embodiments, the control is a sample that has not been exposed to UVR or a non-UVR exposed sample obtained from the test subject. In some embodiments, the control is a skin sample whose exposure to UVR has been blocked or attenuated. In some embodiments, the control is a historical control or standard reference value or range of values (i.e. a previously tested control sample, such as a group of skin samples that were not exposed to UVR, or group of samples that represent baseline or normal values, such as the level of gene expression in non-UVR exposed tissue).

[0035] The differentially-expressed genes (DEGs) listed in Table 8 are genes or gene products that are modulated in skin in response to UVR exposure. Accordingly, using an assay to measure the level of the expression, function, or

activity of DEGs in skin is diagnostic and prognostic of UVR-induced skin damage, photoaging, or photocarcinogenesis. A DEG may be detected at either the nucleic acid or protein level. The expression level of a given gene measured at the nucleotide level refers to the amount of RNA transcribed from the gene measured on a relevant or absolute quantitative scale, and in general refers to the relative abundance of the accumulated mRNA transcript. The expression level of a given gene measured at the protein level refers to the amount of protein translated from the transcribed RNA measured on a relevant or absolute quantitative scale.

[0036] Differential expression, as used herein, means that the expression levels of certain genes, as measured at the RNA or protein level, are different between biological samples in different states, tissues, or type of cells. Differential expression may also be observed relative to a reference standard. Such standard may be determined based on the context of the expression experiments, the biological properties of the genes under study, and/or statistical significance criteria.

[0037] In some embodiments, comparing the expression levels of the UVR-induced DEGs to a control skin sample may require a quantitative or semi-quantitative determination. Other embodiments may involve a relative determination (e.g. a ratio relative to another marker, or a measurement relative to the same marker in a control sample), and other embodiments may involve a threshold determination (e.g. a yes/no determination whether a level is above or below a threshold).

[0038] In some embodiments, the analyzing step comprises carrying out next-generation sequencing of an RNA sample from the subject to identify genes from Table 8, or a subset thereof, that have a different expression profile compared to controls.

[0039] Preferably, the next-generation sequencing is whole transcriptome shotgun sequencing (RNA-Seq). Other methods of analyzing expression levels are well known in the art, and may include microarrays, ChIP sequencing, SAGE (serial analysis of gene expression), tiling arrays, nucleic acid hybridization techniques, nucleic acid reverse transcription methods, nucleic acid amplification methods, western blots, northern blots, southern blots, ELISA, immunoprecipitation, immunofluorescence, flow cytometry, and immunocytochemistry.

[0040] The present invention also provides methods of identifying or monitoring skin cancer in a test subject. In some embodiments, the method comprises: a) analyzing expression levels in a biological sample obtained from the subject of UVR-induced differentially expressed genes (DEGs) listed in Table 8, or a subset thereof; b) comparing the expression levels of the UVR-induced DEGs in the biological sample with a predetermined reference standard for the genes; and c) identifying or monitoring skin cancer in the test subject based on the comparison in b).

[0041] A "predetermined reference standard" as used herein may be determined empirically or historically from a single or multiple control samples. For monitoring a test subject, the predetermined reference standard may be a prior level of expression from the same test subject, a control subject or subjects, or a previously established range of normal, control values.

[0042] The present invention also provides kits for detecting ultraviolet radiation (UVR)-induced skin damage in a subject. In some embodiments, the kit comprises: a set of primers or probes that specifically bind to UVR-induced differentially expressed genes (DEGs) listed in Table 8 or a subset thereof, packaged together with instructions for its use.

[0043] The phrase “specifically bind” and the like refers to a binding reaction between two molecules that is at least two times the background and more typically more than 10 to 100 times background molecular associations under physiological conditions.

[0044] The present invention also provides methods for measuring the effectiveness of a test agent in reducing ultraviolet radiation (UVR)-induced damage. In some embodiments, the method comprises: a) irradiating a test skin sample, to which the test agent has been applied, with UV radiation; b) obtaining an expression profile of the UVR-induced differentially expressed genes (DEGs) listed in 8 Table 8, or a subset thereof, in the test skin sample; and c) comparing the expression profile of the UVR-induced DEGs, or a subset thereof, from the test skin sample, with an expression profile of the same genes in a reference skin sample and a control skin sample, wherein the reference skin sample is irradiated in the absence of the test agent, and the normal, control skin sample is not irradiated; wherein if the gene expression profile of the test skin sample is the same or substantially similar to the gene expression profile of the normal, control skin sample, the test agent is effective at reducing UVR-induced damage, whereas if the gene expression profile of the test skin sample is the same or substantially similar to the gene expression profile of the reference skin sample, the test agent is not effective at reducing UVR-induced damage.

[0045] As used herein, the phrase "same or substantially similar to" refers to statistically no significant difference in the expression level between the test skin sample and the control skin sample. Conversely, the phrase “different from” and the like refers to a statistically significant difference in expression.

[0046] The present invention also provides methods for diagnosing and treating UVR-induced skin damage in a subject. In some embodiments, the method comprises: analyzing a sample from the subject for an expression profile of UVR-induced DEGs listed in Table 8 or a subset thereof that is different from an expression profile of the same genes in a normal, control sample, wherein the subject is diagnosed with UVR-induced skin damage if the expression profile of the subject differs from the expression profile from the normal, control sample; and administering a treatment for UVR-induced skin damage to the diagnosed subject.

[0047] As used herein, the terms "treat," "treating," "treatment" and grammatical variations thereof mean subjecting an individual subject to a protocol, regimen, process or remedy, in which it is desired to obtain a physiologic response or outcome in that subject, e.g., a patient. In particular, the methods of the present invention may be used to slow the development of symptoms or delay the onset of the disease or condition, or halt the progression of disease development. However, because every treated subject may not respond to a particular treatment protocol, regimen, process or remedy, treating does not require that the desired physiologic response or outcome be achieved in each and every subject or subject population, e.g., patient population. Accordingly, a given subject or subject population, e.g., patient population may fail to respond or respond inadequately to treatment.

[0048] The embodiments described in this disclosure can be combined in various ways. Any aspect or feature that is described for one embodiment can be incorporated into any other embodiment mentioned in this disclosure. While various novel features of the inventive principles have been shown, described and pointed out as applied to particular embodiments thereof, it should be understood that various omissions and substitutions and changes may be made by those skilled in

the art without departing from the spirit of this disclosure. Those skilled in the art will appreciate that the inventive principles can be practiced in other than the described embodiments, which are presented for purposes of illustration and not limitation.

[0049] Skin cancer is the most common cancer in the United States. According to Skin Cancer Foundation statistics, one in every five Americans will develop skin cancer in their lifetime. Skin cancer greatly affects quality of life and creates substantial health care costs for individuals, families and the nation. Despite the fact that most skin cancer cases are preventable, its rates continue to rise mainly due to unnecessary UV radiation exposure and a lack of reliable biomarkers that can effectively monitor UV damage to help evaluate and predict skin cancer risk. Accordingly, embodiments of the disclosure relate to a UV radiation biomarker panel that can serve as sensitive tool for UV damage assessment and risk prediction to facilitate skin cancer prevention and reduce skin cancer-related illness, death and health care costs.

[0050] In one embodiment, an assay is provided for evaluating the effect of ultraviolet radiation (UVR) on a tissue sample. The assay comprises a system to evaluate expression of a plurality of UVR-responsive biomarker genes in the tissue sample, wherein expression of one or more of the plurality of UVR-responsive biomarker genes is associated with exposure of the tissue sample to ultraviolet radiation. In one embodiment, the system is a gene array system to evaluate expression of the plurality of UVR-responsive biomarker genes. In another embodiment, the assay is a high-capacity screening assay configured to evaluate the expression of the plurality of UVR-responsive biomarker genes in a plurality of tissue samples.

[0051] In one embodiment, the plurality of UVR-responsive biomarker genes are those associated with at least one of skin damage due to UV exposure, cancer risk and cancer progression. In yet another embodiment, the plurality of UVR-responsive biomarker genes are those that are involved at least one of inflammation, cell growth and proliferation, DNA repair, and cancer pathogenesis. In yet a further embodiment, the plurality of UVR-responsive biomarker genes are those selected from the group consisting of CYP24A1, GJA5, SLAMF7 and ETV1.

[0052] In one embodiment, the tissue sample that is evaluated by the assay is a mammalian tissue sample. For example, in one embodiment, the tissue sample is a human tissue sample. As yet another example, in one embodiment, the tissue sample comprises human keratinocytes.

[0053] In one embodiment, the assay is capable of correlating the expression of each of the UVR-responsive biomarker genes with at least one of UV damage to the tissue sample and/or a disease state, such as via a gene expression profile correlation system to correlate.

[0054] In one embodiment, a method of evaluating ultraviolet damage to tissue comprises evaluating the expression of a plurality of UVR-responsive biomarker genes in a sample of the tissue, and determining whether the expression of one or more of the plurality of UVR-responsive biomarker genes is indicative of ultraviolet damage. For example, in one embodiment, the plurality of UVR-responsive biomarker genes are those associated with at least one of skin damage due to UV exposure, cancer risk and cancer progression. In yet another embodiment, the plurality of UVR-responsive biomarker genes are those selected from the group consisting of CYP24A1, GJA5, SLAMF7 and ETV1. In one embodiment, the

expression of the plurality of UVR-responsive biomarker genes is evaluated via a high-capacity gene array screening system.

[0055] Accordingly to one embodiment, the tissue that is evaluated for UV damage is mammalian tissue. According to yet another embodiment, the tissue that is evaluated for UV damage is human tissue.

[0056] In one embodiment, a method of diagnosing skin cancer or predicting skin cancer risk in a subject comprises evaluating the expression of a plurality of UVR-responsive biomarker genes in a sample of the tissue, and determining whether the expression is indicative of skin cancer or skin cancer risk. For example, in one embodiment, the plurality of UVR-responsive biomarker genes are those selected from the group consisting of CYP24A1, GJA5, SLAMF7 and ETV1. In one embodiment, the subject is a mammalian subject. In yet another embodiment, the subject is a human subject.

[0057] In one embodiment, a method of evaluating a sunscreen formulation comprises applying the sunscreen formulation to a tissue sample, irradiating the tissue sample with ultraviolet radiation, evaluating the expression of a plurality of UVR-responsive biomarker genes in the tissue sample, and determining whether the expression of the plurality of UVR-responsive biomarker genes is indicative of efficacy of sunscreen formulation in providing a UV protective effect to the tissue sample.

[0058] One embodiment of the present disclosure is directed to providing UVR biomarkers having better reliability and accuracy. Accordingly, to obtain UVR biomarkers with better reliability and accuracy, a panel of UVR-responsive genes have been identified through comprehensive transcriptomic profiling studies. Functions of these carefully selected UVR biomarker genes span several biological

pathways including inflammation, cell growth and proliferation, DNA repair, and cancer pathogenesis. The panel of genes has been subjected to rigorous validations by both bioinformatics and experimental approaches to confirm that their mRNA expressions are consistently responsive to UVR among different skin types. Furthermore, the UVR-induced mRNA expression changes in the biomarker genes persist long after UVR, highlighting their potential as reliable UVR biomarkers.

[0059] According to one embodiment, the UV biomarker panel can serve to set a new industrial standard in testing UVR-protective effects of sunscreen products in preventing cancer-inducing dose of sun damage. According to yet another embodiment, it can be used in clinical diagnosis to assist health care providers with a sensitive tool in assessing excessive sun exposure and skin cancer risk. In yet another embodiment, to facilitate industrial and clinical applications, a gene array system in a 96-well plate format is designed to allow simultaneous detections of the expression of the UVR biomarker genes from multiple samples. In one embodiment, the UVR biomarker panel together with the high capacity screening assay system may be capable of revolutionizing the assessment of sun damage and skin cancer risk predication to allow for early prevention and effective reduction of skin cancer-related illness, death, and health care costs.

[0060] Embodiments of the disclosure may involve (1) validation and optimization of the selection of biomarker genes for gene-array preparation; (2) development and optimization of a compact gene array system that can process multiple samples on the same array to achieve high screening capacity; and (2) development of algorithms to enable autonomous processing of gene expression data.

[0061] In one embodiment, a UVR biomarker panel is provided for monitoring sun damage and predicting skin cancer risk with a high level of sensitivity and accuracy. Associated analytical regents, test kits and diagnostic models for sun damage detection and cancer risk prediction can also be provided.

[0062] In one embodiment, the UVR biomarker panel can be applied in the sunscreen industry to evaluate the efficacy of sunscreen products in UVR protection and reducing sun exposure damage of the skin.

[0063] In one embodiment, the tissue and/or subject being evaluated is mammalian, such as preferably human. In other aspects of this embodiment, the tissue and or subject is that of a laboratory animal. In addition to humans, categories of mammals within the scope of aspects of the present disclosure include, for example, agricultural animals, veterinary animals, laboratory animals, etc. Some examples of agricultural animals include cows, pigs, horses, goats, etc. Some examples of veterinary animals include dogs, cats, etc. Some examples of laboratory animals include rats, mice, rabbits, guinea pigs, etc.

[0064] In one embodiment, methods and/or steps in methods described herein may be carried out in vitro. In other embodiments, the methods and/or steps in the methods described herein are carried out in vivo or ex vivo.

[0065] As used herein, in vitro refers to a process performed in an artificial environment created outside a living multicellular organism (e.g., a test tube or culture plate) used in experimental research to study a disease or process. As used herein, in vitro includes processes performed in intact cells growing in culture.

[0066] As used herein, in vivo means that which takes place inside an organism and more specifically to a process performed in or on the living tissue of a

whole, living multicellular organism (animal), such as a mammal, as opposed to a partial or dead one.

[0067] As used herein, ex vivo refers to a process performed in an artificial environment outside the organism on living cells or tissue which are removed from an organism and subsequently returned to an organism.

[0068] An Appendix is attached hereto which provides additional details regarding the inventive principles described in this disclosure. The Appendix is explicitly incorporated herein by reference in its entirety. In the event of a conflict between the teachings of this application and those of the incorporated document, the teachings of this application control.

[0069] The embodiments described in this disclosure can be combined in various ways. Any aspect or feature that is described for one embodiment can be incorporated into any other embodiment mentioned in this disclosure. While various novel features of the inventive principles have been shown, described and pointed out as applied to particular embodiments thereof, it should be understood that various omissions and substitutions and changes may be made by those skilled in the art without departing from the spirit of this disclosure. Those skilled in the art will appreciate that the inventive principles can be practiced in other than the described embodiments, which are presented for purposes of illustration and not limitation.

EXAMPLES

First Series of Experiments

EXAMPLE 1

Materials and Methods

Human keratinocyte cultures, human SCC and normal skin tissues

[0070] Primary human keratinocytes were established from neonatal foreskins through the Columbia University Skin Disease Research Center tissue culture core facility. The protocol was exempt by our Institutional Review Board. Keratinocytes were isolated from separate individual neonatal foreskins (N0, N1, N2, and N6), and cells from each individual were maintained and analyzed separately for assessing individual variations. Keratinocytes were cultured in 154CF medium supplemented with human keratinocyte growth supplement (Life Technologies, Grand Island, NY). Human SCC tumor tissues and matched normal skin tissues from two patients were obtained from the Molecular Pathology Shared Resource/ Tissue Bank of the Herbert Irving Comprehensive Cancer Center of Columbia University under CUMC IRB protocol AAAB2667.

UVB radiation

[0071] Keratinocytes were rinsed once with PBS and irradiated with UVB supplied by four FS20T12/UVB tubes (National Biological Corp., Beachwood, OH). The intensity of UVB lights was measured using an IL1400 radiometer connected to a SEL240/UVB-1/TD detector (International Light, Newburyport, MA). Cells were irradiated with a total dose of 10, 20, and 30 mJ/cm^2, respectively. Cells were collected at different times points after exposure including four hours or one, three, or 21 days as indicated.

RNA isolation and RNA-Seq analysis

[0072] Total RNA was isolated from cultured keratinocytes and human tissues using the RNeasy Kit (QIAGEN, Gaithersburg, MD) and treated with DNase I (Life Technologies, Grand Island, NY) according to the manufacturers' protocols. All RNA samples were subsequently analyzed using an RNA 6000 nano chip (Agilent

Technologies, Wilmington, DE) to confirm that the RNA integrity index was 8.0 or above. For RAN-Seq, 500 ng of total RNA from each sample was subjected to poly-A pull-down to enrich mRNAs for library preparation by using Illumina TruSeq RNA prep kit (Illumina, San Diego, CA). The resulting libraries were sequenced using Illumina HiSeq2000 at Columbia Genome Center. Samples were multiplexed in each lane, which yielded targeted number of paired-end 100bp reads for each sample, as a fraction of 180 million reads for the whole lane. We used RTA (Illumina) for base calling and bcl2fastq (version 1.8.4, Illumina) for converting BCL to fastq format, coupled with adaptor trimming. The reads were mapped to the human reference genome (NCBI/build37.2) using Tophat (version 2.0.4). Relative gene expression levels were calculated using Cufflinks (version 2.0.2) with default settings. Differentially expressed genes (DEGs) under various UVR conditions were determined using the DESeq software package (Anders 2010), with a fold change cutoff set at >2 or <0.5 between irradiation and non-irradiated keratinocytes. Genes with FPKM values <10 were subjected to higher FC cutoffs to be selected in the final DEG list (details available upon request). A False Discovery rate (FDR) <0.05 was used to control for false discoveries.

Bioinformatics and statistical analyses

[0073] DEG lists were used in principal component analysis (PCA) to characterize the variations in transcriptomic responses to different UVR conditions among the keratinocyte lines. To uncover pathways that were most significantly affected by UVR, we performed pathway analysis using DAVID to identify which biological pathways the differentially expressed genes were enriched in. Gene enrichment analysis (GSEA) was performed to determine the overlap between UVR signature genes and gene sets that were dysregulated in different human

malignancies. Paired t-test was used to identify genes displaying time-dependent UVR responses from Day 1 to Day 3 following exposure. To identifying genes manifesting dose-dependent changes in response to UVR, we constructed a linear regression model using UVR dosage as an independent variable and gene expression as a dependent variable for each gene in the same keratinocyte line and at the same time point. We then performed the same analysis for all three keratinocyte lines (N0, N1, and N2) and at both time points (Day 1 and 3), which generated six expression models for each gene. In each model, a low coefficient p-value ($p < 0.05$) indicated a significant association between UVR dosage and gene expression. To evaluate the overall effects of the various UVR dosage on the expression of a specific gene, we integrated the multiple p-values from every regression analysis for that gene using Fisher's Method. P-values from the above analyses were FDR-corrected. To obtain cancer-specific gene signatures for various human malignancies, we retrieved and selected RNA-Seq data sets from the TCGA database that were available for both primary tumor cases and matched normal control tissues from same patient for each tumor type. We used DESeq package to normalize the raw counts and determine genes that were differentially expressed between each primary tumor and matched normal control tissue to obtain dysregulated gene sets for each tumor type. To identify genes that are critical to skin cancer cell proliferation or survival, we queried the Achilles database with 67 of the UVR signature genes that were upregulated by UVR. (Cowley 2014) Genes were considered essential to skin cancer cell survival if their corresponding shRNAs became depleted after 40 days or 16 population doublings following shRNA infection. Normalized shRNA depletion scores were downloaded from the "cBOTv8_sbsv3_allreps_log.gct2" file in Achilles database. For multiple shRNAs

targeting the same gene, we selected the ones whose depletion scores were consistent across all cancer cell lines and then took the median value as the final depletion score for each shRNA. All statistical analyses were performed using R.

EXAMPLE 2

Transcriptomic responses to different UVR conditions

[0074] In addition to its mutagenic effect, UVR has been shown to cause transcriptomic instability affecting thousands of genes. To fully characterize UVR-induced transcriptomic changes, we took advantage of the recent advances in RNA-Seq to profile UVR-induced kinetic changes in human primary keratinocytes exposed to different UVR conditions (Table 1). We used keratinocytes isolated from four individual neonatal foreskins to generate UVR-induced differentially expressed gene (DEG) lists in response to each of the UVR conditions (Table 1). Together with four DEG lists representing transcriptomic profiles at four hours after exposure, we performed principle component analysis (PCA) to differentiate the DEG profiles under various UVR conditions. As shown in the PCA plot (FIG. 1A), DEG profiles from Day 1 and 3 groups, but not the 4 hour group, demonstrated great similarities with each other in the first principle component (PC1). Along the second principle component (PC2) axis, however, the range of differences within the Day 3 DEG group appeared smaller than that of the Day 1 DEG group, demonstrating a clear time-dependent transcriptomic effect of UVR that became less differentiated among different UVR conditions 3 days after exposure.

To uncover the biological pathways that were mostly affected by UVR, we took the average of the fold change (FC) of each gene between irradiated and non-irradiated cells from the 19 DEG lists (Table 1). Using a FC cutoff of 2, we obtained a total of

531 genes that were up-regulated (FC>2) and 610 genes that were down-regulated (FC<0.5) in response to different UVR conditions (Table 2 and Table 3). We performed DAVID pathway analysis to categorize the functions of the up-regulated genes and down-regulated genes, respectively, which revealed multiple pathways that were significantly modulated by UVR. The down-regulated genes were significantly enriched in the following top four biological pathways: cell cycle regulation (83 genes), chromosome structure (19 genes), DNA damage response (59 genes) and microtubule organization (23 genes); whereas the up-regulated genes were largely enriched in pathways such as apoptosis (33 genes), defense inflammatory response (43 genes), ectoderm epithelium development (36 genes), cell adhesion (4 genes) and leukocyte activation (9 genes) (FIG. 1B).

Table 1. Keratinocyte lines and experimental UVR conditions

Keratinocyte lines	UVR conditions					
	10 mJ/cm² 24h	20 mJ/cm² 24h	30 mJ/cm² 24h	10 mJ/cm² 72h	20 mJ/cm² 72h	30 mJ/cm² 72h
N0	1	2	3	4	5	6
N1	7	8	9	10	11	12
N2	13	14	15	16	17	18
N6						19

Table 2. Genes up-regulated by UVR

Gene ID	Log2FC	Gene ID	Log2FC	Gene ID	Log2FC
A2ML1	1.25542	GGT6	2.012062	OVOL1	2.085033
A4GALT	1.217168	GIPR	1.443944	P4HTM	1.543172
ABCA12	1.377908	GJA5	1.128834	PADI1	1.763089
ABCD1	1.252331	GJB4	1.442723	PAPL	1.978976
ABHD4	1.15769	GLRX	1.411782	PCDH1	2.520425
ABLIM3	1.065562	GLS2	1.635732	PDE6B	1.230008
ACAP1	1.359902	GPNMB	1.547934	PGPEP1	1.267001

ACBD4	1.075352	GPR172B	2.315739	PHLDB3	1.019073
ACER2	2.006333	GPR37	1.273549	PHYHIP	1.46292
ACTA2	1.169663	GPRASP1	1.081898	PI3	2.404414
ADAMTS13	1.111708	GPRC5A	3.036593	PIDD	1.246663
ADAMTS7	1.803072	GRB7	1.812811	PIK3IP1	1.63279
ADAMTSL4	1.579834	GREB1	3.918492	PKIB	1.88435
ADCK3	1.407755	GRHL1	1.549886	PLA2G4C	1.366493
ADH6	1.037455	GRHL3	2.137244	PLA2G4D	1.768802
ADHFE1	1.308802	GRIN3B	1.04264	PLA2G4E	1.233771
ADSSL1	1.567365	GRIP2	1.741655	PLAC2	1.196007
AIFM3	1.051368	GSDMA	1.531598	PLAUR	1.160952
AIM1L	1.309328	GTF2IP1	1.31404	PLEKHG1	1.058571
AKR1B10	1.680432	GUCA1B	1.103181	PLEKHG6	1.612271
AKR1C1	1.734541	H1F0	1.009822	PLIN4	2.008771
AKR1C2	1.63357	H1FX-AS1	1.000064	PNLIPRP3	1.06203
AKR1C3	1.442466	HAP1	2.66275	PNMAL1	1.138815
ALDH3B2	1.885289	HAPLN3	1.002183	PNRC1	1.363591
ALOX12B	1.627145	HBEGF	1.037813	POU2F3	1.906488
ALOX15B	1.148359	HBP1	1.070321	POU3F1	1.472181
ANKRD22	1.505822	HCAR2	2.227049	PPL	1.079871
ANKRD29	1.004008	HCAR3	2.061033	PPP1R15A	1.250187
APOE	1.10496	HCP5	1.022373	PPP1R3B	1.200822
ARHGAP30	2.227763	HDAC5	1.191311	PRDM1	1.492528
ARNT2	2.347534	HDAC9	1.014098	PRICKLE4	1.141436
ARRDC4	1.377681	HEPHL1	1.084285	PRODH	1.239592
ASPRV1	2.393802	HES2	1.815118	PROM2	1.239982
ATF3	2.600626	HIST1H1C	2.570588	ProSAPiP1	1.008596
ATP12A	1.440183	HIST1H2AC	1.751416	PRSS22	3.207114
AVPI1	1.283781	HIST1H2BD	2.723667	PRSS8	1.194038
B3GALT4	1.300773	HIST1H2BK	1.243929	PSORS1C1	1.553438
B3GNT3	1.049928	HIST2H2BE	1.850329	PTGES	1.511422
BBC3	1.612703	HIST3H2A	1.005484	PTGS2	1.301506
BCL2L1	1.077692	HLA-G	2.460471	PVRL4	3.274905
BCL6	1.022801	HMOX1	2.320076	QPCT	1.121274
BIK	1.899355	HSD17B14	1.463513	RAB11FIP1	1.050886
BIRC3	1.411982	HSD17B2	1.779269	RAET1G	1.355114
BLNK	2.166166	HSD3B7	1.356109	RASSF5	1.541771
BMF	2.369338	HSH2D	1.030704	REEP6	1.077737
BNIP3L	1.036609	HSPB8	2.738695	RET	1.243314
BST2	1.416924	ICAM1	2.087607	RGAG4	1.507274
BTBD19	1.135608	ICAM4	1.355522	RGS16	2.736892
BTG1	1.148244	ID2	1.7539	RGS2	1.778959
BTG2	1.403243	IDUA	1.182603	RHBDL1	1.204067
C10orf99	2.924011	IFI27	1.601052	RHCG	2.079265
C11orf35	1.369906	IFIT2	1.077206	RHPN1	1.365829
C11orf9	1.682084	IGFBP3	1.96108	RIBC1	1.098573
C16orf5	1.006965	IGFL3	1.932189	RiNL	1.033176
C17orf103	1.565166	IL1B	1.223292	RNASE7	1.870734

C18orf56	1.11554	IL1R2	2.283708	RND2	1.440745
C19orf46	1.466501	IL1RN	1.278581	RNF208	1.265198
C1orf126	1.008004	IL23A	1.378554	RORA	1.140093
C1orf38	1.298954	IL32	1.122006	RRAD	3.850695
C1orf51	1.552331	IL33	1.109746	RRM2B	1.324419
C1orf74	1.732929	IL36RN	2.089587	RSAD2	1.549139
C1orf88	1.324512	IL8	1.751882	RUNDC3A	1.48569
C20orf46	1.04507	INPP5D	1.925148	RYR1	1.065997
C5orf41	1.546868	INPP5J	1.016762	S100A4	1.430196
C6orf138	1.094879	IRAK2	1.116631	S100A6	1.054154
C7orf10	1.941839	IRF5	1.327517	S100A8	2.129619
C7orf53	1.249614	IRF6	1.395184	SAA1	1.335856
C9orf7	1.060832	ISG20	1.350179	SALL4	2.057745
CA2	1.243123	ISYNA1	1.381921	SAMD10	1.014837
CALML3	1.255207	ITIH4	1.029668	SBK1	2.558557
CALML5	2.024878	ITPKC	1.126402	SBSN	1.878689
CAPNS2	1.210126	IVL	2.375886	SCNN1A	1.524209
CARD14	1.278924	KCNN4	1.802118	SDPR	1.22298
CARD18	2.472437	KCTD11	1.081291	SELPLG	1.687573
CASP9	1.091866	KIAA1257	1.865952	SEMA3B	2.411019
CBX7	1.169991	KIAA1370	1.146223	SEMA3G	1.572456
CCDC11	1.24824	KLHDC9	1.432303	SERPINB1	1.159593
CCDC64B	1.433373	KLHL24	1.889937	SERPINB2	1.49504
CCK	1.062617	KLK10	1.414561	SERPINB3	1.529827
CCL20	1.568576	KLK11	1.551882	SERPINB7	1.343932
CD55	1.028517	KLK5	1.255347	SERTAD1	1.03668
CD68	1.471241	KLK7	1.405181	SESN1	1.171176
CD74	1.002605	KLRG2	1.233281	SGPP2	1.075454
CDKN1A	1.898547	KRT13	4.582385	SIK1	1.048194
CDKN1C	1.344886	KRT15	2.227083	SIRPB2	1.315647
CDKN2B	1.337026	KRT16	1.445009	SLAMF7	2.122482
CDKN2D	1.103006	KRT19	1.292513	SLC28A3	1.767182
CDSN	2.193489	KRT23	2.654857	SLC2A12	1.185052
CEACAM1	1.521198	KRT34	2.056054	SLC44A3	1.096887
CEBPA	1.068886	KRT37	2.786469	SLC46A1	1.177566
CEL	1.833995	KRT42P	1.383759	SLC7A4	1.156152
CES3	1.495162	KRT6B	1.218162	SLPI	2.205451
CES4A	1.145926	KRT7	1.20472	SMOC1	1.596494
CFB	1.525458	KRT75	1.204212	SNCG	1.231876
CGN	1.243352	KRT80	2.425273	SORT1	1.427147
CHI3L2	2.22442	KRTDAP	1.404801	SPATA18	1.077252
CHST2	1.153737	KYNU	1.234901	SPINK6	1.288906
CITED2	1.362391	LACC1	1.348361	SPNS2	1.783244
CLCF1	1.746694	LBH	1.964427	SPOCD1	1.028304
CLDN1	2.164861	LCE1B	2.863596	SPON2	3.073135
CLDN23	1.949484	LCE1C	1.5978	SPRR1A	1.79158
CLDN4	3.387876	LCN2	1.410005	SPRR1B	1.458382
CLDN7	1.756154	LIF	2.020803	SPRR2A	1.281665

CLEC2B	1.823128	LINC00086	2.475568	SPRR2D	1.021259
CLIC3	1.327201	LMO7	1.453974	SPRR2E	1.628479
CLU	1.438944	LOC100049716	1.166231	SPRR3	2.813864
CNFN	2.155499	LOC100129781	1.088847	SQSTM1	1.526918
COX6B2	1.34408	LOC100131096	1.015925	STEAP4	4.22635
CPT1C	1.277061	LOC100131564	1.109901	SULT1A1	1.332854
CRB3	1.066881	LOC100132909	1.081642	SULT2B1	1.729219
CRCT1	3.196832	LOC100133190	1.059472	SYNGR3	1.134232
CRISPLD2	2.63943	LOC100287177	1.060091	SYTL2	1.420285
CRYAB	2.080253	LOC100505623	1.290074	TACSTD2	1.167671
CSF1	1.150493	LOC100505974	1.072712	TCP11L2	1.288639
CSF3	1.528244	LOC100506119	1.199105	TGFB2	1.111166
CST6	3.096074	LOC100506377	1.931858	TGM1	1.556176
CTSS	1.384918	LOC100506538	1.582621	THBD	1.570713
CUL9	1.146301	LOC100506746	1.093062	TIMP2	1.624976
CYFIP2	2.012293	LOC100507429	1.577794	TLCD2	1.203551
CYGB	1.278952	LOC100507452	1.034674	TLR2	1.209706
CYP2S1	1.111609	LOC100507656	1.387791	TM7SF2	1.094312
CYP3A5	2.134077	LOC151475	2.864213	TMEM125	1.769122
DAPK1	2.489445	LOC151534	1.798543	TMEM184A	1.403734
DBNDD1	1.697917	LOC284080	1.116795	TMEM27	2.26327
DBP	1.548785	LOC284440	1.232691	TMEM38A	1.428279
DCN	1.917867	LOC284837	2.507131	TMEM45B	1.329869
DEFB1	4.538491	LOC441869	1.405387	TMEM61	1.417963
DENND1C	1.052741	LOC554223	1.05486	TMEM86A	1.280883
DGAT2	1.066686	LOC646471	1.010308	TMEM91	1.277979
DHDH	1.977426	LOC728975	1.150382	TMPRSS11D	1.097904
DHRS3	1.150886	LOC730755	1.127336	TMPRSS13	2.538018
DKFZp434J0226	1.581589	LY6D	2.375439	TMPRSS4	1.673327
DPP4	1.635675	LY6G6C	1.478579	TNF	1.380011
DQX1	1.282541	LYNX1	1.569974	TNFAIP2	2.133214
DUSP10	2.217671	LYPD3	1.202858	TNFAIP8L3	1.078872
DYRK1B	1.133527	LYPD5	1.938955	TNFRSF10C	4.084906
EDA2R	1.650437	MAFB	1.976484	TNFRSF14	1.154539
EGR3	1.055599	MAP1LC3A	1.524844	TNFSF4	1.328395
ELFN2	1.454605	MAP3K8	1.266091	TOB1	1.129999
ENO2	1.176432	MAPK8IP2	1.267615	TP53INP1	1.898305
ENTPD3	1.13432	MCHR1	2.376182	TP53INP2	1.709985
EPHB2	1.0814	MDM2	1.857866	TPPP	1.126332
EPHB3	1.28144	MEG3	1.680548	TRAF1	1.270284
EPPK1	1.03793	METRNL	1.850228	TRAF3IP3	1.885624
ERBB3	1.176234	MEX3B	1.293473	TREM2	1.406591
ESPN	1.898346	MIR21	1.056403	TRIM17	1.097686
ETV7	1.992978	MLPH	1.048951	TRIM22	1.107816
FAM131C	1.195041	MME	1.279362	TSPAN1	1.043978
FAM13C	1.660195	MNT	1.093418	TSPAN10	1.145679
FAM198B	1.546092	MUC1	1.323749	TTC39A	1.513684
FAM43A	2.281964	MXD1	1.221816	TTC9	1.775748

FAM46A	1.142838	MXD4	1.119169	TTLL3	1.07677
FAM84A	1.217675	MXI1	1.012704	TXNIP	1.324999
FAM86HP	1.398758	MYBPHL	2.469553	UCA1	3.144775
FBXO32	1.762987	MYH16	1.669449	ULBP1	1.718077
FDXR	1.123815	MYO15B	1.769726	ULK1	1.155636
FGF11	1.057493	N4BP2L1	1.302932	UNC13D	1.284158
FLJ32255	1.396227	NCCRP1	2.25184	VAMP5	1.10333
FLJ35776	1.045777	NCF2	1.956338	VASN	1.070314
FLJ43663	1.505095	NDRG4	1.724837	VGLL3	1.526916
FLJ45831	1.688516	NEAT1	1.17292	VNN1	1.585207
FLNC	1.840758	NFATC4	1.144891	VWCE	2.339601
FN3K	1.042252	NFKBIA	1.085284	WDR63	1.100921
FOLR3	1.453421	NFKBIZ	1.055574	WFDC5	1.623134
FTH1	1.02617	NHLH2	1.783285	YPEL2	1.093046
FTL	1.293257	NINJ1	1.360009	YPEL3	1.333902
FUT2	1.130622	NIPAL4	1.035101	YPEL4	2.050039
FUT3	1.400397	NLRP10	2.908381	ZFHX2	1.14507
FXYD3	1.235707	NOD2	1.045928	ZFYVE1	1.004115
G0S2	1.507978	NOTCH3	2.10179	ZNF185	1.058878
GABARAPL1	1.12635	NR1D1	1.830782	ZNF425	1.493712
GALK1	1.028271	NR1D2	1.034866	ZNF432	1.264009
GAMT	1.499196	NR4A1	1.502722	ZNF610	1.214798
GBP2	2.981328	NR4A2	1.09004	ZNF702P	1.114955
GDA	1.668244	NUPR1	1.436536	ZNF750	1.98419
GDF15	4.934651	OCLN	1.834442	ZNF763	1.068978
GGT1	1.76415	OVGP1	1.381053	ZNF812	1.677638

Table 3. Genes down-regulated by UVR

Gene ID	Log2FC	Gene ID	Log2FC	Gene ID	Log2FC
ABCC4	-1.348205778	FAM54A	-1.308473296	PCSK5	-1.300996825
ABI3BP	-1.592845354	FAM64A	-2.300111494	PDE4D	-1.179913183
ADAMTSL1	-3.057818112	FAM72A	-2.02193515	PDGFC	-1.025319775
AGTPBP1	-1.059225614	FAM72B	-2.376888348	PDIA2	-1.385271
AKAP6	-1.065270643	FAM72D	-2.569570317	PDIA4	-1.259521447
AKAP7	-1.191007938	FAM83D	-1.9457666	PEG10	-1.227483825
AKT3	-1.063141722	FANCA	-1.30500965	PFAS	-1.051620468
ALDH1L2	-1.71329721	FANCB	-1.681934488	PHGDH	-1.227080584
ALG14	-1.390158117	FANCC	-1.226225604	PID1	-1.453305805
ALMS1	-1.39725398	FANCD2	-1.605305539	PIF1	-2.616987868
ANK2	-2.852547236	FANCI	-1.236564911	PIK3C2G	-2.501961882
ANKRD44	-3.201509809	FAR2	-1.708513767	PKI55	-1.083926432
ANLN	-2.074462024	FARS2	-1.344824882	PKMYT1	-1.844074552
ANO1	-1.455452126	FBN2	-1.282186621	PLCB4	-1.013542456
ANXA6	-1.214603625	FBXL17	-1.373090742	PLK1	-2.434416727
APBA1	-1.03839454	FBXL7	-2.52127296	PLK4	-1.534332316
APCDD1	-1.068852998	FBXO43	-2.669021178	PLXDC2	-1.404520551

APLN	-1.995875214	FBXO5	-1.501898367	PLXNC1	-1.085076724
ARHGAP11A	-1.932775855	FEN1	-1.059637367	PLXND1	-1.348170161
ARHGAP11B	-1.97626487	FGFBP1	-1.649445744	POLA1	-1.343856772
ARHGAP18	-1.090237869	FGGY	-1.201858562	POLE2	-1.769737957
ARHGAP19	-1.34032156	FHIT	-2.966326239	POLN	-1.486625284
ARHGAP33	-1.316757909	FIGN	-1.270062012	POLQ	-2.072375564
ARSB	-1.490168103	FKBP11	-1.262078361	POLR3G	-1.005696232
ASF1B	-1.507991707	FOXD2	-1.119795421	PRC1	-1.947640952
ASNS	-1.325921219	FOXM1	-2.05641668	PRDM5	-1.585370558
ASPM	-2.485501797	FOXP2	-1.900599816	PRICKLE1	-1.498603086
ATAD2	-1.092034263	FRAS1	-1.154333269	PRIM1	-1.160571677
ATAD5	-1.198810998	FUT4	-1.003805317	PRIM2	-1.004231581
ATG10	-1.012583207	FUT8	-1.067042768	PRKCA	-1.601780357
AURKA	-1.605879285	GALNT10	-1.185419938	PRR11	-1.833215683
AURKB	-2.266234804	GALNTL4	-1.125279056	PRTFDC1	-1.228474421
B3GALTL	-1.098025255	GAS2L3	-2.204825541	PRUNE2	-3.224761055
BARD1	-1.245055616	GHR	-1.168281527	PSAT1	-1.204185638
BBS9	-1.716979874	GINS1	-1.262554478	PSMC3IP	-1.085977037
BCAS3	-1.500580847	GINS2	-1.836989185	PSRC1	-2.121773024
BCAT1	-1.262972667	GINS4	-1.304293072	PTGS1	-1.085302707
BCL2	-1.345519919	GIPC2	-1.366213219	PTPRG	-1.65358899
BEND6	-1.554214214	GJB2	-1.157268298	PTPRZ1	-1.507226274
BIRC5	-2.468776552	GLI1	-1.607809436	PYCR1	-1.057369077
BLM	-1.833991479	GLT8D2	-1.021420114	RABGAP1L	-1.289087491
BORA	-1.11351262	GMDS	-1.894237011	RACGAP1	-1.234902292
BRCA1	-1.433568205	GNB3	-1.024028547	RAD51	-1.480782503
BRCA2	-1.738870791	GNG11	-1.308698968	RAD51AP1	-1.372089728
BRIP1	-1.365404961	GNG2	-1.267535939	RAD51B	-1.42302095
BUB1	-2.232101679	GPC6	-3.413041607	RAD54B	-1.21691423
BUB1B	-2.463047443	GPHN	-1.639685734	RAD54L	-1.432880045
C11orf82	-1.734657367	GPR113	-1.006074874	RANBP17	-1.427466251
C12orf26	-1.02533073	GPR39	-1.182345041	RAPGEF4	-1.594354405
C12orf48	-1.731440454	GPR63	-1.082603164	RBL1	-1.430172588
C12orf55	-1.155331766	GPSM2	-1.114318389	RBMS3	-1.312042071
C14orf49	-1.046892915	GRB14	-1.016641502	RECQL4	-1.184607991
C14orf80	-1.158411353	GREB1L	-1.343457163	RFC3	-1.107780232
C15orf42	-1.43469073	GRIA1	-3.531086354	RFX3	-1.411661589
C16orf59	-1.251575133	GRIP1	-2.0507268	RGMB	-1.153194674
C1orf112	-1.026418432	GSG2	-1.568691237	RGPD5	-1.371696038
C21orf58	-1.347413053	GTDC1	-1.532315383	RGS5	-1.453690846
C3orf26	-1.633777304	GTSE1	-2.383747263	RMI1	-1.121325391
C4orf21	-1.638019979	H2AFX	-1.343555024	RNLS	-1.262777743
C5	-1.896229619	HAUS8	-1.092972486	ROBO1	-1.187476219
C9orf100	-1.416508411	HELLS	-1.088366116	ROR1	-1.51612717
C9orf140	-1.512229	HIST1H2BH	-1.024808608	RPL22L1	-1.338137604
C9orf93	-3.645734034	HJURP	-2.4592233	RPS6KA2	-1.461033057
CADPS2	-2.749447365	HMCN1	-2.204217467	RRM2	-1.991311534
CAMKMT	-1.560519775	HMGB2	-1.263166086	RSRC1	-1.178787776

CASC2	-1.210566387	HMGCS1	-1.182070599	RUNDC2A	-1.265189228
CASC5	-2.254998502	HMMR	-2.404579608	RUNDC3B	-2.323290022
CBS	-1.047490252	HNRNPA3P1	-1.036139918	RYR3	-1.010652199
CCBE1	-1.49186818	HPDL	-1.042909973	S1PR1	-1.018299255
CCDC109B	-1.008132116	HS6ST2	-1.493151016	SAMD3	-1.661703151
CCDC150	-1.777877107	HSP90B1	-1.544477225	SCAPER	-1.144478129
CCDC152	-1.563498921	HSP90B3P	-1.317944538	SCFD2	-1.922440965
CCDC18	-1.539219671	HSPA5	-1.420064786	SCLT1	-1.080112469
CCDC3	-2.188282435	HYOU1	-1.068804209	SCMH1	-1.052116405
CCNA2	-2.040850548	IL7R	-1.477457922	SCN9A	-1.398160949
CCNB1	-1.992477017	IMMP2L	-1.066160828	SDF2L1	-1.284992898
CCNB2	-2.023197257	INCENP	-1.107627737	SDK1	-2.13313528
CCNE2	-1.166174946	IQCK	-1.064764335	SEMA3D	-2.01252048
CCNF	-1.319421617	IQGAP3	-2.061688996	SEMA3E	-2.516404159
CDC20	-2.788887669	ISPD	-1.879226849	SEMA5A	-2.929174239
CDC25A	-1.345444577	ITGA1	-1.353730434	SERGEF	-1.093861415
CDC25C	-1.941854577	ITGA4	-1.756671957	SFTA1P	-1.191338272
CDC45	-1.66938146	ITPR1	-1.290522642	SFXN2	-1.409000972
CDC6	-1.746559274	ITPR2	-1.233472544	SGOL1	-2.176977698
CDC7	-1.022925655	KCNK10	-2.68829958	SGOL2	-1.985641318
CDCA2	-1.900385914	KCNQ5	-2.008072711	SHCBP1	-2.176358987
CDCA3	-2.659044568	KHDRBS3	-1.145560989	SIRPB1	-1.073654141
CDCA5	-1.747593013	KIAA0101	-1.461639006	SKA1	-2.292700912
CDCA7	-1.343204821	KIAA0825	-1.622878808	SKA3	-2.130705608
CDCA8	-1.959093261	KIAA1524	-1.392420329	SKP2	-1.100554338
CDH4	-2.389925028	KIAA1644	-1.799956723	SLC16A9	-1.437744237
CDK1	-1.949360908	KIF11	-1.878590906	SLC2A13	-1.400132755
CDK14	-1.182597074	KIF14	-2.53528912	SLC43A1	-1.088907499
CDKAL1	-1.326316704	KIF15	-2.216792744	SLC43A3	-1.115380732
CDKN2C	-1.321626434	KIF18A	-2.041415274	SLC7A11	-1.101550321
CDKN3	-2.415696295	KIF18B	-2.456303841	SLC7A2	-1.316982859
CDON	-1.278358612	KIF20A	-2.8739185	SLC7A5	-1.092962509
CDT1	-1.295120529	KIF20B	-1.335643536	SLC8A1	-3.890468578
CENPA	-2.730714266	KIF23	-1.80247136	SLC9A9	-1.772424605
CENPE	-1.89935139	KIF24	-1.392867165	SLFN11	-1.344303011
CENPF	-2.568066958	KIF26B	-1.838433497	SLFN13	-1.001484977
CENPH	-1.270674947	KIF2C	-2.287148765	SLIT2	-1.635335628
CENPI	-1.767622737	KIF4A	-2.522518287	SLIT3	-2.106888295
CENPJ	-1.102370738	KIF4B	-2.278006561	SMC2	-1.07784523
CENPK	-1.271103299	KIFC1	-2.018332665	SMC4	-1.372671433
CENPM	-1.567908583	KLHL13	-1.355922156	SMYD3	-1.914279342
CENPN	-1.330259855	KNTC1	-1.005796394	SNORA51	-1.176748219
CENPO	-1.394874643	KPNA2	-1.290854042	SNORD101	-1.349751243
CENPW	-1.348316188	L3MBTL4	-1.577144676	SNORD12	-1.264153814
CEP112	-1.785492351	LARGE	-2.256213738	SNORD14C	-1.373015383
CEP128	-1.931644843	LBR	-1.031056323	SNORD14E	-1.065302198
CEP170P1	-3.902232714	LEF1	-1.277296868	SNORD17	-1.364493668
CEP55	-2.535959714	LEPR	-1.166781312	SNORD28	-1.221337171

CHAF1A	-1.060713699	LFNG	-1.599869881	SNORD88B	-1.055543084
CHEK1	-1.204412215	LHFP	-1.064934578	SNX10	-1.079060213
CHRNA5	-1.310278551	LIMCH1	-1.292609661	SNX29	-1.410602348
CHSY3	-2.63674892	LINC00341	-1.013052052	SOX11	-1.223375096
CIT	-2.093026219	LMCD1	-1.009878102	SOX6	-1.032166298
CKAP2L	-2.259036313	LMNB1	-2.526637995	SPAG17	-1.659735287
CKS1B	-1.089031731	LNP1	-1.303478188	SPAG5	-1.65235008
CLDN11	-1.745869165	LOC100128191	-1.134938013	SPATA13	-1.075647439
CLMP	-2.630409593	LOC100128881	-1.090189815	SPATA17	-2.430679132
CLSPN	-1.755066048	LOC100129961	-1.331714119	SPATA5	-1.14726314
CMTM1	-1.092242876	LOC100288637	-1.889382704	SPATA6	-1.379798818
CNTLN	-1.002235788	LOC100506711	-1.459828788	SPC24	-1.942352943
CNTN1	-1.717727031	LOC100506844	-1.238994387	SPC25	-2.181086004
CNTNAP3	-1.50024013	LOC100506994	-1.030046919	SPEF2	-1.218600348
COL12A1	-1.225388115	LOC100507552	-3.443851009	SSBP2	-1.270375221
COL18A1	-1.039211617	LOC100652789	-1.082283866	ST8SIA4	-1.171785056
COL24A1	-1.275030048	LOC285141	-1.573604306	STAG1	-1.211513978
COL4A1	-1.469924365	LOC642846	-1.033203026	STAG3L1	-1.346197566
COL4A2	-1.669276381	LOC647946	-2.25998556	STAMBPL1	-1.060856801
COL4A4	-1.048165114	LRBA	-1.087162349	STAR	-1.769078887
COL5A1	-1.270708967	LRIG1	-1.024924857	STIL	-1.496402119
COL8A1	-1.928088788	LRP8	-1.42572786	STK32B	-2.069785601
COMMD1	-1.133528646	LRRC6	-1.488389369	STK33	-2.30665232
COMMD10	-1.332882925	LRRIQ1	-1.751414291	STS	-1.532500152
CPS1	-1.70577865	LTBP1	-1.813158937	STX8	-1.127540559
CREB5	-1.013904928	LZTS1	-1.66064357	STXBP4	-1.351053971
CRELD2	-1.101683675	MAD2L1	-1.591320994	SULT1E1	-1.560657669
CSRNP3	-1.459413081	MAGI3	-1.089745698	SUPT3H	-1.559626944
CTNNAL1	-1.404403365	MAP6	-1.031260549	SUV39H1	-1.055427461
CYP39A1	-1.023008589	MAPK10	-1.33357193	SVEP1	-1.172034978
DBF4	-1.254245876	MATN3	-1.028109037	SYT1	-1.850488964
DBF4B	-1.335142658	MBOAT1	-1.196601248	TACC3	-1.807917227
DCDC2	-1.495206045	MCM10	-2.303622809	TBC1D3P1-DHX40P1	-1.718629676
DCHS1	-1.786705555	MCM3	-1.173047908	TBC1D5	-1.034717598
DDX12P	-1.054548291	MCM5	-1.300923302	TBX1	-1.002975218
DENND1A	-1.056858676	MCM6	-1.364315385	TCF19	-1.331891307
DEPDC1	-2.480768329	MCM7	-1.074498906	TDRD9	-1.056032287
DEPDC1B	-1.167668186	MEF2C	-2.000689675	TGM4	-1.037262874
DERL3	-2.51482921	MELK	-1.057551244	THBS1	-1.017293581
DHFR	-1.297735908	METAP1D	-1.067957808	THBS2	-1.724598457
DIAPH2	-1.696949962	MGC16121	-1.04238246	TIMELESS	-1.088272778
DIAPH3	-2.033597387	MKI67	-2.74797697	TK1	-1.51351299
DLEU1	-1.121028106	MMP2	-1.17402456	TLL1	-1.746038163
DLEU2	-2.107581325	MMS22L	-1.149026385	TLR6	-1.761305528
DLGAP5	-2.608879588	MND1	-1.741478459	TMEM117	-1.208085002
DLL1	-1.015920318	MOXD1	-1.460995365	TMEM97	-1.212401251
DMC1	-3.630542564	MPHOSPH9	-1.15786143	TMTC2	-1.815467237
DNAH5	-1.37639111	MSH5-C6orf26	-1.040129645	TNC	-1.600248019

DOCK10	-1.918039738	MSRA	-2.240412801	TNS1	-1.554340131
DOCK11	-1.395693649	MTBP	-1.01902842	TOP2A	-2.386015457
DOCK4	-1.143979182	MYBL1	-1.698796151	TPK1	-2.246074973
DPY19L2	-1.056133483	MYBL2	-2.022262666	TPX2	-1.813159472
DPYD	-3.389239421	MYH15	-2.192048185	TRAIP	-1.18054426
DPYSL3	-1.926485306	MYLK4	-1.05279565	TRAPPC9	-1.031296849
DRP2	-2.641906925	NAV3	-1.110567684	TRIM59	-1.075976395
DSCAM	-1.906670101	NCALD	-1.199097373	TRIP13	-1.57140204
DSCC1	-1.403031606	NCAPD2	-1.224817576	TROAP	-2.358691763
DTL	-1.948891786	NCAPG	-2.247458098	TTC26	-1.066910781
DTWD2	-1.523560971	NCAPG2	-1.585127369	TTC28	-1.43380084
DUSP9	-1.171136132	NCAPH	-2.170881812	TTK	-2.183953926
DYNC2H1	-1.083013559	NCKAP5	-1.342371268	TUBA1B	-1.549605554
DZIP3	-1.080806672	NCOA1	-1.154674374	TUBA1C	-1.06766931
E2F1	-1.637960738	NDC80	-2.165240026	TXNDC5	-1.014330286
E2F2	-1.587033082	NEIL3	-2.29503331	TYW1B	-1.055561674
E2F8	-1.073325681	NEK11	-1.026289133	UBE2C	-2.550014168
EDA	-1.827607348	NEK2	-2.208099443	UBE2S	-1.293876674
EDNRA	-1.659792405	NOS1	-1.310961641	UCHL1	-1.000277324
EFCAB11	-1.584503864	NRGN	-1.689312634	UHRF1	-1.654077016
EFCAB2	-1.527976301	NTM	-2.048027621	USP13	-1.211411674
EFHC2	-1.933530011	NTNG1	-1.415593761	UTP20	-1.159131427
ELAVL2	-1.125514972	NUBPL	-1.096121588	WDPCP	-1.986624455
ELOVL6	-1.188535907	NUCB2	-1.074994468	WDR17	-1.469613807
ELP4	-1.033572654	NUF2	-2.143706843	WDR4	-1.122037801
EME1	-1.532128786	NUSAP1	-1.570361409	WDR62	-1.327456068
ENOX1	-2.429551313	ODC1	-1.192092225	WDR65	-1.366210497
EPB41L2	-1.070473848	ODZ3	-1.844793468	WDR7	-1.053132054
ERCC6L	-1.837917859	ODZ4	-1.318047355	WDR76	-1.760139175
ESCO2	-1.704405316	OIP5	-1.387288305	WHSC1	-1.36218294
ESPL1	-1.810339548	ORC1	-1.957553549	WNT10B	-1.302096355
ETV1	-1.384595787	ORC6	-1.113974953	WWOX	-2.010534417
EXO1	-2.035852802	OSBPL6	-1.004909427	XRCC2	-2.075258306
EXOC4	-1.386101999	OXCT1	-1.088317263	XRCC4	-1.285559504
EXTL2	-1.239584151	P4HA3	-3.230028297	XYLT1	-1.538493127
FAAH2	-1.104705621	PALM2	-1.258674299	ZNF367	-1.804784888
FAF1	-1.009982162	PALMD	-1.231475809	ZNF492	-1.476335538
FAM111B	-2.120125967	PARD3B	-2.825199287	ZNF546	-1.044266261
FAM132B	-1.187212606	PBK	-2.22936512	ZNF724P	-1.23386724
FAM151B	-1.125962764	PCDH18	-1.489762025	ZNF730	-1.15988286
FAM167A	-1.03677525	PCDHAC2	-1.484449311	ZRANB3	-1.691812182
FAM172A	-1.639239582	PCLO	-1.276919308	ZWINT	-1.120333991

EXAMPLE 3

Time-dependent transcriptomic changes in response to UVR

[0075] Our PCA analysis in Fig. 1A revealed time-dependent variations in UVR-responsiveness. To identify genes exhibiting time-dependent cumulative UVR responsiveness, we performed paired t-tests to compare the gene expression signatures of Day 3 versus those of Day 1 for each keratinocyte cell line (N0, N1 and N2) under the same UVR dose. 164 out of the 531 up-regulated genes showed higher expressions at Day 3 than at Day 1 (FDR-corrected p-value < 0.05); while 239 out of the 610 down-regulated genes were more repressed at Day 3 than at Day 1 at the same p-value threshold (Table 4). Two examples of time-dependent up-regulation include ADAMTSL4, encoding a disintegrin and metalloproteinase; and CST6, encoding a cystatin superfamily protein. Examples of time-dependent down-regulation include UHRF1, encoding a member of a subfamily of RING-finger type E3 ubiquitin ligases; and TRIP13, which encodes a protein that interacts with thyroid hormone receptors (FIG. 2).

Table 4. Genes displaying time-dependent changes in mRNA expression following UVR

		Down-regulated		
ANLN	CENPH	GINS1	MND1	SGOL1
ARHGAP11A	CENPI	GINS2	MTBP	SGOL2
ARHGAP11B	CENPJ	GINS4	MYBL1	SHCBP1
ASF1B	CENPK	GLT8D2	MYBL2	SKA1
ASPM	CENPM	GPR63	MYH15	SKA3
ATAD2	CENPN	GSG2	NCAPG	SKP2
ATAD5	CENPO	GTSE1	NCAPG2	SLC43A3
AURKA	CENPW	H2AFX	NCAPH	SLFN13
AURKB	CEP55	HAUS8	NDC80	SMC2
BARD1	CHAF1A	HELLS	NEIL3	SMC4
BIRC5	CHEK1	HIST1H2BH	NEK2	SNORD17
BLM	CHRNA5	HJURP	NRGN	SNORD28
BORA	CKAP2L	HMGB2	NUF2	SOX11
BRCA1	CKS1B	HMMR	NUSAP1	SPAG5
BRCA2	CLSPN	HPDL	OIP5	SPC24
BRIP1	DBF4	HYOU1	ORC1	SPC25
BUB1	DBF4B	IL7R	ORC6	STAMBPL1
BUB1B	DDX12P	INCENP	PALMD	STIL

C11orf82	DEPDC1	IQGAP3	PBK	SULT1E1
C14orf80	DHFR	KIAA0101	PCDH18	SUV39H1
C15orf42	DLEU1	KIAA1524	PCDHAC2	TACC3
C16orf59	DLGAP5	KIF11	PEG10	TCF19
C1orf112	DSCC1	KIF14	PFAS	TGM4
C9orf100	DTL	KIF15	PKMYT1	THBS1
CASC5	DUSP9	KIF18A	PLK1	TIMELESS
CCDC150	E2F1	KIF18B	PLK4	TK1
CCNA2	E2F8	KIF20A	POLE2	TMEM97
CCNB1	EDNRA	KIF20B	POLQ	TOP2A
CCNB2	EME1	KIF23	POLR3G	TPX2
CCNE2	ERCC6L	KIF24	PRC1	TRAIP
CCNF	ESCO2	KIF2C	PRIM1	TRIM59
CDC20	ESPL1	KIF4A	PSMC3IP	TRIP13
CDC25A	EXO1	KIF4B	PTGS1	TROAP
CDC25C	FAM111B	KIFC1	RACGAP1	TTK
CDC45	FAM167A	KPNA2	RAD51	UBE2C
CDC6	FAM54A	LBR	RAD51AP1	UBE2S
CDC7	FAM64A	LMNB1	RAD54B	UHRF1
CDCA2	FAM72A	LOC100128191	RAD54L	UTP20
CDCA3	FAM72B	LOC100506711	RBL1	WDR4
CDCA5	FAM83D	MAD2L1	RECQL4	WDR62
CDCA8	FANCA	MCM10	RFC3	WDR65
CDK1	FANCB	MCM3	RGMB	WDR76
CDKN2C	FANCD2	MCM5	RMI1	XRCC2
CDKN3	FANCI	MCM7	RRM2	ZNF367
CDT1	FBXO5	MELK	S1PR1	ZNF492
CENPA	FEN1	MKI67	SEMA3D	ZNF724P
CENPE	FKBP11	MMP2	SFTA1P	ZWINT
CENPF	FOXM1	MMS22L	SFXN2	

	Up-regulated	
ABCA12	GAMT	NOTCH3
ABLIM3	GDA	NUPR1
ACBD4	GGT1	PAPL
ACTA2	GIPR	PIK3IP1
ADAMTS13	GPNMB	PLA2G4C
ADAMTS7	GRIN3B	PLEKHG1
ADAMTSL4	HBEGF	PNLIPRP3
ADHFE1	HIST1H2AC	ProSAPiP1
ADSSL1	HLA-G	PRSS22
AIFM3	HSD17B14	PRSS8
ALDH3B2	HSD17B2	PSORS1C1
ALOX15B	ICAM1	QPCT
ANKRD29	ICAM4	REEP6
APOE	IDUA	RET
ATP12A	IL32	RHBDL1

B3GALT4	IL33	RNF208
BLNK	IRAK2	RUNDC3A
BNIP3L	IRF5	RYR1
BTBD19	ITIH4	S100A4
C11orf35	ITPKC	S100A6
C19orf46	KCTD11	SAA1
C1orf126	KIAA1370	SGPP2
C1orf38	KLHDC9	SIRPB2
C1orf88	KLHL24	SLC28A3
C5orf41	KLK11	SLPI
C6orf138	KRT15	SORT1
C7orf10	KRT19	SPNS2
C9orf7	KRT23	SULT1A1
CARD14	KRT37	TCP11L2
CBX7	KYNU	TIMP2
CCDC64B	LCN2	TLCD2
CCL20	LINC00086	TLR2
CD68	LOC100049716	TM7SF2
CLDN7	LOC100129781	TMEM38A
COX6B2	LOC100131096	TMEM61
CRCT1	LOC100131564	TMEM91
CST6	LOC100505623	TMPRSS4
CTSS	LOC100507452	TNFAIP8L3
CUL9	LOC284080	TNFRSF14
CYGB	LOC284440	TREM2
DKFZp434J0226	LOC646471	TSPAN10
DPP4	LOC728975	TTC39A
DQX1	LYNX1	TTC9
DYRK1B	MEG3	TTLL3
EPHB2	MIR21	TXNIP
ESPN	MLPH	VAMP5
FBXO32	MME	VNN1
FGF11	MNT	WFDC5
FN3K	MUC1	YPEL2
FOLR3	MXD4	YPEL3
FTH1	MXI1	YPEL4
FTL	MYO15B	ZFHX2
FXYD3	N4BP2L1	ZNF185
G0S2	NDRG4	ZNF610
GABARAPL1	NFATC4	

EXAMPLE 4

Dose-dependent transcriptomic changes in response to UVR

[0076] In addition to the time-dependent UVR-responsiveness described above, we were also interested in identifying genes that may display dose-dependent changes in response to UVR. To do so, we fitted linear regression models for each of the differentially expressed genes using UVR doses (10, 20 and 30 mJ/cm^2) as independent variables and gene expression as the dependent variable for each keratinocyte cell line (N0, N1, N2) at the same time point (Day 1 or 3). For each gene, we constructed six models representing the following six conditions: N0-1d, N0-3d, N1-1d, N1-3d, N2-1d and N2-3d, We then integrated the six coefficient p-values from the six models using Fisher's method. We found that 285 out of the 531 up-regulated genes showed dose-dependent up-regulation with FDR-corrected p-value < 0.05; and 452 out of the 610 down-regulated genes demonstrated significant dose-dependent decreases in gene expression at the same FDR threshold (Table 5). Dose-dependent changes in four representative genes from each group were illustrated in FIG. 3.

Table 5. Genes displaying dose-dependent changes in mRNA expression following UVR

		Down-regulated		
ABCC4	CEP112	FKBP11	MCM10	RUNDC3B
ABI3BP	CEP128	FOXM1	MCM3	RYR3
ADAMTSL1	CEP55	GALNT10	MCM5	SCAPER
AGTPBP1	CHAF1A	GALNTL4	MCM6	SCFD2
AKAP6	CHEK1	GINS1	MCM7	SCLT1
AKAP7	CHRNA5	GINS2	MELK	SCMH1
ALDH1L2	CHSY3	GINS4	METAP1D	SCN9A
ALG14	CIT	GIPC2	MGC16121	SDF2L1
ALMS1	CKAP2L	GLI1	MKI67	SDK1
ANKRD44	CKS1B	GLT8D2	MMP2	SEMA3D
ANLN	CLMP	GMDS	MMS22L	SEMA3E
ANXA6	CLSPN	GNB3	MND1	SEMA5A
APLN	CNTLN	GPC6	MOXD1	SERGEF
ARHGAP11A	CNTN1	GPHN	MSRA	SFXN2
ARHGAP11B	COL12A1	GPR39	MTBP	SGOL1
ARHGAP19	COL18A1	GPR63	MYBL2	SGOL2

ARHGAP33	COL4A1	GPSM2	NCAPD2	SHCBP1
ARSB	COL4A2	GRB14	NCAPG	SKA1
ASF1B	COL8A1	GRIA1	NCAPG2	SKA3
ASNS	COMMD1	GRIP1	NCAPH	SKP2
ASPM	COMMD10	GSG2	NCKAP5	SLC16A9
ATAD2	CPS1	GTDC1	NCOA1	SLC2A13
ATAD5	CREB5	GTSE1	NDC80	SLC43A1
AURKA	CTNNAL1	H2AFX	NEIL3	SLC7A5
AURKB	DBF4	HAUS8	NEK2	SLC8A1
B3GALTL	DBF4B	HELLS	NTM	SLFN13
BARD1	DCHS1	HJURP	NUF2	SLIT3
BBS9	DDX12P	HMCN1	NUSAP1	SMC2
BCAT1	DEPDC1	HMGB2	ODZ3	SMC4
BCL2	DEPDC1B	HMGCS1	ORC1	SMYD3
BEND6	DHFR	HMMR	ORC6	SNORA51
BIRC5	DIAPH2	HS6ST2	OSBPL6	SNX29
BLM	DIAPH3	INCENP	OXCT1	SPAG17
BORA	DLEU1	IQCK	P4HA3	SPAG5
BRCA1	DLEU2	IQGAP3	PALM2	SPATA13
BRCA2	DLGAP5	ISPD	PBK	SPATA17
BRIP1	DLL1	ITGA1	PCDHAC2	SPATA5
BUB1	DMC1	ITGA4	PDE4D	SPATA6
BUB1B	DNAH5	ITPR1	PDGFC	SPC24
C11orf82	DOCK10	ITPR2	PEG10	SPC25
C12orf26	DPYD	KCNK10	PFAS	SPEF2
C12orf48	DPYSL3	KCNQ5	PHGDH	STAG1
C14orf80	DRP2	KHDRBS3	PID1	STIL
C15orf42	DSCC1	KIAA0825	PIF1	STK33
C16orf59	DTL	KIAA1524	PIK3C2G	STS
C21orf58	DTWD2	KIF11	PKI55	STXBP4
C3orf26	DYNC2H1	KIF14	PKMYT1	SUPT3H
C4orf21	DZIP3	KIF15	PLK1	SUV39H1
C5	E2F1	KIF18A	PLK4	SYT1
C9orf100	E2F8	KIF18B	PLXNC1	TACC3
C9orf93	EDA	KIF20A	PLXND1	TBX1
CADPS2	EFCAB11	KIF20B	POLA1	TCF19
CAMKMT	EFCAB2	KIF23	POLE2	TDRD9
CASC2	EFHC2	KIF24	POLQ	THBS1
CASC5	ELAVL2	KIF26B	POLR3G	THBS2
CBS	ELOVL6	KIF2C	PRC1	TIMELESS
CCDC150	ELP4	KIF4A	PRDM5	TK1
CCDC152	EME1	KIF4B	PRICKLE1	TLL1
CCDC18	ENOX1	KIFC1	PRIM1	TLR6
CCDC3	EPB41L2	KLHL13	PRKCA	TMEM97
CCNA2	ERCC6L	KNTC1	PRR11	TMTC2
CCNB1	ESPL1	KPNA2	PRTFDC1	TNC
CCNB2	EXO1	L3MBTL4	PRUNE2	TNS1
CCNF	EXTL2	LARGE	PSAT1	TOP2A

CDC20	FAF1	LBR	PSMC3IP	TPK1
CDC25C	FAM111B	LEF1	PSRC1	TPX2
CDC45	FAM167A	LFNG	PTGS1	TRAIP
CDC6	FAM172A	LHFP	PTPRG	TRAPPC9
CDC7	FAM54A	LMCD1	PTPRZ1	TRIM59
CDCA2	FAM64A	LMNB1	PYCR1	TRIP13
CDCA3	FAM72A	LNP1	RACGAP1	TROAP
CDCA5	FAM72B	LOC100128191	RAD51	TTC26
CDCA7	FAM72D	LOC100288637	RAD51AP1	TTK
CDCA8	FAM83D	LOC100506711	RAD51B	TUBA1C
CDH4	FANCA	LOC100506994	RAD54B	TYW1B
CDK1	FANCB	LOC100507552	RAD54L	UBE2C
CDKAL1	FANCC	LOC100652789	RANBP17	UHRF1
CDKN3	FANCD2	LOC642846	RAPGEF4	USP13
CDON	FANCI	LOC647946	RBL1	UTP20
CDT1	FAR2	LRIG1	RECQL4	WDPCP
CENPA	FARS2	LRP8	RFC3	WDR4
CENPE	FBN2	LRRC6	RMI1	WDR62
CENPF	FBXL17	LRRIQ1	RNLS	WDR65
CENPH	FBXL7	LTBP1	ROBO1	WDR7
CENPI	FBXO43	LZTS1	ROR1	WDR76
CENPJ	FBXO5	MAD2L1	RPL22L1	WHSC1
CENPM	FGFBP1	MAGI3	RPS6KA2	WWOX
CENPN	FGGY	MAP6	RRM2	XRCC2
CENPO	FHIT	MATN3	RSRC1	XRCC4
CENPW	FIGN	MBOAT1	RUNDC2A	XYLT1
			ZNF730	ZNF367

	Up-regulated	
A4GALT	GGT6	NLRP10
ABCD1	GIPR	NR1D1
ABHD4	GJB4	NR4A1
ABLIM3	GLRX	OCLN
ACAP1	GLS2	P4HTM
ACER2	GPR172B	PAPL
ADCK3	GPR37	PCDH1
AIM1L	GPRASP1	PDE6B
AKR1B10	GPRC5A	PGPEP1
AKR1C1	GRB7	PHLDB3
AKR1C2	GREB1	PI3
ARHGAP30	GRHL3	PIDD
ARNT2	GSDMA	PLAUR
ATF3	H1F0	PLEKHG6
AVPI1	HAP1	PNLIPRP3
B3GNT3	HAPLN3	PNMAL1
BCL2L1	HBEGF	PNRC1
BCL6	HBP1	PPP1R15A

BIK	HCAR2	PPP1R3B
BIRC3	HCAR3	PRDM1
BMF	HDAC5	PRICKLE4
BNIP3L	HDAC9	ProSAPiP1
BTBD19	HEPHL1	PRSS22
BTG1	HES2	PRSS8
C11orf35	HIST1H1C	PTGS2
C11orf9	HIST1H2AC	PVRL4
C16orf5	HIST1H2BD	QPCT
C17orf103	HIST1H2BK	RAB11FIP1
C1orf51	HIST2H2BE	RASSF5
C1orf74	HIST3H2A	REEP6
C5orf41	HLA-G	RET
C9orf7	HMOX1	RGAG4
CARD18	HSD17B14	RGS16
CASP9	HSD3B7	RGS2
CCDC11	HSPB8	RHCG
CCK	ICAM1	RHPN1
CD55	ID2	RNASE7
CD68	IL1B	RND2
CD74	IL1RN	RORA
CDKN1A	IL23A	RRAD
CDKN2B	IL36RN	RRM2B
CDKN2D	IL8	RUNDC3A
CDSN	INPP5J	S100A4
CGN	IRAK2	SALL4
CHST2	IRF5	SAMD10
CITED2	IRF6	SBK1
CLCF1	ISG20	SCNN1A
CLDN1	ISYNA1	SELPLG
CLDN23	ITPKC	SEMA3B
CLDN4	KCNN4	SERPINB1
CLDN7	KCTD11	SERPINB2
CLEC2B	KIAA1257	SERTAD1
CLU	KIAA1370	SESN1
CNFN	KLHL24	SLAMF7
CRB3	KLK10	SLC46A1
CRCT1	KLK11	SLPI
CRISPLD2	KLRG2	SMOC1
CRYAB	KRT13	SPRR1B
CSF1	KRT15	SPRR3
CST6	KRT19	SQSTM1
CTSS	KRT34	SYNGR3
CYP2S1	KRT37	TCP11L2
DAPK1	KRT7	THBD
DBNDD1	KRT80	TLR2
DEFB1	LACC1	TM7SF2
DENND1C	LBH	TMEM125

DHDH	LCE1B	TMEM184A
DHRS3	LCE1C	TMEM27
DKFZp434J0226	LCN2	TMEM61
DPP4	LIF	TMPRSS13
DUSP10	LOC100133190	TNFAIP2
DYRK1B	LOC100505974	TNFRSF10C
EDA2R	LOC100506377	TNFRSF14
ENO2	LOC100506746	TOB1
ENTPD3	LOC100507429	TP53INP1
ERBB3	LOC100507452	TP53INP2
FAM131C	LOC151475	TPPP
FAM43A	LOC441869	TRAF1
FAM46A	LOC728975	TRAF3IP3
FAM84A	LYPD5	TRIM17
FAM86HP	MAP1LC3A	TSPAN10
FDXR	MCHR1	TTC9
FLJ32255	MDM2	UCA1
FLJ43663	MEG3	ULBP1
FLNC	MUC1	ULK1
FN3K	MXD1	VAMP5
FOLR3	MXD4	VNN1
FTH1	MYBPHL	VWCE
FTL	MYH16	YPEL3
FUT2	NCF2	YPEL4
FUT3	NDRG4	ZFYVE1
G0S2	NEAT1	ZNF425
GDA	NFKBIA	ZNF432
GDF15	NFKBIZ	ZNF610
GGT1	NIPAL4	ZNF702P

EXAMPLE 5

Identification of conserved UVR transcriptomic signature genes

[0077] UVR is a potent regulator of the transcriptome, but its effect on the majority of genes is often transient and diminishes with time after exposure. The time-dependent kinetic changes illustrated in Fig. 2, nevertheless, suggested that UVR might exert persistent effects on a subset of genes that might serve as UVR transcriptomic signature. We speculated that such UVR signature may persist in the progeny cells of UVR-exposed cells and may have important biomarker values in assessing UVR-induced molecular damages. To characterize the genes consisting

the UVR transcriptomic signature, we focused on DEG lists derived from 30 mJ/cm^2 UVR exposure to identify UVR-induced DEGs that were common among different keratinocyte lines (N0, N1, N2, and N6) at Days 1 and 3 after exposure. Through rigorous bioinformatics and statistical analyses, we identified 401 conserved UVR-induced DEGs that we designated as UVR transcriptomic signature (Table 6).

To test whether protein-protein interactions (PPIs) exist among these UVR signature gene products, we performed network analysis using the Pajek software (version 3.1) (Batagelj 2004) based on the known and predicted protein interactions available in the STRING database (version 10). (Szlarczyk 2015) A STRING cutoff score at 0.7 was used to select PPIs with high confidence. Altogether, we found 54 vertices (genes) and 106 edges (interactions) among the UVR signature gene products (FIG. 4). Clustering analysis using the VOS algorithm (van Eck 2010) to maximize modularity within each cluster further revealed eleven modules that were all connected among each other except the histone protein cluster (FIG. 4). Among the UVR signature genes, 13 of them showed more than five interacting neighbors (degree), also known as the hubs on the PPI network, including IL6, PTGS2, IL1B, CDKN1A, BCL2L1, ICAM1, HMOX1, VAV1, PLA2G16, MMP1, HIST1H4H, CYP4F3, and CD8A, highlighting the potentially central roles of these genes in mediating UVR responses.

Table 6. Conserved UVR signature genes in response to 30mJ/cm^2 UVR among different keratinocyte lines

ABCD1	DUSP13	KISS1	MIR23A	SCN3B
ABLIM3	ELF3	KLHL34	MIR29A	SCNN1B
ADAMTS14	ENKUR	KLK10	MIR614	SCNN1D
AGAP11	ENTPD3	KLK14	MME	SCNN1G
ALG1L	EPHB2	KLK6	MMP1	SEMA3B
ALOX5	ESM1	KPNA7	MMP3	SERPINB1
ANGPTL4	FA2H	KPRP	MSH4	SERPINB2

ANKRD20A5P	FAM110C	KRT13	MSX1	SHBG
ANKRD29	FAM115C	KRT19	MUC20	SHC2
ANKRD33	FAM167B	KRT23	MUC3A	SHC4
ANKRD56	FAM182B	KRT34	MUM1L1	SIGLEC15
APOBEC3H	FAM25A	KRT37	MYBPHL	SLAMF7
ARC	FAM46C	KRT38	MYH16	SLC22A14
ARHGAP30	FAM65C	KRT4	MYO7A	SLC25A41
ARNT2	FAM83E	KRT7	MYPN	SLC25A45
ASPRV1	FBP1	KRT78	NCCRP1	SLC40A1
ATG9B	FER1L4	KRT80	NCF4	SLC44A4
B3GNT3	FLJ34208	KRT81	NDRG4	SLC6A14
BCAN	FLJ43663	KRTAP19-1	NFE2	SLC6A20
BCL2L1	FLNC	KYNU	NKAIN4	SLC6A9
BMF	FOXA1	LBH	NKD2	SLC7A11
BMP7	FTL	LCE1A	NLGN3	SLCO2A1
C10orf10	FUT2	LCE1B	OCLN	SLPI
C14orf34	FUT3	LCE1D	OXER1	SMOC1
C15orf48	GABBR2	LCE1E	PADI1	SNORD119
C15orf52	GAD1	LCE1F	PAPL	SNX32
C17orf28	GAS7	LCE2A	PCDH1	SOD3
C17orf67	GAST	LCE3A	PCDHAC1	SPNS2
C1orf228	GCKR	LCE3D	PCDHGB8P	SPP1
C1orf68	GDA	LCE3E	PDE4C	SPRR2B
C20orf195	GDF15	LCE6A	PDE9A	SPRR2G
C2orf54	GDNF	LCN2	PDGFRA	SPRR3
C3orf25	GEM	LDB3	PIK3R5	SPRR4
C6orf15	GGT1	LEMD1	PKD2L2	STC2
C7orf10	GJB4	LGI2	PLA2G10	STRC
CAMP	GLRX	LIF	PLA2G16	STX16-NPEPL1
CAPN12	GOLT1A	LINC00086	PLA2G2F	SULT1A1
CARD18	GPR172B	LINC00303	PLA2G4C	SULT1A2
CASKIN1	GPRC5A	LOC100049716	PLAC8L1	SYNPO2L
CATSPERG	GREB1	LOC100128342	PLEKHB1	SYT5
CCDC110	GRIN3B	LOC100129617	PNLIPRP3	TCTEX1D4
CCDC62	GRIP2	LOC100130331	PNMAL1	TIMP2
CCIN	HAP1	LOC100287036	POLD4	TJP3
CD68	HCAR3	LOC100287082	POSTN	TLCD2
CD70	HIST1H1C	LOC100289251	POU4F1	TM4SF19
CD8A	HIST1H2AC	LOC100505623	PRPS1L1	TMEM125
CDH16	HIST1H2AE	LOC100505639	PRR9	TMEM22
CDKN1A	HIST1H2BC	LOC100505710	PRSS22	TMEM38A
CDKN2D	HIST1H2BD	LOC100505974	PRSS27	TMEM40
CDSN	HIST1H2BG	LOC100505994	PSCA	TMEM88
CEACAM1	HIST1H3D	LOC100506328	PSG2	TMIE
CEACAM6	HIST1H4H	LOC100506377	PSG6	TMPRSS11B
CELF5	HIST2H2BE	LOC100506411	PSG7	TMPRSS11E
CHRNA9	HIST2H2BF	LOC100506801	PTCH2	TMPRSS13
CLCF1	HLA-G	LOC100506810	PTGS2	TNFAIP2

CLDN17	HMOX1	LOC100507025	PTPN22	TNFRSF10C
CLDN23	HPGD	LOC100507065	PVRL4	TNXB
CLDN4	HRASLS	LOC100507140	RAB6B	TP53INP2
CLDN7	HSD17B14	LOC100507145	RASSF5	TREML1
CLDN9	HSD17B2	LOC100507452	REN	TRIM63
CLEC18B	HSPB8	LOC100653024	RET	TRPV3
CLEC3B	ICAM1	LOC145757	RGS16	TSPAN1
CLGN	IGFL1	LOC151475	RNASE7	TTC9
CLIC6	IGFN1	LOC152225	RNF182	UCA1
CNFN	IGSF22	LOC284080	RNF222	UPK2
CRCT1	IL13RA2	LOC284804	RNF223	USP2
CRISPLD2	IL1B	LOC285095	RNF224	USP44
CRYM	IL1RL1	LOC388282	RPLP0P2	VAV1
CSF3	IL23A	LOC440993	RPTN	VNN1
CST6	IL36B	LOC643401	RRAD	VWCE
CT62	IL6	LOC646329	RRAGD	ZEB2
CTSL3	IL8	LOC692247	RUNDC3A	ZMYND15
CYGB	ILDR1	LOC728741	S100A12	ZNF425
CYP24A1	INSC	LOC728975	S100A5	ZP4
CYP4F3	KC6	LRRC4	S100A6	ZPLD1
CYTH4	KCNG1	LYPD5	S100A7	ZSCAN1
DAPK1	KCNN4	MAP1LC3A	S100P	ZSCAN4
DEFB1	KHDC1L	MARCO	SALL4	
DHRS9	KIAA1239	MCHR1	SCARF1	
DKK4	KIAA1683	MEOX1	SCARNA16	
DPP4	KIF26A	MESP1	SCG2	

EXAMPLE 6

Similarities between UVR transcriptomic signature and human SCC signature

[0078] Compelling evidence supports that UVR is the main etiological factor in SCC pathogenesis. (Fartasch 2012) To test whether the identified UVR signature genes were dysregulated in human SCCs, we performed similar RNA-Seq analyses to generate DEGs in human SCC tumor tissues compared to matched normal skin tissues from patients with SCC tumors in the upper back or facial areas. We then performed gene set enrichment analysis (GSEA) (Subramanian 2005) between the UVR signature gene set and the SCC DEG set to determine the enrichment of the

UVR signature in the SCC signature, or vice versa. As shown in FIG. 4A and FIG. 4B, GSEA analyses revealed a significant mutual enrichment between the UVB signature and the SCC signature (p=0.006 and 0.02, respectively). When we used a SCC signature discovered by microarray-based analyses (Hudson 2010), we observed a significant enrichment between the SCC signature and our UVR signature as well (p=5.19e-05 by fisher exact test analysis), reinforcing the molecular similarities between UVR signature and SCC signature.

To test whether the identified UVR signature is specific for skin cancer, we performed additional GSEA analyses to compare the UVR signature with gene sets dysregulated in 14 other human cancer types (obtained from the TGCA RNA-Seq database). Each cancer type contained at least six pairs of matched primary tumor and normal control tissues (Table 7). Using paired t-test, we generate DEG sets specific for each cancer type using RNA-Seq data from matched primary tumor and normal tissues. Each of resulting cancer DEG set was then used in GSEA analyses to assess the mutual enrichment between the UVR signature and the respective cancer DEG set. As summarized in Table 7, there was no significant enrichment between the UVR signature and DEG sets of other cancers ($p > 0.05$) except for thyroid cancer ($p = 0.0222$, Table 7). The similarity between the UVR signature and thyroid cancer-specific gene set might be related to the fact that ionizing radiation is a significant risk factor for thyroid cancer (Boice 2005) and that UVR and other radiations may share common gene signatures involved in pathways such as DNA damage and inflammation. A recent prospective study also found a non-linear association between UVR and thyroid cancer (Lin 2012). Further studies are warranted to determine whether UVR may truly increase thyroid cancer risk.

Table 7. Summary of GSEA results between UVR signature genes and gene sets dysregulated in different human cancer derived from the TCGA database.

Cancer tissue origin	# of matched tumor/normal samples	NES of tumor gene set on UVR signature genes	NES of UVR signature genes on tumor gene set	Average NES	p-value (lower T=F)
Bladder	19	-2.96	-1.93	-2.445	0.993
Breast	110	-3.11	-1.43	-2.27	0.988
Colon	41	-1.47	-0.762	-1.116	0.868
Head & Neck	40	-1.87	-1.46	-1.665	0.952
Kidney (renal)	72	1.64	1.47	1.555	0.06
Kidney (papillary)	32	-0.999	-1.22	-1.1095	0.866
Liver	50	-3.19	-2.17	-2.68	0.996
Lung (adeno)	57	-2.54	-1.41	-1.975	0.976
Lung (Squamous)	50	-3.29	-1.96	-2.625	0.996
Prostate	52	-1.42	-1.44	-1.43	0.924
Rectal	8	-0.944	-1.08	-1.012	0.844
Stomach	29	-1.85	0.356	-0.747	0.772
Thyroid **	59	2.17	1.85	2.01	0.0222
Uterine	23	-3.35	-1.1	-2.225	0.987

NES: normalized enrichmetn score

To test the stability of the UVR transcriptomic signature over an extended period after exposure, we performed RNA-Seq on keratinocytes exposed to 30 mJ/cm^2 of UVR to generate a UVR-induced DEG list at Day 21 after exposure. Cross comparison of the UVR signature with the D21 DEG list revealed an overlap of 144 genes (FIG. 4C and Table 8) ($p < 2.2e-16$ per Fisher's exact test), suggesting that a significant portion of the UVR signature genes maintained their initial UVR responsiveness long after exposure. Similar analyses revealed that the UVR transcriptomic signature gene set were significantly enriched in two SCC-specific DEGs sets ($p < 2.2e-16$ per Fisher's exact test) (FIG. 4D and FIG. 4E), highlighting their potential as biomarkers in UVR damage assessment and skin cancer risk prediction.

Table 8. Overlapping genes between UVR transcriptomic gene set and the DEG set from 21 days after UVR exposure

ADAMTS14	LOC646329	MCHR1
ANGPTL4	HIST1H2AC	MIR23A
ANKRD20A5P	HIST1H2AE	MME
ANKRD56	HIST1H2BC	MMP1
ARHGAP30	HIST1H2BD	MMP3
ATG9B	HIST1H2BG	MYPN
BCAN	HIST1H3D	OCLN
C10orf10	HIST1H4H	PADI1
C14orf34	HIST2H2BE	PCDHAC1
C15orf52	HIST2H2BF	PKD2L2
C1orf68	HMOX1	PLAC8L1
C20orf195	HSD17B2	POSTN
C7orf10	ICAM1	PRSS22
CAPN12	IL13RA2	PSCA
CCDC62	IL1RL1	PTCH2
CD8A	IL23A	PTGS2
CEACAM1	IL6	PVRL4
CLDN4	IL8	RGS16
CLDN7	KIAA1239	RPLP0P2
CLEC18B	KLK10	RRAD
CLEC3B	KPRP	S100A12
CRCT1	KRT13	S100A7
CRYM	KRT19	SCARF1
CSF3	KRT23	SCARNA16
CST6	KRT7	SCNN1D
CT62	KRTAP19-1	SHC2
CYGB	KYNU	SHC4
DEFB1	LBH	SLAMF7
DPP4	LCE1F	SLC22A14
ENTPD3	LCE3D	SLC44A4
FER1L4	LCN2	SPNS2
FLJ43663	LEMD1	SPP1
FLNC	LGI2	STX16-NPEPL1
FUT3	LIF	SULT1A2
GAD1	LINC00086	TM4SF19
GDA	LOC100129617	TMEM88
GLRX	LOC100130331	TMPRSS11E
GOLT1A	LOC100287036	TMPRSS13
GPR172B	LOC100506377	TNXB
GRIP2	LOC100506801	TREML1
HCAR3	LOC100507025	VNN1
LOC152225	LOC100507452	

EXAMPLE 7

Role of UVR signature genes in skin cancer cell proliferation and viability

[0079] Project Achilles leverages both biological and computational analyses to identify genes that affect cancer cell survival and/or proliferation using a genome-wide shRNA library screening in over 200 cancer cell lines. (Cowley 2014) Based on the degree of depletion of a specific shRNA following infection into cancer cells, a depletion score is assigned to each shRNA. The depletion score is therefore inversely correlated with the role of its target gene in cancer cell survival based on the assumption that loss of a key cancer survival gene (as a result of RNAi triggered by its targeting shRNA) is detrimental to the infected cells. (Cowley 2104) Given that Achilles data were derived from loss-of-function analysis, we focused on 67 UVR signature genes that were up-regulated in both SCC cases and by UVR (FC > 2). 25 of the 67 genes have been validated in the Achilles database in multiple cancer cells lines. We queried the Achilles database with these 25 genes to determine which genes may play a role in skin cancer cell proliferation and/or survival. By Wilcox test, we determined that 11 out of the 25 genes had significantly lower depletion scores in skin cancer cell lines compared to other non-skin cancer lines ($p < 0.05$, Table 9), indicating that this subset of UVR signature genes may play key roles in skin carcinogenesis. The depletion scores of the shRNAs targeting these 11 genes in five skin cancer cell lines, together with the median depletion scores of the same shRNAs in non-skin cancer lines, and the p-values from Wilcox tests were summarized in Table 9. These analyses highlighted the potential of these UVR signature genes as molecular targets in future skin cancer prevention and therapeutic development.

Table 9. Summary of UVR signature genes critical for skin cancer cell survival

Genes	Skin cancer vs. other cancer lines	Skin Cancer Cell Lines (depletion score)					Other cancer lines (depletion score)
	Wilcox.test P-value	A2058	C32	COLO741	HS944T	SKMEL5	Median
SLPI	0.00141	-1.4	-1.33	-1.07	-0.875	-1.68	-0.599
KLK7	0.00468	-0.311	-0.375	-0.962	-0.706	-0.93	0.0862
KRT13	0.00621	-0.439	-0.159	-1.18	0.0826	-0.877	0.54
NHLH2	0.00933	-0.882	-1.78	-0.864	-0.98	-1.63	-0.449
GPRC5A	0.0106	-1.53	-1.78	-2.63	-1.29	-1.63	-0.963
HIST1H2BK	0.0167	-1.3	-0.579	-1.02	-1.44	-0.65	-0.361
IGFBP3	0.017	0.277	-1.22	0.332	0.677	0.286	0.765
SPOCD1	0.022	-0.833	-1.45	-0.861	-0.639	-1.21	-0.342
IFI27	0.0273	-0.0243	-2.92	-1.26	-1.13	-2.22	-0.528
KLK11	0.0286	-1.14	-1.63	-0.566	-0.914	-1.07	-0.577
TNFSF4	0.0374	-1.35	-2.3	-1.87	-1.33	-1.3	-1.17

Discussion

[0080] UVR is a potent environmental carcinogen that can cause dysregulations of thousands of genes in skin cells exposed to sub-erythema UVR doses. Despite decades of research, there is no consensus panel of molecular biomarkers available for accurate assessment of UVR damage and prediction of skin cancer risk after exposure. Gene transcription is a dynamic process, which allows cells to respond and adapt promptly to environmental or physiological cues. mRNA transcripts have been successfully used as molecular biomarkers to offer early and more accurate prediction and diagnosis of disease and disease progression and to identify individuals at risk. To address the currently unmet clinical need of sensitive methods for assessing UVR damage and skin cancer risk, we employed RNA-Seq to identify UVR-induced transcriptomic signatures to establish transcriptome-based next-generation UVR biomarker panel. By means of rigorous bioinformatics and statistical analyses, we obtained a UVR biomarker panel consisting of 401 genes whose UVR-responsiveness was conserved among different keratinocyte lines. We

further demonstrate that alterations in the mRNA expression of the UVR signature genes persisted 21 days after exposure, underscoring the stability and reliability of the identified UVR biomarker panel in future clinical applications. The UVR dose-dependent response among some of the UVR signatures genes also suggests that this novel UVR biomarker panel may offer quantitative assessments of UVR damage and stratification of individual's risk of developing skin cancer.

Different UVR target genes have been reported in previous studies. (Dawes 2014; da le Fuente 2009; Yang 2006; Rieger 2004; Dazard 2003; Takao 2002) Our UVR biomarker panel contains both previously identified UVR-responsive genes and many new UVR target genes, owing to the comprehensive coverage of the entire transcriptome by RNA-Seq compared to previous microarray-based analyses. Our comprehensive UVR experimental designs also provide detailed characterization of the UVR-responsive kinetics in the keratinocyte transcriptome (FIG. 2 and FIG. 3). An important application of the identified UVR biomarker panel is in sun screen testing, where it is expected provide better sensitivity and accuracy at the molecular level to replace the MED-based standard in determining the UVR-protective efficacy of sunscreen products to enhance preventative efforts to reduce risky UVR exposures. In addition, the significant similarity between the UVR signatures and SCC signatures suggests that the UVR biomarker panel may also facilitate clinical diagnosis and risk assessment of skin cancer in individuals following repeated sunburns or subjected to regular occupational UVR exposure. (Fartasch 2012)

[0081] Our transcriptome-based UVR biomarker panel consists of significantly more genes (401) than other biomarker panels currently used in clinical diagnosis of various diseases. (You 2015; Zanotti 2014; Gyorffy 2015) Due to the steep decreases in RNA-Seq run times and costs, profiling an individual's transcriptome

has also become a feasible clinical undertaking within a reasonable time frame. A larger biomarker panel will undoubtedly offer better coverage and accuracy in assessing UVR impact and cancer risk. To facilitate future clinical and industrial applications of the UVR biomarker panel, computational algorithms can be developed to automate transcriptomic data analysis to quantify UVR damage and generate risk scores. With more transcriptomic data being generated and incorporated into the UVR transcriptomic data sets, continuous improvement and perfection of the algorithm can be achieved to produce more accurate risk reports. In addition, skin type-specific algorithms can be developed to generate more precise UVR sensitivity and risk report. We anticipate that the UVR transcriptomic signature panel together with the ever-improving RNA-Seq and bioinformatics tools will offer sensitive and reliable next-generation diagnostic tools to help enforce effective skin cancer prevention, pinpoint individual's susceptibility to UVR, identify skin cancer early, and monitor health status and therapy success to reduce skin cancer-related illness and healthcare costs.

Second Series of Experiments

EXAMPLE 8

Introduction

[0082] Gene and environment interactions play pivotal roles in human disease pathogenesis and etiology. Skin serves as the major barrier structure between the body and the environment to protect the body from environmental stressors. Skin has also been shown to function as a peripheral neuroendocrine organ that regulates both local and global homeostasis through its melatoninergic system1,2 , steroidogenic system3 , and a peripheral equivalent of the hypothalamus–pituitary–adrenal (HPA) axis4 . The epidermis of the skin interfaces directly with the outside

environment. This strategic location makes the epidermis an ideal in vivo model organ for studying the mechanisms underlying gene and environment interactions in development and human diseases. Frequent exposure of the epidermis to environmental carcinogens greatly increases the risk and incidence of skin cancers, including both melanoma and non-melanoma skin cancers. In fact, skin cancers are the most common cancer in the United States, affecting more people than all other cancers combined5,6 , which underscores the adverse effects of direct exposure to environmental carcinogens in human health and cancer susceptibility.

[0083] Solar UV radiation (UVR) is an established environmental carcinogen in skin tumorigenesis. Excessive exposure to solar UVR, particularly its UVB component, can cause a variety of harmful effects on human skin including sunburn, photoaging, immune suppression, and increased susceptibility to cancers7,8 . The skin pigmentary system serves as the primary defense against the harmful effects of UVR9 . The secosteroids produced by epidermal keratinocytes can also protect against the DNA damaging effects of UVB radiation10 . Furthermore, UVR may alter whole-body homeostasis via activation of the skin HPA axis to increase serum levels of corticosterone11. At the molecular level, UV can exert its harmful effects via DNA damage, epigenetic lesions, and dysregulated gene expression. While each of these events may arise independently, they may also impinge on each other in response to UVR. The mutagenic effects of UV have been studied extensively and the mechanisms are relatively well characterized12–14 . In contrast, the impact of UV on the epigenome and its contribution to transcriptome regulation remain poorly understood. Recent DNA methylomics studies have provided some preliminary but interesting insights into how chronic solar UVR may contribute to skin photoaging via aberrant DNA methylation15,16 . However, repeated exposures of normal human

skin cells to low doses of UVR have no recognizable effects on global DNA methylation17 . Additional studies are needed to further elucidate the role of epigenetic mechanisms underlying the pathophysiological impact of UVR in the skin.

[0084] We and others have reported previously that acute UV exposures can cause substantial transcriptomic instability affecting thousands of genes18–20 . Our recent RNA-seq studies have generated a large cohort of UV-responsive transcriptomic data using keratinocytes from different genetic background21 . Furthermore, meta-analysis of the transcriptomic cohorts reveals that UV-induced changes in the transcription of a subset of genes are highly conserved and persistent over time21 . These findings prompt us to test whether UV may induce genetic and/or epigenetic changes to cause persistent target gene dysregulation.

[0085] In this study, we performed concurrent RNA-seq, exome-seq, and H3K27ac (histone 3 lysine 27 acetylation) ChIP-seq studies to simultaneously characterize UV-induced genetic, epigenetic, and transcriptional changes in isogenic human keratinocytes under identical UVR experimental settings. We then performed bioinformatics and statistical analyses on the resulting omics data to decipher the interactions among the genome, epigenome and transcriptome following UVR. These analyses provide new molecular insights into the complex interactions between UV and skin cells. Furthermore, comparison of the UV gene expression signature with a human squamous cell carcinoma (SCC) signature identifies several novel UV target genes for developing targeted prevention and therapy of UV-induced skin cancers.

EXAMPLE 9

Materials and Methods

Human keratinocytes, SCC tissues and adjacent normal skin tissues.

[0086] Primary human keratinocytes from a neonatal foreskin (Caucasian donor) were obtained through the Columbia University Skin Disease Research Center (SDRC) Tissue Culture Core facility as described previously20 . The SDRC routinely collects neonatal foreskins from healthy newborns through the Children's Hospital at Columbia University Medical Center (CUMC) under an IRB protocol (# AAAD6866) that was approved by the CUMC Institutional Review Board. All foreskin samples were de-identified prior to being received by researchers and designated as non-human subject research under 45 CFR Part 46. UV radiation was supplied by 4 FS20T12/UVB tubes (National Biological Corp., Beachwood, OH), which emit UV rays between 290 and 340 nm with 75% emission in the UVB, and 25% emission in the UVA spectra, with an emission peak at 313 nm wavelength20,60 . The UVR dose was measured using an IL1700 radiometer and a SED240 UVB detector (International Light, Newburyport, MA) at a distance of 27 cm from the UV source to the cell culture dishes. Cells were irradiated with 30 mJ/cm2 UVR, and then collected at 4 h or 72 h after exposure. Five pairs of primary human SCC tumors with matched adjacent normal skin tissues were collected through the Molecular Pathology Shared Resource/Tissue Bank of the Herbert Irving Comprehensive Cancer Center at CUMC under IRB protocol AAAB2667. The age, gender, and race of the patients along with information on tumor stages and surgical sites of the SCC and control skin are summarized in Supplemental Table 6.

RNA isolation and RNA-seq analysis.

[0087] Total RNA was isolated from cultured keratinocytes, primary SCC tumors or adjacent normal skin tissues using the RNeasy Kit (QIAGEN, Gaithersburg, MD). All RNA samples were subsequently analyzed using an RNA 6000 nano chip (Agilent Technologies, Wilmington, DE) to confirm that the RNA

integrity index was 8.0 or above. Total RNA (500 ng) from each sample was subjected to poly-A pull-down to enrich mRNAs for library preparation by using Illumina TruSeq RNA prep kit (Illumina, San Diego, CA). The resulting libraries were sequenced using Illumina HiSeq2000 at Columbia Genome Center. Sequencing reads were mapped to the human reference genome (NCBI/build37.2) using Tophat (version 2.0.4). Differentially gene expression (DGE) between irradiated and non-irradiated keratinocytes were determined using the DESeq software package61 , with a fold change (FC) cutoff set at >2 or <0.5.

H3K27ac ChIP-seq analysis.

[0088] For ChIP-seq studies, cells were fixed with 1% (final concentration) freshly prepared formaldehyde at 37 °C for 15 min. The fixation was stopped by incubation in 125 mM (final concentration) glycine solution for 5 min at RT. Cells were washed with PBS containing proteinase inhibitor cocktail (1x final concentration), scraped and collected as cell pellets in Eppendorf tubes. Subsequent ChIP assays and sequencing were performed by Active Motif using the H3K27ac HistonePath™ Kit following standard protocols (Active Motif, Carlsbad, CA). The 75-nt sequence reads generated by Illumina sequencing were mapped to the human reference genome hg19 using the BWA algorithm with default settings. Duplicate reads were removed, and the number of aligned reads ("tags") was adjusted to 24.2 million for each sample (by down sampling the larger data sets). These normalized tag files were used in all downstream analysis. ChIP-seq tags were extended at their 3'-ends to 200 bp. We used the model-based analysis of ChIP-seq (MACS) algorithm for peak calling to identify chromatin regions with H3K27ac tags compared to the input control33. Using a p-value cutoff at 1e-7, approximately 38,000 to 40,500 peaks were identified for each sample. Genes were annotated if the distance

between peak-interval and gene body-interval was within 10 kb. MACS peaks (excluding promoter peaks) were used as "constituent enhancers" input into the ROSE (Rank Ordering of Super Enhancers) software to identify super enhancers (SEs). Default settings were used for the stitching (12.5 kb distance). Genes were annotated to be associated with SEs if they were within 25 kb upstream or downstream of a SE. To identify UV-induced enrichment of transcription factor (TF) motifs, we used the HOMER software for motif analysis by comparing the enhancer regions from the irradiated sample with those from the control sample.

Whole exome-seq (WES) analysis.

[0089] Genomic DNA was isolated from UV-irradiated and control samples using the Wizard Genomic DNA Purification Kit (Promega). WES was performed at the Columbia Genome Center following standard Illumina TruSeq multiplexing protocol to generate targeted number of reads with more than 85% coverage of the targeted regions by = 15 reads and 90% covered by = 10 reads. The resulting reads were mapped to the human reference genome hg19 using the BWA algorithm with default settings. Mapped reads were sorted and indexed using the Samtools program. Duplicate reads were marked using Picard-tools. UV-induced somatic mutations between the paired UV-4h vs. control or UV-72h vs. control were called using Samtools mpileup and bcftools with default settings. Variants with fewer than 10 reads depth were discarded from the analysis.

Identification of UV target genes in skin carcinogenesis in the Achilles database.

[0090] To identify UV target genes that are critical to skin cancer cell proliferation or survival, we queried the Achilles database with genes that were upregulated by UV. A gene was considered essential to skin cancer cell survival if

their corresponding shRNAs became depleted after 40 days or 16 population doublings following shRNA infection40. We downloaded the raw normalized shRNA depletion score (DS) (Normalized shRNA value = log2 [(Raw read value for shRNA)/(Total raw read value for Replicate) × 1e6] + 1) from the Achilles database. We normalized each shRNA DS by subtracting the median DS of the negative control shRNAs, including luciferase, GFP, RFP, and LacZ in the same sample. We then performed Wilcoxon tests to compare the distribution of DS among the shRNAs targeting the same gene to the distribution of the pairwise DS of all shRNAs (the null model). If the DS of shRNAs targeting the same gene was significantly similar when compared to that of the null model ($p < 0.1$), we took the median DS of these shRNAs in the replicate samples as the gene-level DS for every cell line. Finally, we used the Wilcoxon test to identify genes whose DS was significantly lower in skin cancer cells than non-skin cancer cells ($p < 0.05$), which were considered as skin cancer-specific cancer genes. All statistical analyses were performed using the R software package.

Immunofluorescence staining.

[0091] Primary antibodies were purchased from Abcam (SLAMF7, ab202840) or One World Lab (PTGS2, TA805307_OWL; CYP24A1: 52761_OWL; GJA5: 5361_OWL). Immunofluorescence staining was performed as we previously reported62 . Briefly, cultured cells on glass coverslips or frozen tissue sections (8 μ M thickness) were fixed in 4% paraformaldehyde for 10 min or in cold acetone for 20 min. Fixed cells or tissue sections were then washed 3 times with PBS and then incubated with blocking buffer (0.1% Triton X-100 and 10% normal serum in PBS) for 1 h before being incubated with primary antibodies overnight at 4°C in a humidified chamber. After 3 consecutive 5-min washes with PBS, cells or tissue sections were

incubated with secondary antibodies for 1 h before being washed with PBS and mounted with gelvatol mounting media containing 4,6-diamidino-2-phenylindole dihydrochloride (DAPI). Images were acquired using a fluorescence confocal microscope (Zeiss, Thornwood, NY, USA).

Statistics.

[0092] Statistical analysis of each omics data set between UV-irradiated and non-irradiated keratinocytes was performed using methods included in each software package as described above. A false discovery rate <0.05 wa s used to control for false discoveries. The gene depletion scores between skin cancer cells and non-skin cancer cells were compared using Wilcoxon tests (R software package) and $p < 0.05$ was considered significant.

EXAMPLE 10

Multi-omics analysis of UV-induced molecular abnormalities

[0093] The mutagenic and transcriptional effects of UV have been studied extensively in the past, but relatively few studies have investigated the impact of UV on the epigenome. H3K27ac is an epigenetic mark that is frequently present at promoters or enhancers, which also separates active enhancers from poised enhancers22–24 . To test whether UV-induced differential gene expression (DGE) may be functionally linked with differential H3K27 acetylation (DHA), we performed parallel RNAseq and ChIP-seq studies to profile global DGE and DHA in UV-irradiated human keratinocytes. As shown in FIG. 6A, UV induced substantial transcriptomic changes as highlighted in the DGE plots by red or blue dots (representing significant DGEs, $p < 0.05$). Similarly, ChIP-seq analysis revealed that UV caused a genome-wide loss of H3K27ac with regional gains in H3K27ac levels (FIG. 6B, slope value <1). T o isolate genes associated with DHA, we calculated the

FC between the average peak value of H3K27ac peaks assigned to a specific gene (within 10 kb of the start or end of a nearby gene) in the UV-irradiated sample and that in the control sample. DHA was defined using a FC cutoff at 2. Altogether, we obtained 1,041 DHA genes at 4 h and 2,508 DHA genes at 72 h following UVR, suggesting a progressive genome-wide redistribution of H3K27ac marks. Genes with significant changes in both mRNA expression (DGE) and H3K27ac (DHA) are highlighted in blue in the DGE plots in FIG 6A.

[0094] In addition to DGE and DHA analyses, we performed concurrent WES studies using cells from the same experiment. Mutation calling using the Samtools program identified 463 and 417 single nucleotide variations (SNVs) at 4 h and 72 h (FIG. 6C, and Supplementary Tables 1 and 2), respectively, revealing a relatively moderate mutagenic effect compared to the substantial changes in global gene expression and H3K27ac in response to UVR. There were 75 common SNVs between the 4 h and 72 h mutation profiles, with 54 of them mapped within or near genes (26 in introns, 15 in exons, 2 in the 3'-UTR, 9 in the 5'-UTR, 2 in 1 kb upstream, Supplementary Table 3), and 21 in intergenic regions. Genomic distribution of UV-induced SNVs is schematically illustrated in FIG. 6D. Overall, SNVs mostly occurred in introns and intergenic regions, followed by exons, 5'-UTR, 3'-UTR, and 1 kb upstream or downstream of the genes.

[0095] Accumulating evidence supports the role of introns in regulating gene expression through cis-acting elements25–27. The predominant distribution of SNVs in introns and intergenic regions indicated that UV-induced mutations might alter gene activities transcriptionally. Indeed, GSEA analysis revealed that genes with intronic mutations were significantly enriched in the DGE list at 72 h after exposure ($p = 0.001$, FIG.6E, left panel). Among them, CYP24A1 was dramatically upregulated

by UVR (Log2FC = 7). CYP24A1 is an enzyme that can metabolize vitamin D3 to generate biologically active hydroxyderivatives with effcient anti-tumorigenic activities on melanoma cells. Elevated levels of CYP24A1 are associated with increased aggressiveness and proliferative potential of colorectal and prostate tumors28,29 . Besides the effect of intronic mutation on gene expression, GSEA also revealed a significant overlap between genes with intronic mutations and genes showing reduced H3K27ac marks (p = 2.6e-06, FIG. 6E, right panel), consistent with the accumulating evidence supporting the role of chromatin conformation in modulating DNA repair activity during UV-induced mutagenesis14,30 .

EXAMPLE 11

UV induced dynamic reorganization of super enhancers (SEs).

[0096] SEs are large clusters of enhancers that regulate the activity of key genes during development and disease pathogenesis31,32 . H3K27ac is one of the best characterized epigenetic marks for mapping genome-wide SE structures33,34 . To test whether UVR may alter SEs to modulate its target gene activities, we used the ROSE algorithm to map SEs in both control and UV-irradiated keratinocytes. We sorted the enhancer regions based on their H3K27ac signals from the lowest to the highest. Enhancers whose signals were higher than the transition point of the curve (FIG. 7A) were designated as SEs. A total of 1,342 SEs were identified in control keratinocytes. Following UV irradiation, the total number of SEs decreased to 1,223, and 1,209 SEs at 4 h and 72 h after exposure, respectively (FIG. 7A), revealing a net loss of SEs following UVR. Venn diagram in FIG. 7B illustrates that UV induced 214 unique SEs at 4 h, and 294 unique SEs at 72 h after UV exposure, with 77 UV-specific SEs conserved between the 4 h and 72 h SE sets. The majority of the SEs in non-irradiated cells (814 out of 1,342), however, remained intact after UVR.

Separate analyses further revealed that UVR also decreased global H3K27ac signals at promoter regions (FIG. 7C).

[0097] Next, we isolated genes associated with either the common SEs or UV-induced SEs as indicated in FIG. 7B. We used the ToppGene Suite program to identify top biological pathways in which each group of SE-associated genes were enriched. As summarized in Table 10, many of the SE-associated genes play important roles in tumorigenesis. The common SE-associated genes were enriched in integrin-dependent signaling pathways, which are essential in epidermal development and homeostasis35,36 . In contrast, genes associated with UV-induced SEs were enriched in cancer-, DNA damage-, and endocytosis-related pathways (Table 10). Examples of UV-induced changes in SEs are shown in Table 10, where UV reduced H3K27ac signal of the SE associated with PHACTR3 but increased H3K27ac signal of the SE associated with TMPRSS11B. DNA hypermethylation of PHACTR3 is frequently observed in HPV-induced immortalization of keratinocytes and in human cancers37,38 , highlighting the importance of epigenetic regulation of its activity in human diseases.

Table 10. Top biological pathways and relevant disease pathways in which the conserved SE-associated genes or UV-induced SE-associated genes are enriched. P-values were obtained using the hypergeometric distribution test to examine the overlap between the identified gene sets and the known pathways. Bonferroni correction was used to have adjusted p-values.

Conserved SE-associated genes		
Biological pathway	p-Value	Bonferroni
α9β1 integrin signaling	3.868E-10	8.588E-7
Integrin signaling pathway	6.781E-10	1.503E-6
α6β4 integrin signaling pathway	8.588E-10	1.903E-6
Regulation of actin cytoskeleton	7.360E-9	1.636E-5
Focal adhesion	2.159E-7	4.803E-4
Disease relevance	**p-Value**	**Bonferroni**
Tumor Progression	8.246E-21	5.308E-17
Mammary Neoplasms	9.642E-17	6.333E-13
Malignant neoplasm of lymph node	3.622E-15	2.331E-11
Non-Small Cell Lung Carcinoma	4.468E-15	2.874E-11
Ovarian Carcinoma	6.162E-15	3.965E-11

UV-induced SE-associated genes		
Biological pathway	p-Value	Bonferroni
Pathways in cancer	7.319E-7	1.273E-3
Androgen receptor signaling pathway	1.323E-6	2.301E-2
FOXM1 transcription factor network	1.818E-6	3.158E-2
DNA damage response (only ATM dependent)	9.398E-6	1.634E-1
Endocytosis	1.522E-4	2.647E-1
Disease relevance	**p-Value**	**Bonferroni**
Leukemia	1.023E-12	4.460E-9
Tumor Progression	4.283E-12	1.867E-8
Glioblastoma	8.107E-10	3.534E-6
Malignant neoplasm of pancreas	5.226E-9	2.278E-5
Pancreatic carcinoma	1.252E-8	5.458E-5

EXAMPLE 12

Functional associations between global H3K27ac and gene expression regulation.

[0098] To test the impact of H3K27ac redistribution on transcriptome dysregulation following UVR, we divided DHA gene set and DGE gene set into three groups based on their respective Log2FC values, including Log2FC > 1, Log2FC < -1, or - 1 < Log2FC < 1 (which was considered less or non-responsive to UVR). We plotted UV-induced DGE set against DHA set at 4 h or 72 h using the R software package. As shown in FIG. 8A, we found significant correlations between genes showing increased H3K27ac (Log2FC > 1) and upregulated expression at both 4 h and 72 h after UVR. In contrast, significant correlations existed between decreased H3K27ac (Log2FC < - 1) and reduced gene expression only at 72 h but not 4 h after UVR, suggesting a time-dependent effect on H3K27ac change on gene expression regulation. Representative genes with concordant changes in gene expression and H3K27ac are shown in FIG. 8B. Genome-wide associations between H3K27ac and gene expression of UV target genes are summarized in FIG. 8C, where positive

correlations are highlighted in pink and inverse correlations are highlighted in green. The majority of the UV-responsive genes displayed discordant changes in H3K27ac and expression regulation. DAVID Pathway analysis of the UV target genes using the DAVID program identified top-ranked UV-responsive pathways including keratinocyte differentiation, epithelial cell differentiation, calcium-independent cell-cell adhesion, and epidermal development (FIG. 8D). A parallel H3K27ac analysis of the genes involved in these pathways demonstrated, however, the regulation of their gene expression was largely independent of H3K27ac changes, suggesting that other transcription regulatory mechanisms were involved to alter UV target gene expression.

EXAMPLE 13

UV-responsive TF motifs and target genes in skin cancer cell growth and survival.

[0099] Previous chromatin accessibility analysis shows that UV can induce genome-wide chromatin compaction39 , which coincides with the global loss of H3K27ac after UVR. To test whether UVR-induced changes in chromatin accessibility may occur at TF binding sites, we performed TF motif analysis focusing on H3K27 DHA regions using the HOMER algorithm. We found a significant enrichment of multiple TF motifs occurred at UV-induced DHA regions (FIG. 9A), suggesting that binding of these TFs was modulated by UVR. The majority of the identified UV-responsive TFs, such as JUN, TP53 and FOSIL1, showed moderate changes in their mRNA levels (FIG. 9B). They may contribute to the differential expression of UV target genes through chromatin accessibility changes after UVR.

[00100] Project Achilles focuses on identifying genetic vulnerabilities and generating high quality gene essentiality datasets and rigorous analytical tools. The

Achilles database consists of experimental data on the function of selected genes in cancer cell growth and/or survival based on genome-wide shRNA screenings studies40 . To test the role of UV-responsive TFs in skin carcinogenesis, we queried the Achilles database for experimental evidence on which TFs are critical to skin cancer cell growth and survival. As shown in FIG. 9C, shRNA-mediated knockdown of 6 UV-responsive TFs were significantly more toxic for cutaneous melanoma cells (A2058, C32, HS944T, SKMEL5) than other types of cancer cells ($p < 0.05$). Similarly, we queried the Achilles database to test the role of UV target genes in skin cancer growth and survival. We found multiple UV target genes to be critical to the survival of skin cancer cells, including CD200, GJA5, GPR115, KLK7, SLAMF7 and SLP1 (FIG. 9D). Given the lack of RNA-seq data on cutaneous SCCs in The Cancer Genome Atlas (TCGA), we performed RNA-seq studies on 5 pairs of cutaneous SCC tumors and matched adjacent normal skins to generate a SCC-specific DGE cohort containing genes that were dysregulated in SCCs. We then queried this SCC DGE cohort to determine the expression of the UV-responsive TF genes and UV target genes shown in FIG. 9C and FIG. 9D. As illustrated in FIG. 9E, many of these TF genes and UV target genes displayed individual variations in their DGE status among the SCC patients. SLAMF7, ARNTL, ETV1, and GPR115 were consistently upregulated in SCCs and in response to UVR, whereas GJA5 was frequently down-regulated in SCCs but upregulated by UVR in keratinocytes.

EXAMPLE 14

Validation of selected UV target genes in human SCCs.

[00101] Comparison of the UV gene expression signature derived in keratinocytes with the SCC signature revealed numerous UV target genes to be consistently dysregulated in human SCCs. mRNA expression changes of selected

UV target genes in SCCs relative to matched normal tissues are shown in FIG. 10A. ChIP-seq profiles at these selected gene loci demonstrated that UV induced pronounced increases in H3K27ac 72 h after UVR (FIG. 10B), consistent with the upregulation of their mRNA expression by UVR. By immunofluorescence staining, we confirmed that protein expression of SLAMF7, GJA5, CYP24A1 and PTGS2 were all elevated in UV-irradiated keratinocytes (FIG. 10C). PTGS2 is a well-characterized UV target gene that is frequently upregulated in skin carcinogenesis41,42 . Next, we performed immunofluorescence staining to compare the protein expression of the UV target genes between SCC tumors and normal skins. We found that PTGS2, SLAMF7, and CYP24A1 protein levels were elevated in human SCC tissues, but GJA5 was decreased in SCCs (FIG. 10D). SLAMF7 is an established therapeutic target for multiple myeloma, and a monoclonal antibody (elotuzumab) targeting SLAMF7 can activate natural killer cells to selectively kill myeloma cells43. The GJA5 protein is a component of gap junctions. The biological significance of its inverse regulation by UVR and in SCCs awaits further investigations. CYP24A1 mRNA expression is elevated in multiple malignancies. In addition to the UV-induced mutation in CYP24A1 intron, increased H3K27ac may also contribute to its aberrant upregulation in skin SCC.

Discussion

[00102] Elucidating the complex molecular mechanisms underlying UV-gene interaction will offer new insights into how UVR modulates skin homeostasis and disease pathogenesis to help improve the prevention of UV-induced skin diseases. Our study represents the first concurrent multi-omics analysis of UV interactions with the genome, epigenome and transcriptome using isogenic cells from the same UV experiment, which minimizes genetic and experimental variations. While our analysis

reveals a positive functional correlation between DHA and DGE among a subset of UV target genes, the majority of the UV target genes display discordant changes or, in some cases, inverse correlations between DHA and DGE after UVR, suggesting that H3K27ac alone is insufficient to predict gene expression. UV may cause other epigenetic changes such as DNA methylation and differential histone modifications to dynamically modulate its target gene activity. In this study, we focused on H3K27ac mainly because it is one of the best-characterized epigenetic marks associated with active enhancer and promoter regions22,44 . The open chromatin regions marked by H3K27ac may be indicative of frequent binding of transcription factors. The ultimate outcome of gene expression regulation may be co-determined by a combination of other histone modifications including acetylation of H3K9 and H3K18 45,46 , or methylation of H3K4me1/3, H3K9me3,

H3K27me3 that are linked with either active or poised enhancers and promoters23,47,48 . The diverse repertoire of histone modifications together with their interacting regulatory proteins underscore the importance and need of systematic omics-based studies to better understand the mechanisms underpinning UV-gene interactions in skin disease pathogenesis.

[00103] UV irradiation is a primary risk factor for both melanoma and non-melanoma skin cancers49,50 . Excessive exposure to solar UVR can cause cumulative genetic and epigenetic damages that disrupt gene expression preceding malignant transformation in sun-exposed skin areas. We have validated that some of the novel UV target genes discovered by our RNA-seq studies are dysregulated in human SCCs, which may also have important implications for melanomagenesis. CYP24A1, for example, is an enzyme that can metabolize vitamin D3 to generate biologically active hydroxyderivatives of 20(OH)D3, which possesses effcient anti-

tumorigenic activities on melanoma cells51 . Paradoxically, elevated levels of CYP24A1 have been reported in melanocytic nevi and early stage melanomas, highlighting the complex role of CYP24A1 in skin tumorigenesis52 . SLAMF7 is a receptor present on immune cells including natural killer (NK) cells that mediates inhibition of NK cells in the absence of EAT-2. Elotuzumab, a monoclonal antibody targeting SLAMF7, has been approved recently as an immunotherapy agent for treating multiple myeloma43 . SLAMF7 expression is undetectable in normal skin. SLAMF7 mRNA and protein levels are elevated in a subset of human melanoma tissues (data from The Cancer Genome Atlas and The Human Protein Atlas), making SLAMF7 an attractive immunotherapeutic target in for treating SLAMF7-positive melanoma patients. UV-induced epigenetic effects via H3K27ac may persist in UV-irradiated cells and contribute to the malignant transformation of UV-damaged cells over time. While regional gains of H3K27ac occur following UVR, UV induces progressive global losses of H3K27ac that are especially pronounced at 72 h after exposure. The genomewide loss of H3K27ac may be due to suppressed HATs activities53 , while the regional gain in H3K27ac may occur due to the binding of UV-responsive TFs such as JUN/FOS or TP53 that in turn recruits HATs to their target regions. A survey of mRNA expression of 17 histone acetyltransferases (HATs) and 18 histone deacetylases (HDACs) based on the RNA-seq results reveals an initial downregulation of HAT members (CLOCK, KAT6, KAT7 and NCOAs) and HDAC members (HDAC4, HDAC7, HDAC9, SIRT1) at 4 h after UVR (Supplemental Table 2). By 72 h, however, there are no pronounced changes in mRNA levels of either HATs or HDACs except a 2.9-fold increase in SIRT4 (Supplemental Table 4). SEs are crucial regions of the genome consisting of clusters of enhancer elements that are enriched in H3K27ac and TFs. Despite the dynamic

H3K27ac redistribution, the amount of SEs defined by H3K27ac signal peaks following UVR remains relatively stable. Pathway analyses of genes associated with common SEs in control and UV-irradiated keratinocytes reveal a significant enrichment of genes in epidermal development and function. In contrast, genes associated with UV-induced SEs are enriched in pathways of DNA damage response (CDKN1B, TP73, CDC42), consistent with the proposed function of SEs in the regulation of cell identity and state54 .

[00104] Our concurrent omics analyses also show that the mutagenic effect of UV is relatively moderate compared to the extensive epigenomic and transcriptomic changes affecting thousands of genes. While WES is primarily used to identify mutations in coding regions, WES also generates high-quality sequence reads from noncoding regions including introns, UTRs, and intergenic regions55,56 . Our study reveals that approximately 13% of UV-induced SNVs are located in exons, whereas the rest are found in introns or intergenic regions. While mutations in protein-coding regions have been the primary focus in disease research, there are growing interests in understanding

the role of non-coding mutations after multiple studies demonstrating that the overwhelming majority of mutations, both somatic and germline, occur in non-coding portions of the genome. Our GSEA analysis identifies a significant correlation between UV-induced intron mutations with both DGE and H3K27ac DHA, indicating that intron mutations may interact with the epigenetic machinery in gene regulation. The C to G mutation at the Chr20:52789743 site in the CYP24A1 intron is within a region containing the binding sites of multiple chromatin modifiers such as EZH2, RBBP5, and USF1, highlighting the potential role of this CYP24A1 mutation in its expression regulation.

Our WES analysis demonstrates that C > T/G > A are the most common UV-induced SNVs (Supplemental Table 5), consistent with the UV signature mutation as seen in skin cancers57–59 . The percentage of C > T mutations identified in our WES analysis, however, is lower than the percentage observed in skin cancers. The discrepancy may be due to that the mutation profile discovered in our study represents the effect of one single UV exposure event, whereas the mutation profiles in skin tumors reflect long-term cumulative effects of UV exposures. In support of this possibility, the UV-induced mutation profile in our study is highly similar to the one observed in mouse melanomas that are induced by one single neonatal UV exposure57 .

[00105] In summary, our concurrent multi-omics studies provide new insights into the complex molecular mechanisms underlying UV photobiological effects, which have important implications in understanding its impact on skin homeostasis and disease pathogenesis. Our analysis also identified several new UV target genes, including CYP24A1 and SLAMF7, which are aberrantly expressed in human SCCs. The new UV target genes and UV-responsive TFs that we have identified have important clinical implications in skin carcinogenesis, making them attractive targets for developing novel approaches for skin cancer prevention and treatment.

REFERENCES

Afaq, F., Adhami, V. M. & Mukhtar, H. Photochemoprevention of ultraviolet B signaling and photocarcinogenesis. Mutation research 571, 153–173, doi: 10.1016/j.mrfmmm.2004.07.019 (2005).

Anders, S. & Huber, W. Differential expression analysis for sequence count data. Genome biology 11, R106, doi: 10.1186/gb-2010-11-10-r106 (2010).

Anders, S., and Huber, W. (2010) Differential expression analysis for sequence count data. Genome biology 11, R106

Aubin, F. Mechanisms involved in ultraviolet light-induced immunosuppression. European journal of dermatology: EJD 13, 515–523 (2003).

Batagelj, V., and Mrvar, A. (2004) Pajek - Analysis and visualization of large networks. Math Visual, 77-103

Bens, G. (2014) Sunscreens. Advances in experimental medicine and biology 810, 429-463

Besaratinia, A. et al. Wavelength dependence of ultraviolet radiation-induced DNA damage as determined by laser irradiation suggests that cyclobutane pyrimidine dimers are the principal DNA lesions produced by terrestrial sunlight. FASEB journal: official publication of the Federation of American Societies for Experimental Biology 25, 3079–3091, doi: 10.1096/fj.11-187336 (2011).

Boice, J. D., Jr. (2005) Radiation-induced thyroid cancer--what's new? Journal of the National Cancer Institute 97, 703-705

Bonn, S. et al. Tissue-specific analysis of chromatin state identifies temporal signatures of enhancer activity during embryonic development. Nature genetics 44, 148–156, doi: 10.1038/ng.1064 (2012).

Brash, D. E. UV signature mutations. Photochemistry and photobiology 91, 15–26, doi: 10.1111/php.12377 (2015).

Brozyna, A. A. et al. CYP24A1 expression inversely correlates with melanoma progression: clinic-pathological studies. International journal of molecular sciences 15, 19000–19017, doi: 10.3390/ijms151019000 (2014).

Calo, E. & Wysocka, J. Modification of enhancer chromatin: what, how, and why? Molecular cell 49, 825–837, doi: 10.1016/j.molcel.2013.01.038 (2013).

Cowley, G. S. et al. Parallel genome-scale loss of function screens in 216 cancer cell lines for the identification of context-specific genetic dependencies. Scientific data 1, 140035, doi: 10.1038/sdata.2014.35 (2014).

Cowley, G. S., Weir, B. A., Vazquez, F., Tamayo, P., Scott, J. A., Rusin, S., East-Seletsky, A., Ali, L. D., Gerath, W. F., Pantel, S. E., Lizotte, P. H., Jiang, G., Hsiao, J., Tsherniak, A., Dwinell, E., Aoyama, S., Okamoto, M., Harrington, W., Gelfand, E., Green, T. M., Tomko, M. J., Gopal, S., Wong, T. C., Li, H., Howell, S., Stransky, N., Liefeld, T., Jang, D., Bistline, J., Hill Meyers, B., Armstrong, S. A., Anderson, K. C., Stegmaier, K., Reich, M., Pellman, D., Boehm, J. S., Mesirov, J. P., Golub, T. R., Root, D. E., and Hahn, W. C. (2014) Parallel genome-scale loss of function screens in 216 cancer cell lines for the identification of context-specific genetic dependencies. Scientific data 1, 140035

Creyghton, M. P. et al. Histone H3K27ac separates active from poised enhancers and predicts developmental state. Proceedings of the National Academy of Sciences of the United States of America 107, 21931–21936, doi: 10.1073/pnas.1016071107 (2010).

Dawes, J. M. et al. Genome-wide transcriptional profiling of skin and dorsal root ganglia after ultraviolet-B-induced inflammation. PloS one 9, e93338, doi: 10.1371/journal.pone.0093338 (2014).

Dawes, J. M., Antunes-Martins, A., Perkins, J. R., Paterson, K. J., Sisignano, M., Schmid, R., Rust, W., Hildebrandt, T., Geisslinger, G., Orengo, C., Bennett, D. L., and McMahon, S. B. (2014) Genome-wide transcriptional profiling of skin

and dorsal root ganglia after ultraviolet-B-induced inflammation. PloS one 9, e93338

Dazard, J. E., Gal, H., Amariglio, N., Rechavi, G., Domany, E., and Givol, D. (2003) Genome-wide comparison of human keratinocyte and squamous cell carcinoma responses to UVB irradiation: implications for skin and epithelial cancer. Oncogene 22, 2993-3006

de la Fuente, H., Lamana, A., Mittelbrunn, M., Perez-Gala, S., Gonzalez, S., Garcia-Diez, A., Vega, M., and Sanchez-Madrid, F. (2009) Identification of genes responsive to solar simulated UV radiation in human monocyte-derived dendritic cells. PloS one 4, e6735

Dennis, L. K., Beane Freeman, L. E., and VanBeek, M. J. (2003) Sunscreen use and the risk for melanoma: a quantitative review. Annals of internal medicine 139, 966-978

Djebali, S. et al. Landscape of transcription in human cells. Nature 489, 101–108, doi: 10.1038/nature11233 (2012).

Elbediwy, A. et al. Integrin signalling regulates YAP and TAZ to control skin homeostasis. Development 143, 1674–1687, doi: 10.1242/dev.133728 (2016).

Ernst, J. et al. Mapping and analysis of chromatin state dynamics in nine human cell types. Nature 473, 43–49, doi: 10.1038/nature09906 (2011).

Fartasch, M., Diepgen, T. L., Schmitt, J., and Drexler, H. (2012) The Relationship Between Occupational Sun Exposure and Non-Melanoma Skin Cancer. Dtsch Arztebl Int 109, 715-U714

Gronniger, E. et al. Aging and chronic sun exposure cause distinct epigenetic changes in human skin. PLoS genetics 6, e1000971, doi: 10.1371/journal.pgen.1000971 (2010).

Guo, Y. et al. Exome sequencing generates high quality data in non-target regions. BMC genomics 13, 194, doi: 10.1186/1471-2164-13-194 (2012).

Guy, G. P., Jr., Machlin, S. R., Ekwueme, D. U., and Yabroff, K. R. (2015) Prevalence and costs of skin cancer treatment in the U.S., 2002-2006 and 2007-2011. American journal of preventive medicine 48, 183-187

Gyorffy, B., Hatzis, C., Sanft, T., Hofstatter, E., Aktas, B., and Pusztai, L. (2015) Multigene prognostic tests in breast cancer: past, present, future. Breast cancer research : BCR 17, 11

Hacker, E., Boyce, Z., Kimlin, M. G., Wockner, L., Pollak, T., Vaartjes, S. A., Hayward, N. K., and Whiteman, D. C. (2013) The effect of MC1R variants and sunscreen on the response of human melanocytes in vivo to ultraviolet radiation and implications for melanoma. Pigment cell & melanoma research 26, 835-844

Heckman, C. J., Chandler, R., Kloss, J. D., Benson, A., Rooney, D., Munshi, T., Darlow, S. D., Perlis, C., Manne, S. L., and Oslin, D. W. (2013) Minimal Erythema Dose (MED) testing. Journal of visualized experiments : JoVE, e50175

Heintzman, N. D. et al. Distinct and predictive chromatin signatures of transcriptional promoters and enhancers in the human genome. Nature genetics 39, 311–318, doi: 10.1038/ng1966 (2007).

Hnisz, D. et al. Super-enhancers in the control of cell identity and disease. Cell 155, 934–947, doi: 10.1016/j.cell.2013.09.053 (2013).

Hobaus, J. et al. Impact of CYP24A1 overexpression on growth of colorectal tumour xenografts in mice fed with vitamin D and soy. International journal of cancer. Journal international du cancer 138, 440–450, doi: 10.1002/ijc.29717 (2016).

Hubers, A. J. et al. DNA hypermethylation analysis in sputum for the diagnosis of lung cancer: training validation set approach. British journal of cancer 112, 1105–1113, doi: 10.1038/bjc.2014.636 (2015).

Hudson, L. G., Gale, J. M., Padilla, R. S., Pickett, G., Alexander, B. E., Wang, J., and Kusewitt, D. F. (2010) Microarray analysis of cutaneous squamous cell carcinomas reveals enhanced expression of epidermal differentiation complex genes. Molecular carcinogenesis 49, 619-629

Kadekaro, A. L. et al. Melanocortin 1 receptor genotype: an important determinant of the damage response of melanocytes to ultraviolet radiation. FASEB journal: official publication of the Federation of American Societies for Experimental Biology 24, 3850–3860, doi: 10.1096/fj.10-158485 (2010).

Khurana, E. et al. Role of non-coding sequence variants in cancer. Nature reviews. Genetics 17, 93–108, doi: 10.1038/nrg.2015.17 (2016).

Konger, R. L., Martel, K. C., Jernigan, D., Zhang, Q. & Travers, J. B. The peroxisome proliferator-activated receptor gamma system regulates ultraviolet B-induced prostaglandin e(2) production in human epidermal keratinocytes. PPAR research 2010, 467053, doi: 10.1155/2010/467053 (2010).

Lahtz, C. et al. UVB irradiation does not directly induce detectable changes of DNA methylation in human keratinocytes. F1000Research 2, 45, doi: 10.12688/f1000research.2-45.v1 (2013).

Lautenschlager, S., Wulf, H. C., and Pittelkow, M. R. (2007) Photoprotection. Lancet 370, 528-537

Lin, S. W., Wheeler, D. C., Park, Y., Cahoon, E. K., Hollenbeck, A. R., Freedman, D. M., and Abnet, C. C. (2012) Prospective study of ultraviolet radiation exposure

and risk of cancer in the United States. International journal of cancer. Journal international du cancer 131, E1015-1023

Liu, L. et al. Hairless is a histone H3K9 demethylase. FASEB journal: offcial publication of the Federation of American Societies for Experimental Biology 28, 1534–1542, doi: 10.1096/fj.13-237677 (2014).

Loven, J. et al. Selective inhibition of tumor oncogenes by disruption of super-enhancers. Cell 153, 320–334, doi: 10.1016/j.cell.2013.03.036 (2013).

Mao, P., Smerdon, M. J., Roberts, S. A. & Wyrick, J. J. Chromosomal landscape of UV damage formation and repair at single nucleotide resolution. Proceedings of the National Academy of Sciences of the United States of America 113, 9057–9062, doi: 10.1073/pnas.1606667113 (2016).

Mukhopadhyay, P., Ferguson, B., Muller, H. K., Handoko, H. Y. & Walker, G. J. Murine melanomas accelerated by a single UVR exposure carry photoproduct footprints but lack UV signature C > T mutations in critical genes. Oncogene 35, 3342–3350, doi: 10.1038/onc.2015.386 (2016).

Niederriter, A. R., Varshney, A., Parker, S. C. & Martin, D. M. Super Enhancers in Cancers, Complex Disease, and Developmental Disorders. Genes 6, 1183–1200, doi: 10.3390/genes6041183 (2015).

Osterwalder, U., and Herzog, B. (2009) Sun protection factors: world wide confusion. The British journal of dermatology 161 Suppl 3, 13-24

Palumbo, A. & Sonneveld, P. Preclinical and clinical evaluation of elotuzumab, a SLAMF7-targeted humanized monoclonal antibody in development for multiple myeloma. Expert review of hematology 8, 481–491, doi: 10.1586/17474086.2015.1053866 (2015).

Pentland, A. P., Schoggins, J. W., Scott, G. A., Khan, K. N. & Han, R. Reduction of UV-induced skin tumors in hairless mice by selective COX-2 inhibition. Carcinogenesis 20, 1939–1944 (1999).

Perera, D. et al. Differential DNA repair underlies mutation hotspots at active promoters in cancer genomes. Nature 532, 259–263, doi: 10.1038/nature17437 (2016).

Pfeifer, G. P., You, Y. H. & Besaratinia, A. Mutations induced by ultraviolet light. Mutation research 571, 19–31, doi: 10.1016/j.mrfmmm.2004.06.057 (2005).

Pickering, C. R. et al. Mutational landscape of aggressive cutaneous squamous cell carcinoma. Clinical cancer research: an official journal of the American Association for Cancer Research 20, 6582–6592, doi: 10.1158/1078-0432.CCR-14-1768 (2014).

Pleasance, E. D., Cheetham, R. K., Stephens, P. J., McBride, D. J., Humphray, S. J., Greenman, C. D., Varela, I., Lin, M. L., Ordonez, G. R., Bignell, G. R., Ye, K., Alipaz, J., Bauer, M. J., Beare, D., Butler, A., Carter, R. J., Chen, L., Cox, A. J., Edkins, S., Kokko-Gonzales, P. I., Gormley, N. A., Grocock, R. J., Haudenschild, C. D., Hims, M. M., James, T., Jia, M., Kingsbury, Z., Leroy, C., Marshall, J., Menzies, A., Mudie, L. J., Ning, Z., Royce, T., Schulz-Trieglaff, O. B., Spiridou, A., Stebbings, L. A., Szajkowski, L., Teague, J., Williamson, D., Chin, L., Ross, M. T., Campbell, P. J., Bentley, D. R., Futreal, P. A., and Stratton, M. R. (2010) A comprehensive catalogue of somatic mutations from a human cancer genome. Nature 463, 191-196

Rada-Iglesias, A. et al. A unique chromatin signature uncovers early developmental enhancers in humans. Nature 470, 279–283, doi:10.1038/nature09692 (2011).

Rieger, K. E., and Chu, G. (2004) Portrait of transcriptional responses to ultraviolet and ionizing radiation in human cells. Nucleic acids research 32, 4786-4803

Rippa, A. L., Vorotelyak, E. A., Vasiliev, A. V. & Terskikh, V. V. The role of integrins in the development and homeostasis of the epidermis and skin appendages. Acta naturae 5, 22–33 (2013).

Robinson, J. K. (2005) Sun exposure, sun protection, and vitamin D. Jama 294, 1541-1543

Rogers, H. W., Weinstock, M. A., Feldman, S. R. & Coldiron, B. M. Incidence Estimate of Nonmelanoma Skin Cancer (Keratinocyte Carcinomas) in the U.S. Population, 2012. JAMA dermatology 151, 1081–1086, doi: 10.1001/jamadermatol.2015.1187 (2015).

Rogers, H. W., Weinstock, M. A., Feldman, S. R., and Coldiron, B. M. (2015) Incidence Estimate of Nonmelanoma Skin Cancer (Keratinocyte Carcinomas) in the US Population, 2012. JAMA dermatology 151, 1081-1086

Schick, S. et al. Dynamics of chromatin accessibility and epigenetic state in response to UV damage. Journal of cell science 128, 4380–4394, doi: 10.1242/jcs.173633 (2015).

Schutze, D. M. et al. Longitudinal assessment of DNA methylation changes during HPVE6E7-induced immortalization of primary keratinocytes. Epigenetics 10, 73–81, doi: doi: 10.4161/15592294.2014.990787 (2015).

Seite, S., Fourtanier, A., Moyal, D., and Young, A. R. (2010) Photodamage to human skin by suberythemal exposure to solar ultraviolet radiation can be attenuated by sunscreens: a review. The British journal of dermatology 163, 903-914

Shain, A. H. et al. The Genetic Evolution of Melanoma from Precursor Lesions. The New England journal of medicine 373, 1926–1936, doi: 10.1056/NEJMoa1502583 (2015).

Shen, Y., Kim, A. L., Du, R. & Liu, L. Transcriptome Analysis Identifies the Dysregulation of Ultraviolet Target Genes in Human Skin Cancers. PloS one 11, e0163054, doi: 10.1371/journal.pone.0163054 (2016).

Skobowiat, C. & Slominski, A. T. UVB Activates Hypothalamic-Pituitary-Adrenal Axis in C57BL/6 Mice. The Journal of investigative dermatology 135, 1638–1648, doi: 10.1038/jid.2014.450 (2015).

Slominski, A. et al. Steroidogenesis in the skin: implications for local immune functions. The Journal of steroid biochemistry and molecular biology 137, 107–123, doi: 10.1016/j.jsbmb.2013.02.006 (2013).

Slominski, A. T. et al. Key role of CRF in the skin stress response system. Endocrine reviews 34, 827–884, doi: 10.1210/er.2012-1092 (2013).

Slominski, A. T. et al. Local melatoninergic system as the protector of skin integrity. International journal of molecular sciences 15, 17705–17732, doi: 10.3390/ijms151017705 (2014).

Slominski, A. T. et al. Novel non-calcemic secosteroids that are produced by human epidermal keratinocytes protect against solar radiation. The Journal of steroid biochemistry and molecular biology 148, 52–63, doi: 10.1016/j.jsbmb.2015.01.014 (2015).

Slominski, A. T. et al. Sensing the environment: regulation of local and global homeostasis by the skin's neuroendocrine system. Advances in anatomy, embryology, and cell biology 212, v, vii, 1–115 (2012).

Slominski, A., Tobin, D. J., Shibahara, S. & Wortsman, J. Melanin pigmentation in mammalian skin and its hormonal regulation. Physiological reviews 84, 1155–1228, doi: 10.1152/physrev.00044.2003 (2004).

Stern, R. S. Prevalence of a history of skin cancer in 2007: results of an incidence-based model. Archives of dermatology 146, 279–282, doi: 10.1001/archdermatol.2010.4 (2010).

Subramanian, A., Tamayo, P., Mootha, V. K., Mukherjee, S., Ebert, B. L., Gillette, M. A., Paulovich, A., Pomeroy, S. L., Golub, T. R., Lander, E. S., and Mesirov, J. P. (2005) Gene set enrichment analysis: a knowledge-based approach for interpreting genome-wide expression profiles. Proceedings of the National Academy of Sciences of the United States of America 102, 15545-15550

Sun, X., Kim, A., Nakatani, M., Shen, Y. & Liu, L. Distinctive molecular responses to ultraviolet radiation between keratinocytes and melanocytes. Experimental dermatology, doi: 10.1111/exd.13057 (2016).

Szklarczyk, D., Franceschini, A., Wyder, S., Forslund, K., Heller, D., Huerta-Cepas, J., Simonovic, M., Roth, A., Santos, A., Tsafou, K. P., Kuhn, M., Bork, P., Jensen, L. J., and von Mering, C. (2015) STRING v10: protein-protein interaction networks, integrated over the tree of life. Nucleic acids research 43, D447-452

Takao, J., Ariizumi, K., Dougherty, II, and Cruz, P. D., Jr. (2002) Genomic scale analysis of the human keratinocyte response to broad-band ultraviolet-B irradiation. Photodermatology, photoimmunology & photomedicine 18, 5-13

Tannour-Louet, M. et al. Increased expression of CYP24A1 correlates with advanced stages of prostate cancer and can cause resistance to vitamin D3-based therapies. FASEB journal: offcial publication of the Federation of American

Societies for Experimental Biology 28, 364–372, doi: 10.1096/fj.13-236109 (2014).

The Surgeon General's Call to Action to Prevent Skin Cancer, Washington (DC) (2014)

Thurman, R. E. et al. The accessible chromatin landscape of the human genome. Nature 489, 75–82, doi: 10.1038/nature11232 (2012).

Tieu, E. W. et al. Rat CYP24A1 acts on 20-hydroxyvitamin D(3) producing hydroxylated products with increased biological activity. Biochemical pharmacology 84, 1696–1704, doi: 10.1016/j.bcp.2012.09.032 (2012).

van Eck, N. J., Waltman, L., Dekker, R., and van den Berg, J. (2010) A Comparison of Two Techniques for Bibliometric Mapping: Multidimensional Scaling and VOS. J Am Soc Inf Sci Tec 61, 2405-2416

Vandiver, A. R. et al. Age and sun exposure-related widespread genomic blocks of hypomethylation in nonmalignant skin. Genome biology 16, 80, doi: 10.1186/s13059-015-0644-y (2015).

Wang, Y. et al. A complex network of factors with overlapping affnities represses splicing through intronic elements. Nature structural & molecular biology 20, 36–45, doi: 10.1038/nsmb.2459 (2013).

Warr, A. et al. Exome Sequencing: Current and Future Perspectives. G3 5, 1543–1550, doi: 10.1534/g3.115.018564 (2015).

Wei, Y. et al. SEA: a super-enhancer archive. Nucleic acids research 44, D172–179, doi: 10.1093/nar/gkv1243 (2016).

Whyte, W. A. et al. Master transcription factors and mediator establish super-enhancers at key cell identity genes. Cell 153, 307–319, doi: 10.1016/j.cell.2013.03.035 (2013).

Wu, S. et al. History of Severe Sunburn and Risk of Skin Cancer Among Women and Men in 2 Prospective Cohort Studies. American journal of epidemiology 183, 824–833, doi: 10.1093/aje/kwv282 (2016).

Wu, S., Han, J., Laden, F., and Qureshi, A. A. (2014) Long-term ultraviolet flux, other potential risk factors, and skin cancer risk: a cohort study. Cancer epidemiology, biomarkers & prevention : a publication of the American Association for Cancer Research, cosponsored by the American Society of Preventive Oncology 23, 1080-1089

Yang, G., Zhang, G., Pittelkow, M. R., Ramoni, M. & Tsao, H. Expression profiling of UVB response in melanocytes identifies a set of p53-target genes. The Journal of investigative dermatology 126, 2490–2506, doi: 10.1038/sj.jid.5700470 (2006).

Yang, G., Zhang, G., Pittelkow, M. R., Ramoni, M., and Tsao, H. (2006) Expression profiling of UVB response in melanocytes identifies a set of p53-target genes. The Journal of investigative dermatology 126, 2490-2506

You, Y. N., Rustin, R. B., and Sullivan, J. D. (2015) Oncotype DX((R)) colon cancer assay for prediction of recurrence risk in patients with stage II and III colon cancer: A review of the evidence. Surgical oncology 24, 61-66

Zanotti, L., Bottini, A., Rossi, C., Generali, D., and Cappelletti, M. R. (2014) Diagnostic tests based on gene expression profile in breast cancer: from background to clinical use. Tumour biology : the journal of the International Society for Oncodevelopmental Biology and Medicine 35, 8461-8470

Zentner, G. E., Tesar, P. J. & Scacheri, P. C. Epigenetic signatures distinguish multiple classes of enhancers with distinct cellular functions. Genome research 21, 1273–1283, doi: 10.1101/gr.122382.111 (2011).

Zhang, X. et al. Solar Simulated Ultraviolet Radiation Induces Global Histone Hypoacetylation in Human Keratinocytes. PloS one 11, e0150175, doi: 10.1371/journal.pone.0150175 (2016).

CLAIMS

1. A method of detecting ultraviolet radiation (UVR)-induced skin damage in a subject, said method comprising the steps of:

a) obtaining a skin sample from the subject;

b) analyzing expression levels in the skin sample of UVR-induced differentially expressed genes (DEGs) listed in Table 8 or a subset thereof; and

c) comparing the expression levels of the UVR-induced DEGs to a control skin sample;

wherein, when the expression levels of the UVR-induced DEGs in the skin sample is above or below the level of each of the UVR-induced DEGs in the control sample, the subject is identified as likely being afflicted with UVR-induced skin damage.

2. The method of claim 1, wherein the analyzing step comprises carrying out next-generation sequencing of an RNA sample from the subject to identify genes from Table 8, or a subset thereof, that have a different expression profile compared to controls.

3. The method of claim 1, wherein a first subset of the UVR-induced DEGs from Table 8 is selected from the group consisting of: IL6, PTGS2, IL1B, CDKN1A, BCL2L1, ICAM1, HMOX1, VAV1, PLA2G16, MMP1, HIST1H4H, CYP4F3, and CD8A.

4. The method of claim 1, wherein a second subset of the UVR-induced DEGs from Table 8 is selected from the group consisting of: SLPI, KLK7, KRT13, NHLH2, GPRC5A, HIST1H2BK, IGFBP3, SPOCD1, IFI27, KLK11, and TNFSF4.

5. The method of claim 1, wherein the subject is human.

6. A method of identifying or monitoring skin cancer in a test subject, comprising:

a) analyzing expression levels in a biological sample obtained from the subject of UVR-induced differentially expressed genes (DEGs) listed in Table 8, or a subset thereof;

b) comparing the expression levels of the UVR-induced DEGs in the biological sample with a predetermined reference standard for the genes; and

c) identifying or monitoring skin cancer in the test subject based on the comparison in b).

7. The method of claim 6, wherein expression levels of the UVR-induced DEGs above or below the predetermined reference standard is indicative of skin cancer in the subject.

8. The method of claim 6, wherein the analyzing step comprises carrying out next-generation sequencing of RNA in the biological sample obtained from the subject to identify genes from Table 8, or a subset thereof, that have a different expression profile compared to controls.

9. The method of claim 6, wherein the biological sample is a skin sample.

10. The method of claim 6, wherein a first subset of the UVR-induced DEGs from Table 8 is selected from the group consisting of: IL6, PTGS2, IL1B, CDKN1A, BCL2L1, ICAM1, HMOX1, VAV1, PLA2G16, MMP1, HIST1H4H, CYP4F3, and CD8A.

11. The method of claim 6, wherein a second subset of the UVR-induced DEGs from Table 8 is selected from the group consisting of: SLPI, KLK7, KRT13, NHLH2, GPRC5A, HIST1H2BK, IGFBP3, SPOCD1, IFI27, KLK11, and TNFSF4.

12. The method of claim 6, wherein the test subject is human.

13. A kit for detecting ultraviolet radiation (UVR)-induced skin damage in a subject, comprising: a set of primers or probes that specifically bind to UVR-induced differentially expressed genes (DEGs) listed in Table 8 or a subset thereof, packaged together with instructions for its use.

14. The kit of claim 13, wherein a first subset of the UVR-induced DEGs from Table 8 is selected from the group consisting of: IL6, PTGS2, IL1B, CDKN1A, BCL2L1, ICAM1, HMOX1, VAV1, PLA2G16, MMP1, HIST1H4H, CYP4F3, and CD8A.

15. The kit of claim 13, wherein a second subset of the UVR-induced DEGs from Table 8 is selected from the group consisting of: SLPI, KLK7, KRT13, NHLH2, GPRC5A, HIST1H2BK, IGFBP3, SPOCD1, IFI27, KLK11, and TNFSF4.

16. The kit of claim 13, wherein the subject is human.

17. A kit for identifying or monitoring skin cancer in a subject, comprising: a set of primers or probes that specifically bind to UVR-induced differentially expressed genes (DEGs) listed in Table 8 or a subset thereof, packaged together with instructions for its use.

18. The kit of claim 17, wherein a first subset of the UVR-induced DEGs from Table 8 is selected from the group consisting of: IL6, PTGS2, IL1B, CDKN1A, BCL2L1, ICAM1, HMOX1, VAV1, PLA2G16, MMP1, HIST1H4H, CYP4F3, and CD8A.

19. The kit of claim 17, wherein a second subset of the UVR-induced DEGs from Table 8 is selected from the group consisting of: SLPI, KLK7, KRT13, NHLH2, GPRC5A, HIST1H2BK, IGFBP3, SPOCD1, IFI27, KLK11, and TNFSF4.

20. The kit of claim 17, wherein the subject is human.

21. A method for measuring the effectiveness of a test agent in reducing ultraviolet radiation (UVR)-induced damage, the method comprising:

a) irradiating a test skin sample, to which the test agent has been applied, with UV radiation;

b) obtaining an expression profile of the UVR-induced differentially expressed genes (DEGs) listed in Table 8, or a subset thereof, in the test skin sample; and

c) comparing the expression profile of the UVR-induced DEGs, or a subset thereof, from the test skin sample, with an expression profile of the same genes in a reference skin sample and a control skin sample, wherein the reference skin sample is irradiated in the absence of the test agent, and the normal, control skin sample is not irradiated;

wherein if the gene expression profile of the test skin sample is the same or substantially similar to the gene expression profile of the normal, control skin sample, the test agent is effective at reducing UVR-induced damage, whereas if the gene expression profile of the test skin sample is the same or substantially similar to the gene expression profile of the reference skin sample, the test agent is not effective at reducing UVR-induced damage.

22. A method for diagnosing UVR-induced skin damage in a subject by analyzing a sample from the subject for an expression profile of UVR-induced DEGs listed in Table 8 or a subset thereof that is different from an expression profile of the same genes in a normal, control sample, wherein the subject is diagnosed with UVR-induced skin damage if the expression profile of the subject differs from the expression profile from the normal, control sample.

23. A method for diagnosing skin cancer in a subject by analyzing a sample from the subject for the presence or absence of squamous cell carcinoma or pre-cancerous skin lesion cells by analyzing a sample from the subject for an expression profile of UVR-induced DEGs listed in Table 8 or a subset thereof that is different from an expression profile of the same genes in a normal, control sample, wherein the subject is diagnosed with skin cancer if squamous cell carcinoma or pre-cancerous skin lesion cells are detected.

24. A method for diagnosing and treating UVR-induced skin damage in a subject comprising: analyzing a sample from the subject for an expression profile of UVR-induced DEGs listed in Table 8 or a subset thereof that is different from an expression profile of the same genes in a normal, control sample, wherein the patient is diagnosed with UVR-induced skin damage if the expression profile of the subject differs from the expression profile from the normal, control sample; and administering a treatment for UVR-induced skin damage to the diagnosed subject.

25. A method for treating skin cancer in a subject comprising: requesting a test providing the results of an analysis of whether the subject has an expression profile of UVR-induced DEGs listed in Table 8 or a subset thereof that is different from an expression profile of the same genes in a normal, control sample; and administering a treatment for skin cancer to the subject if the expression profile of the subject differs from the expression profile from the normal, control sample.

26. An assay for evaluating the effect of ultraviolet radiation (UVR) on a tissue sample, the assay comprising:

a system to evaluate expression of a plurality of UVR-responsive biomarker genes in the tissue sample,

wherein expression of one or more of the plurality of UVR-responsive biomarker genes is associated with exposure of the tissue sample to ultraviolet radiation.

27. The assay according to any preceding claim, wherein the system is a gene array system to evaluate expression of the plurality of UVR-responsive biomarker genes.

28. The assay according to any preceding claim, wherein the assay is a high-capacity screening assay configured to evaluate the expression of the plurality of UVR-responsive biomarker genes in a plurality of tissue samples.

29. The assay according to any preceding claim, wherein the plurality of UVR-responsive biomarker genes are those associated with at least one of skin damage due to UV exposure, cancer risk and cancer progression.

30. The assay according to any preceding claim, wherein the plurality of UVR-responsive biomarker genes are those that are involved at least one of inflammation, cell growth and proliferation, DNA repair, and cancer pathogenesis.

31. The assay according to any preceding claim, wherein the plurality of UVR-responsive biomarker genes are those selected from the group consisting of CYP24A1, GJA5, SLAMF7 and ETV1.

32. The assay according to any preceding claim, wherein the tissue sample is a mammalian tissue sample.

33. The assay according to any preceding claim, wherein the tissue sample is a human tissue sample.

34. The assay according to any preceding claim, wherein the tissue sample comprises human keratinocytes.

35. The assay according to any preceding claim, further comprising a gene expression profile correlation system to correlate the expression of each of the UVR-responsive biomarker genes with at least one of UV damage to the tissue sample and/or a disease state.

36. A method of evaluating ultraviolet damage to tissue, the method comprising:

evaluating the expression of a plurality of UVR-responsive biomarker genes in a sample of the tissue; and

determining whether the expression of one or more of the plurality of UVR-responsive biomarker genes is indicative of ultraviolet damage.

37. The method according to any preceding claim, wherein the plurality of UVR-responsive biomarker genes are those associated with at least one of skin damage due to UV exposure, cancer risk and cancer progression.

38. The method according to any preceding claim, wherein the plurality of UVR-responsive biomarker genes are those selected from the group consisting of CYP24A1, GJA5, SLAMF7 and ETV1.

39. The method according to any preceding claim, wherein the expression of the plurality of UVR-responsive biomarker genes is evaluated via a high-capacity gene array screening system.

40. The method according to any preceding claim, wherein the tissue that is evaluated for UV damage is mammalian tissue.

41. The method according to any preceding claim, wherein the tissue that is evaluated for UV damage is human tissue.

42. A method of diagnosing skin cancer or predicting skin cancer risk in a subject, the method comprising:

evaluating the expression of a plurality of UVR-responsive biomarker genes in a sample of the tissue; and

determining whether the expression is indicative of skin cancer or skin cancer risk.

43. The method according to any preceding claim, wherein the plurality of UVR-responsive biomarker genes are those selected from the group consisting of CYP24A1, GJA5, SLAMF7 and ETV1.

44. The method according to any preceding claim, wherein the subject is a mammal.

45. The method according to any preceding claim, wherein the subject is a human.

46. A method of evaluating a sunscreen formulation, comprising:

applying the sunscreen formulation to a tissue sample;

irradiating the tissue sample with ultraviolet radiation;

evaluating the expression of a plurality of UVR-responsive biomarker genes in the tissue sample; and

determining whether the expression of the plurality of UVR-responsive biomarker genes is indicative of efficacy of sunscreen formulation in providing a UV protective effect to the tissue sample.

FIG. 1A

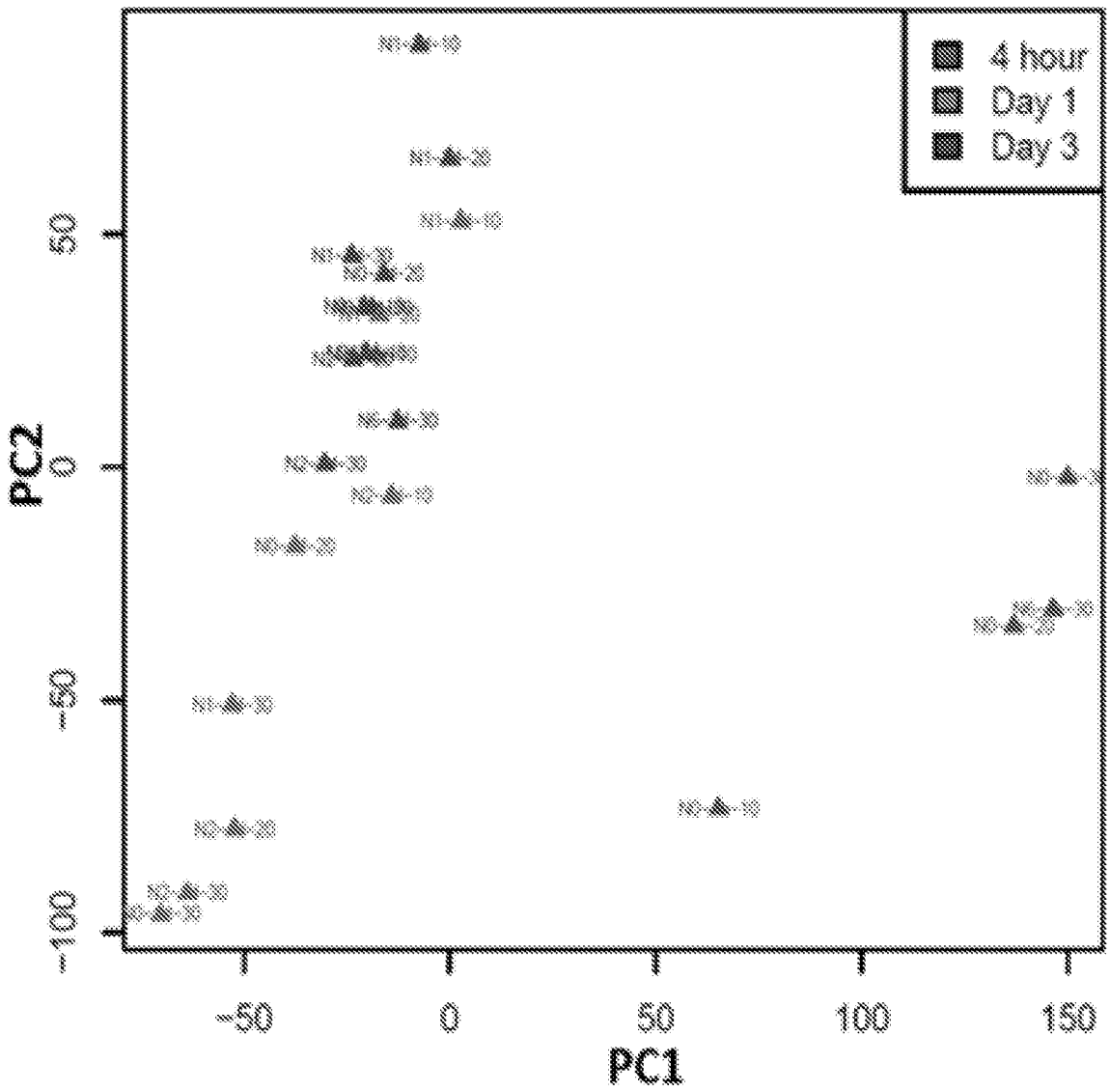

FIG. 1B

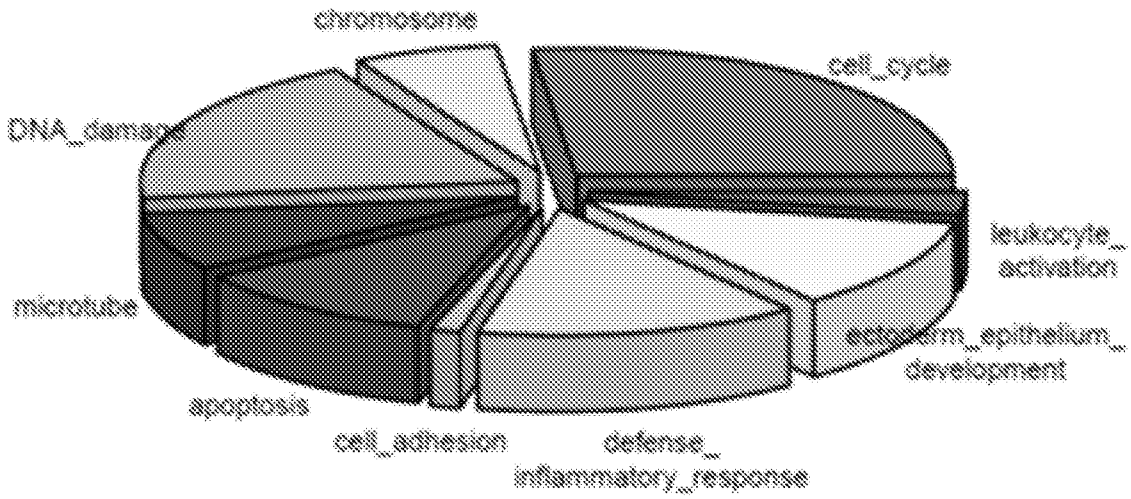
chromosome
cell_cycle
DNA_damage
leukocyte_
activation
microtube
ectoderm_epithelium_
development
apoptosis
cell_adhesion
defense_
inflammatory_response

FIG. 2

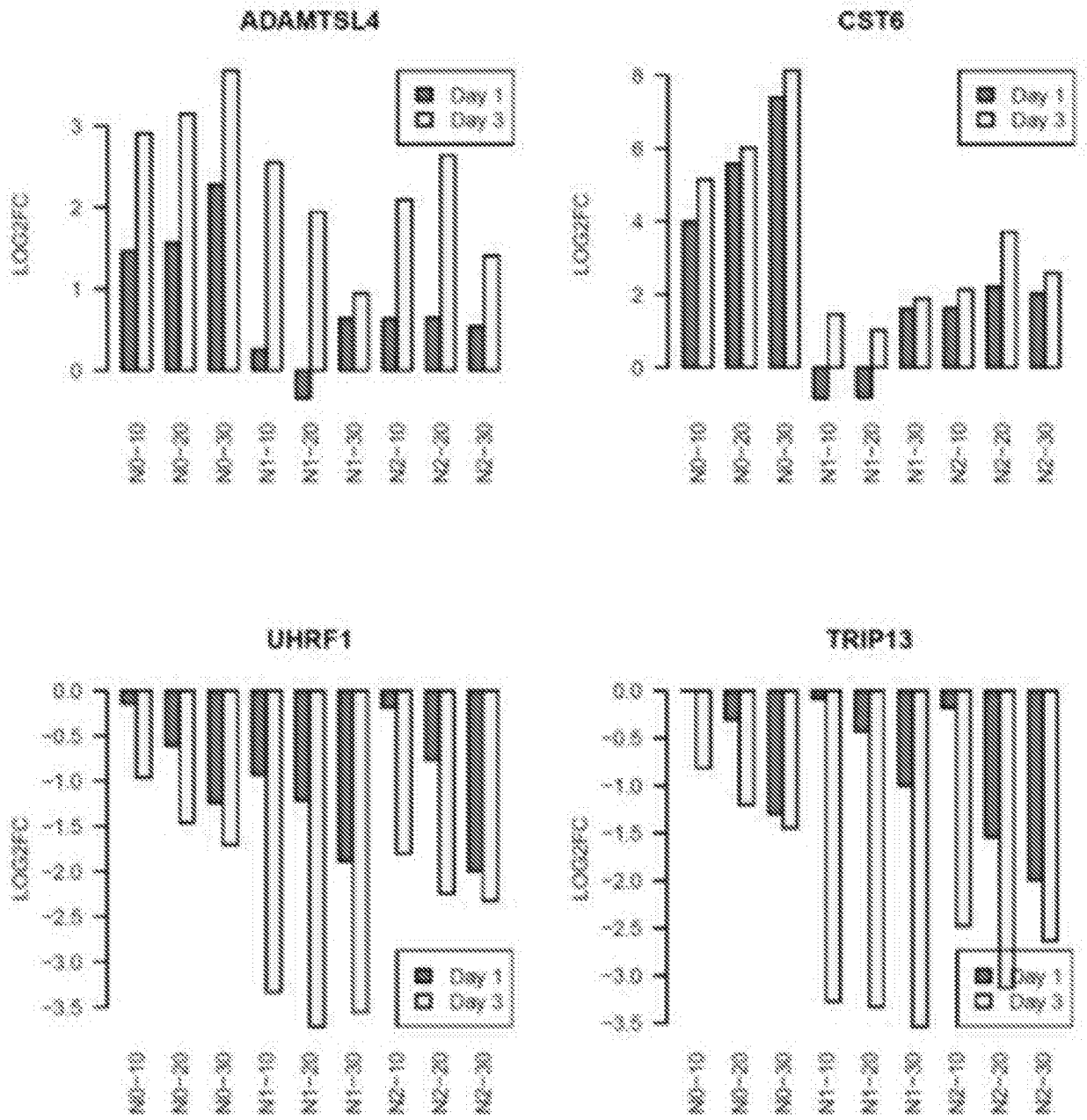
ADAMTSL4
CST6
UHRF1
TRIP13
Log2FC
Day 1
Day 3
NO-10
NO-20
NO-30
N1-10
N1-20
N1-30
N2-10
N2-20
N2-30

FIG. 3

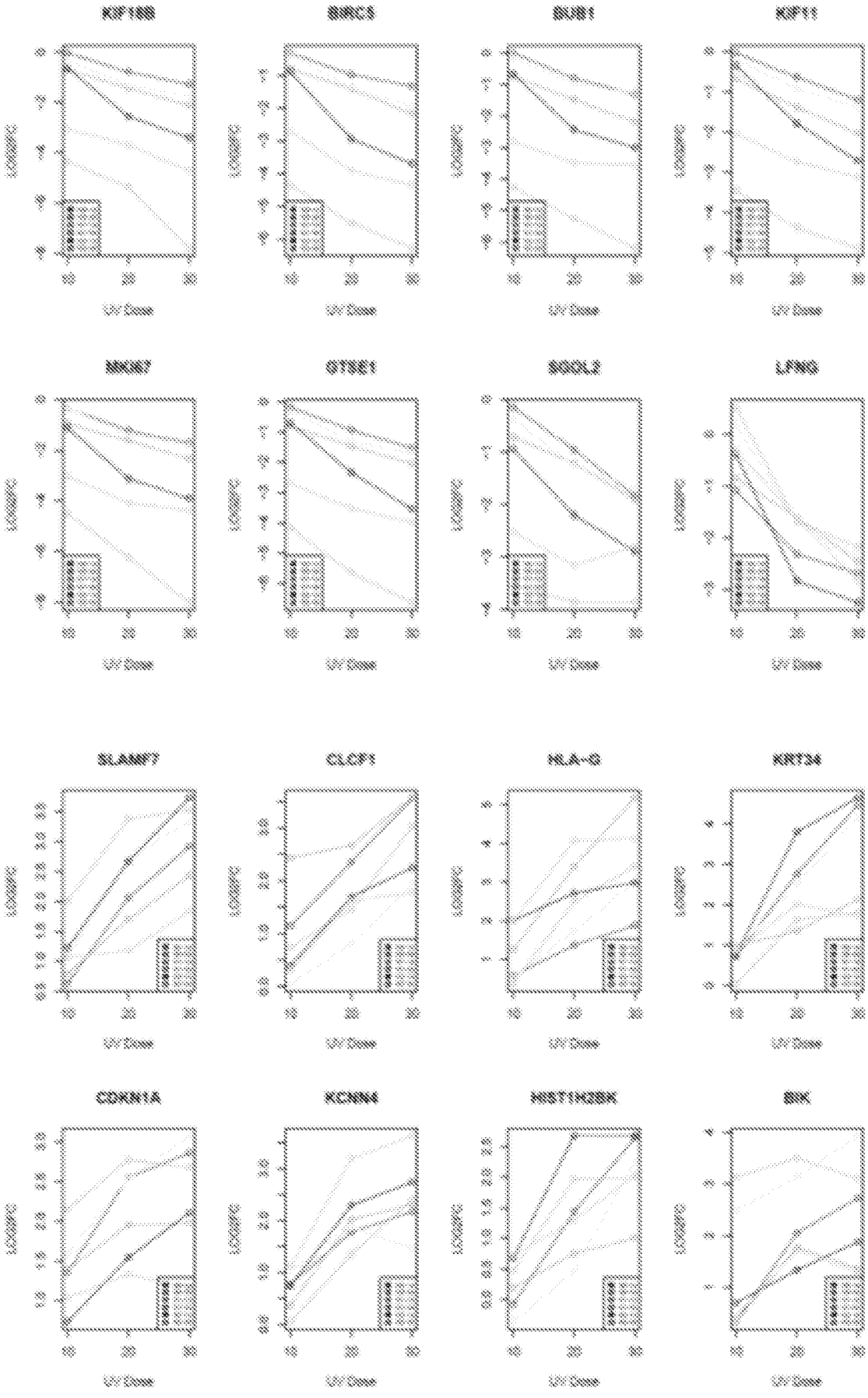
KIF18B
BIRC5
BUB1
KIF11
NUSAP1
GTSE1
SGOL2
LPIN3
SLAMF7
CLCF1
HLA-G
KRT34
CDKN1A
KCNN4
HIST1H2BK
BIK

FIG. 4

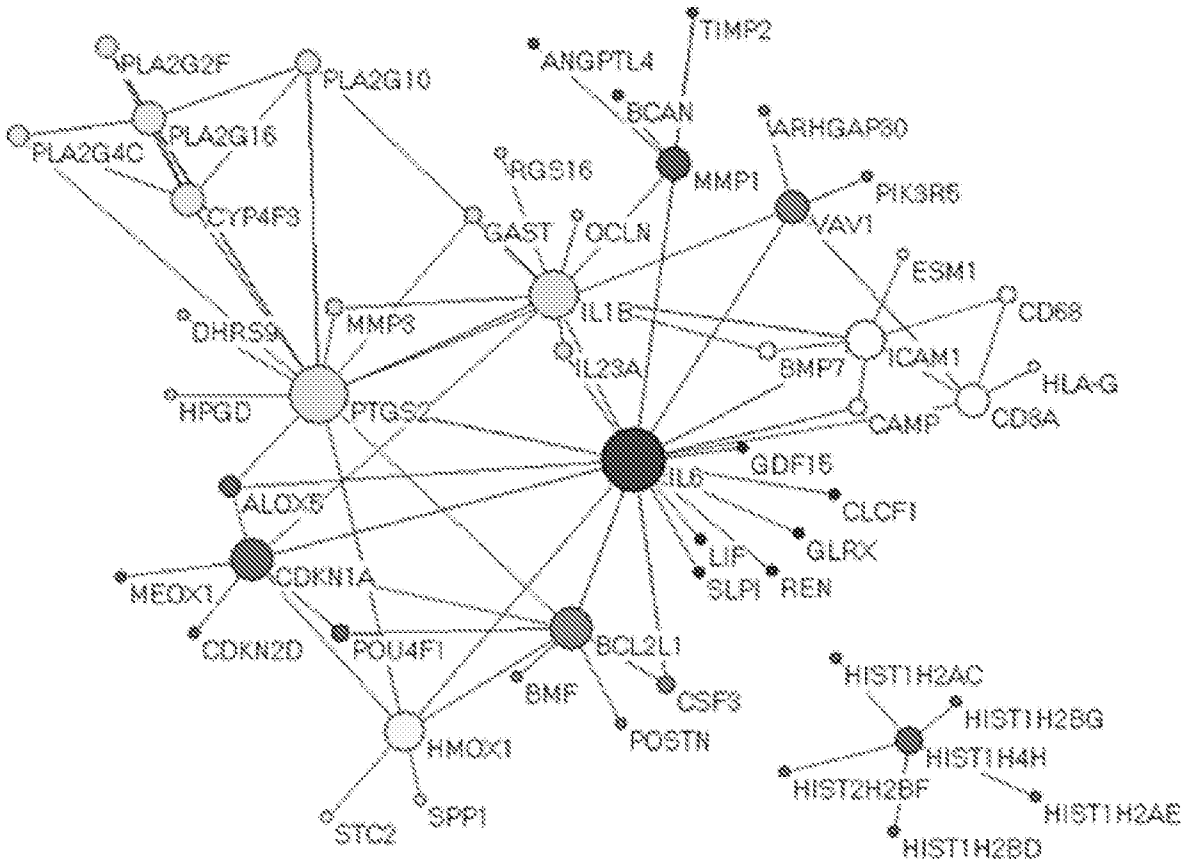
PLA2G2F
PLA2G10
PLA2G16
PLA2G4C
CYP4F3
DHRS9
MMP3
HPGD
PTGS2
ALOX5
MEOX1
CDKN1A
CDKN2D
FOU4F1
HMOX1
SPP1
STC2
RGS16
GAST
OCLN
TIMP2
ANGPTL4
BCAN
MMP1
ARHGAP30
PIK3R6
VAV1
ESM1
IL1B
IL23A
BMP7
ICAM1
CD68
HLA-G
CD8A
CAMP
IL6
GDF15
CLCF1
GLRX
LIF
SLPI
REN
BCL2L1
BMF
CSF3
POSTN
HIST1H2AC
HIST1H2BG
HIST1H4H
HIST2H2BF
HIST1H2AE
HIST1H2BD

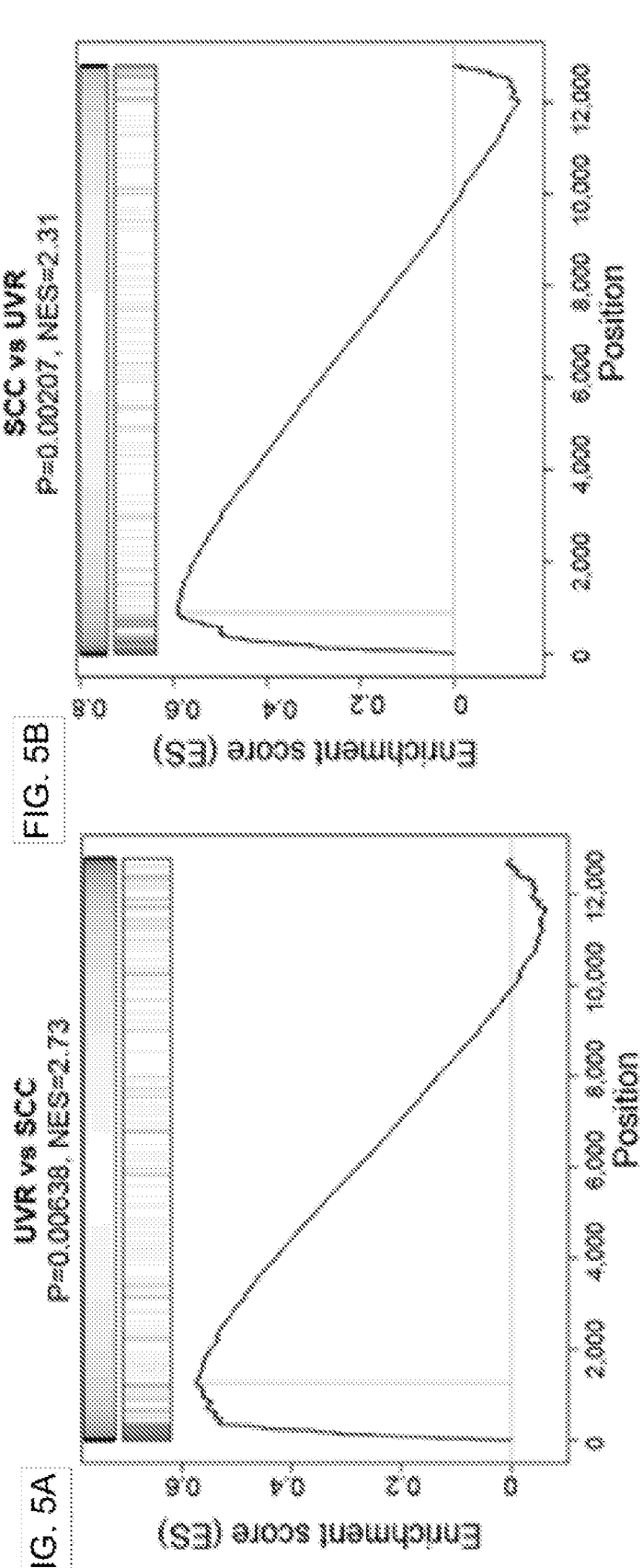

FIG. 5A

FIG. 5B

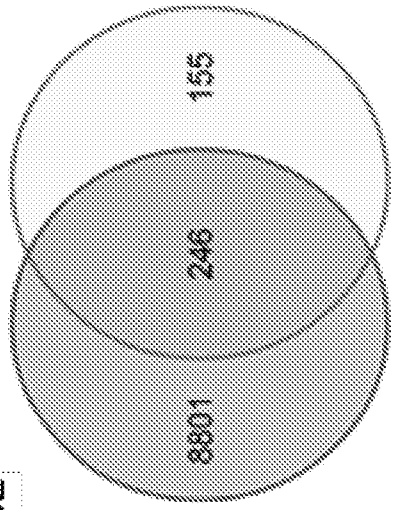

FIG. 5E

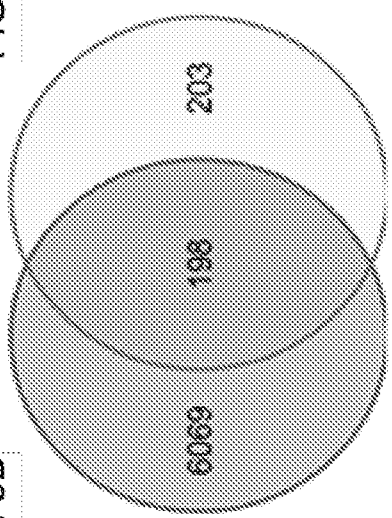

FIG. 5D

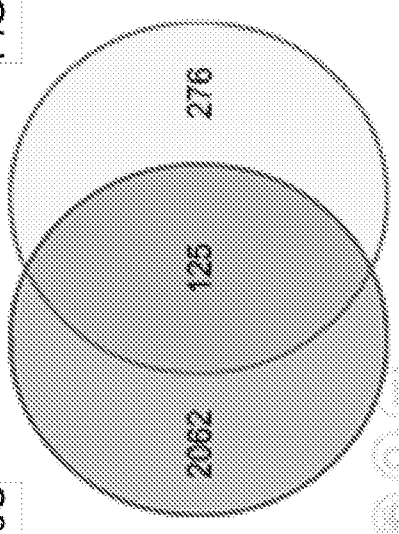

FIG. 5C

FIG. 6A

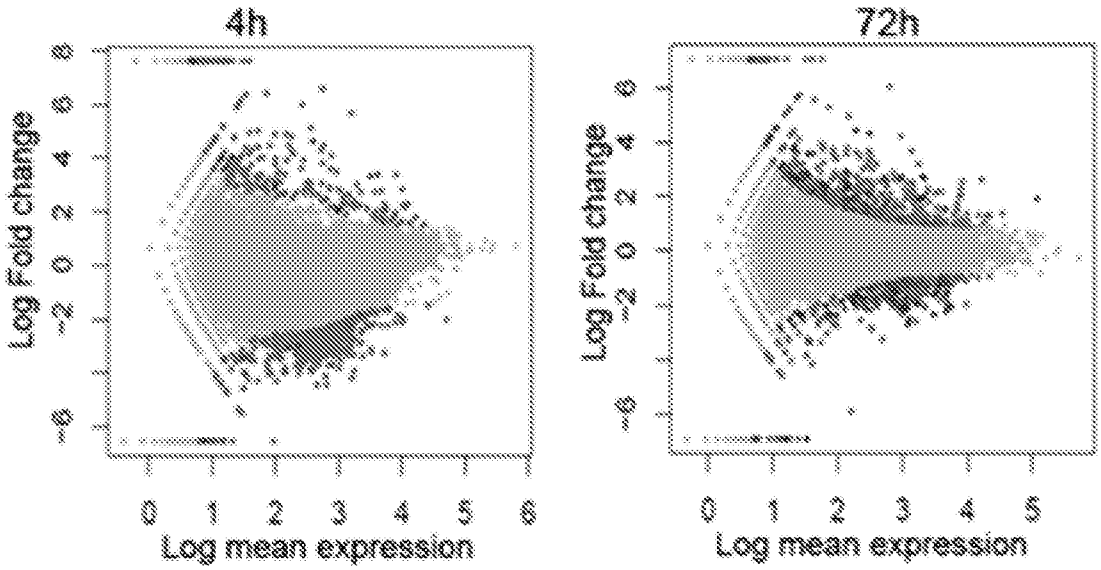
4h
72h
Log Fold change
Log mean expression
−6
−2
0
2
4
6
0
1
2
3
4
5

FIG. 6B

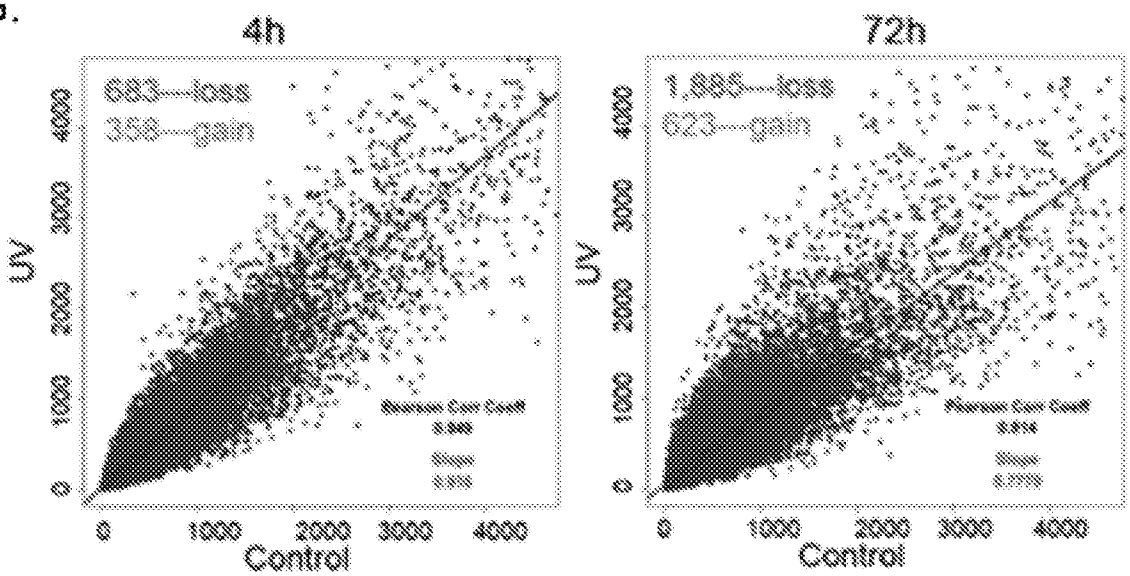
4h
72h
683—loss
358—gain
1,885—loss
623—gain
UV
Control
0
1000
2000
3000
4000

FIG. 6C

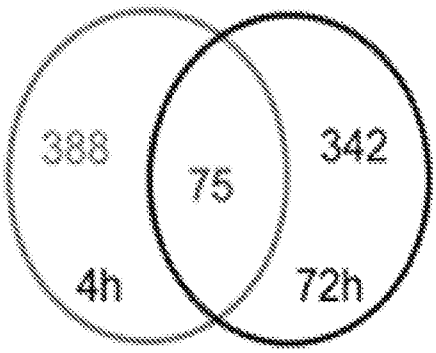

FIG. 6D

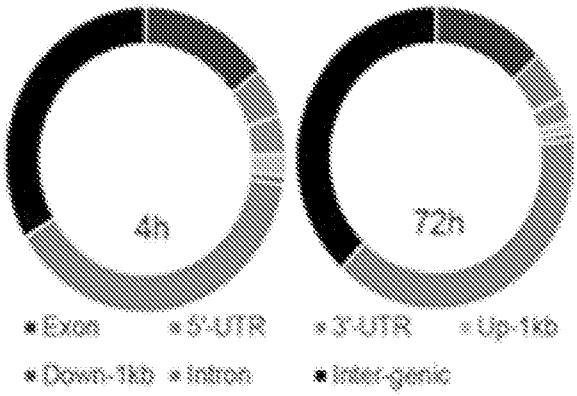

FIG. 6E

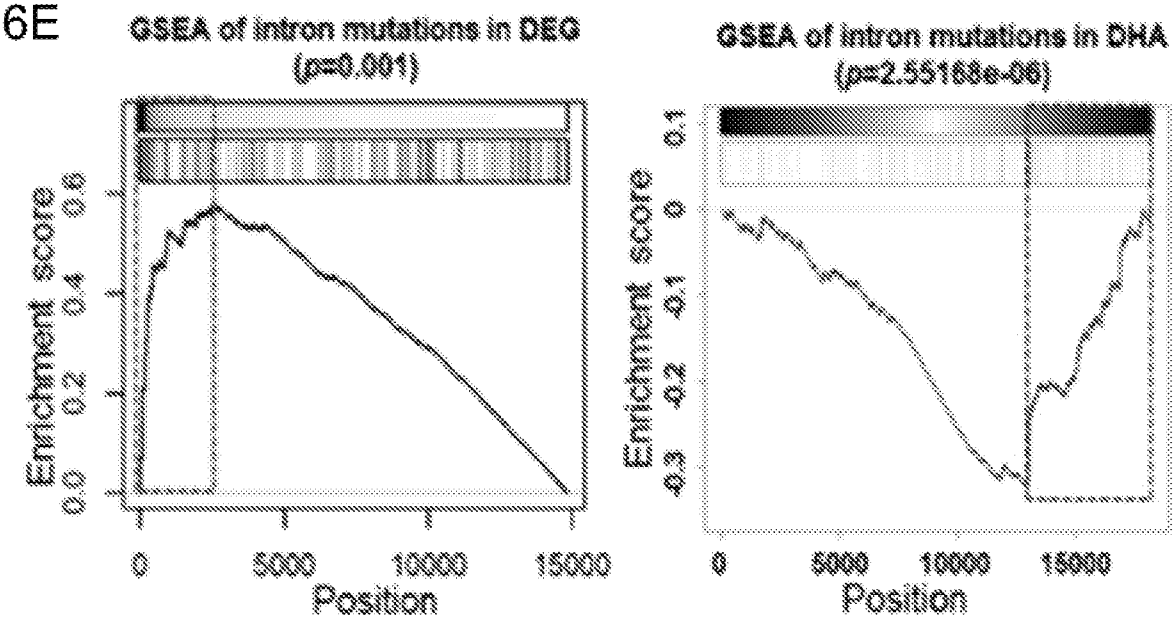

FIG. 7A

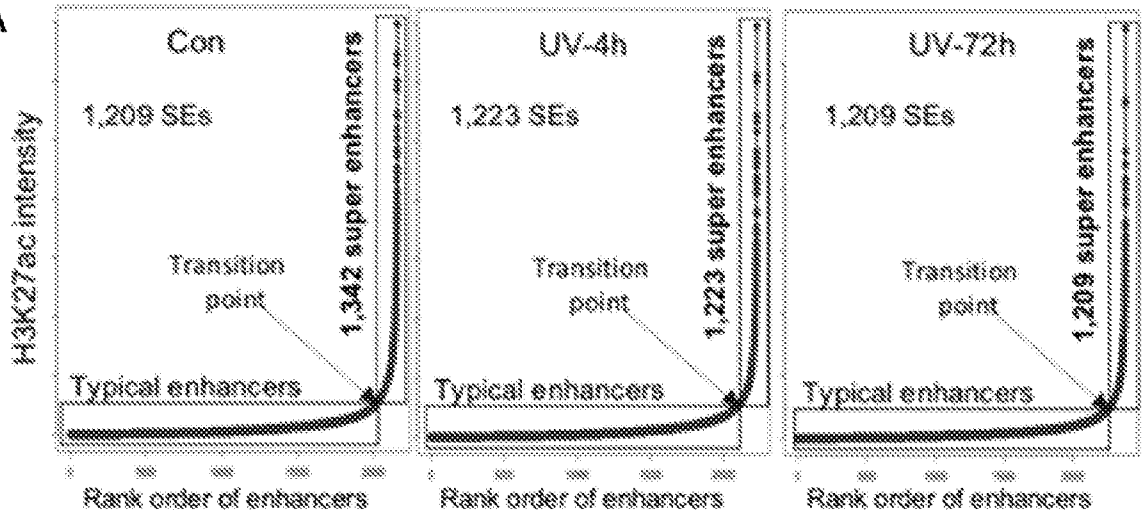

FIG. 7B

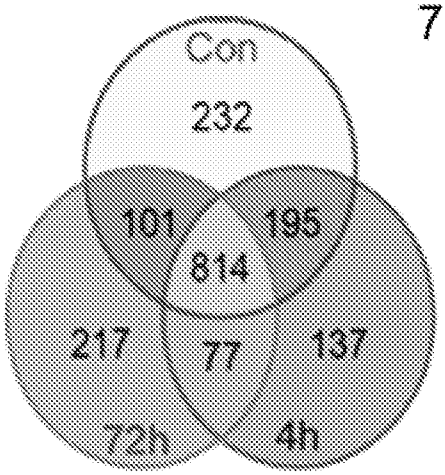

FIG. 7C

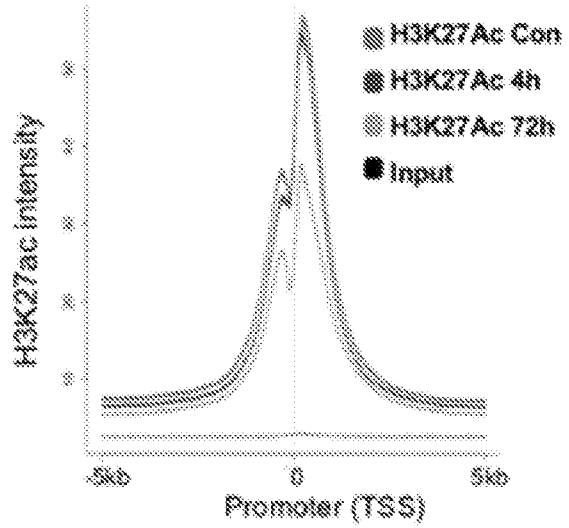

FIG. 7D

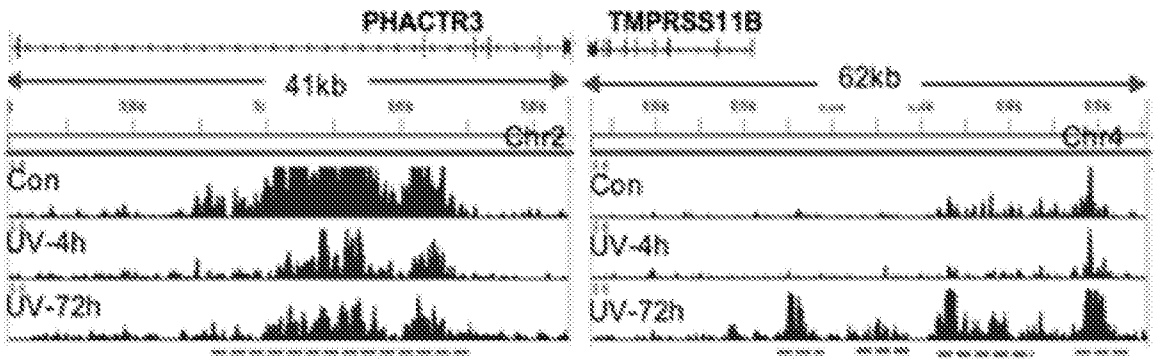

FIG. 8A

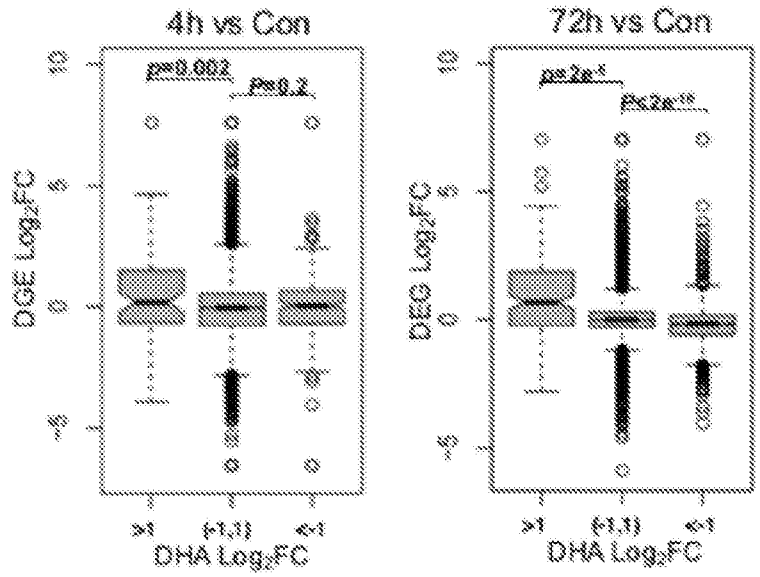
4h vs Con
72h vs Con
DGE Log2FC
DEC Log2FC
DHA Log2FC
DHA Log2FC

FIG. 8B

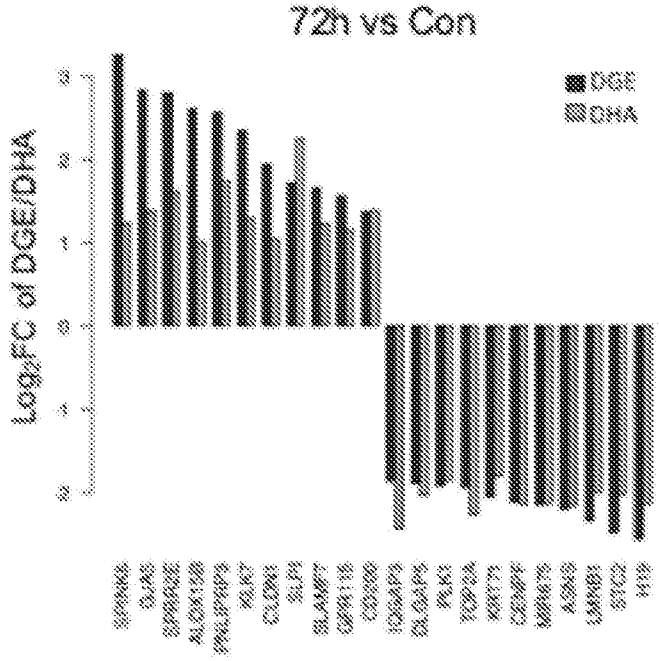
72h vs Con
DGE
DHA
Log2FC of DGE/DHA

FIG. 8C

4 h	DGE > 1	DGE (-1,1)	DGE < -1
DHA > 1	24	38	12
DHA (-1,1)	1275	9010	2643
DHA < -1	39	226	56

72 h	DGE > 1	DGE (-1,1)	DGE < -1
DHA > 1	74	78	15
DHA (-1,1)	800	10700	443
DHA < -1	54	965	170

FIG. 8D

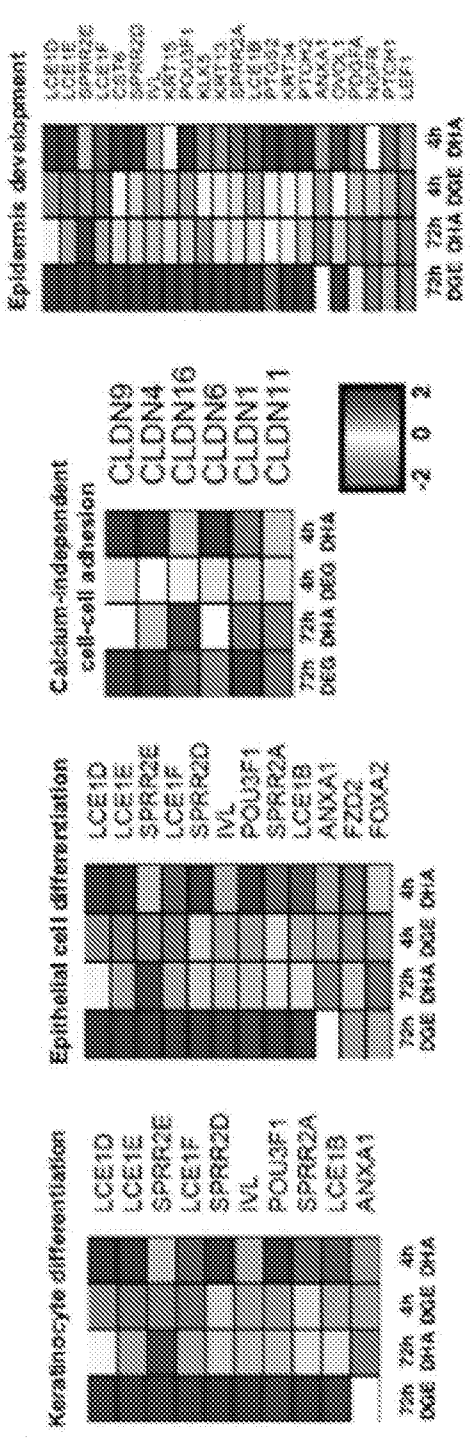

FIG. 9A

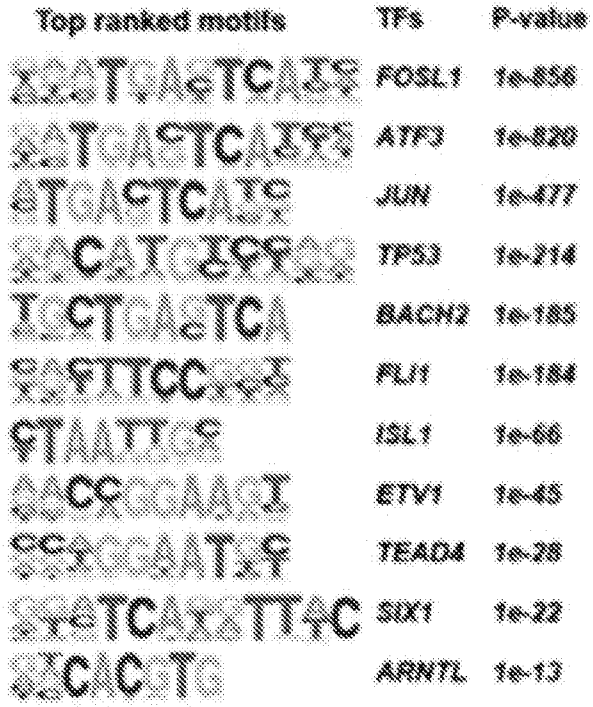
Top ranked motifs
TFs
P-value
FOSL1
1e-856
ATF3
1e-820
JUN
1e-477
TP53
1e-214
BACH2
1e-185
FLI1
1e-184
ISL1
1e-66
ETV1
1e-45
TEAD4
1e-28
SIX1
1e-22
ARNTL
1e-13

FIG. 9B

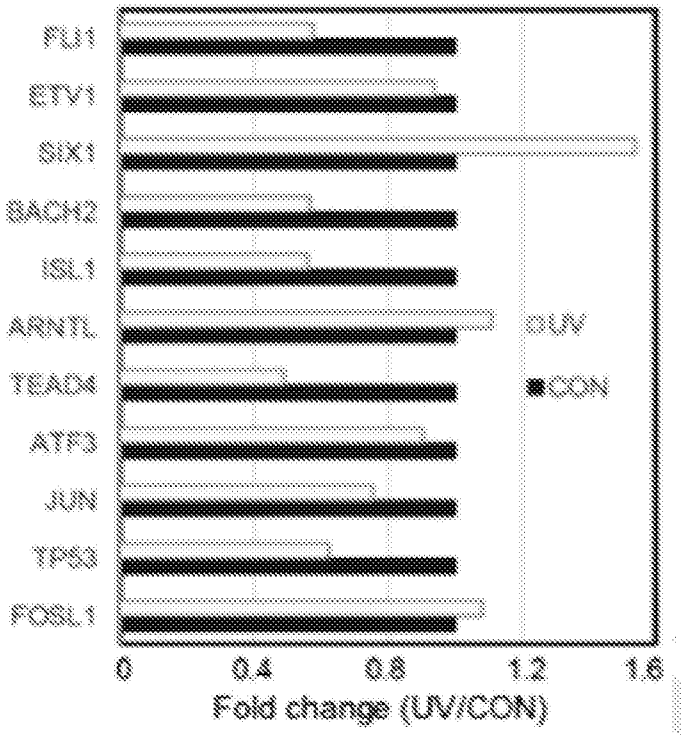
FLI1
ETV1
SIX1
BACH2
ISL1
ARNTL
TEAD4
ATF3
JUN
TP53
FOSL1
UV
CON
0
0.4
0.8
1.2
1.6
Fold change (UV/CON)

FIG. 9D

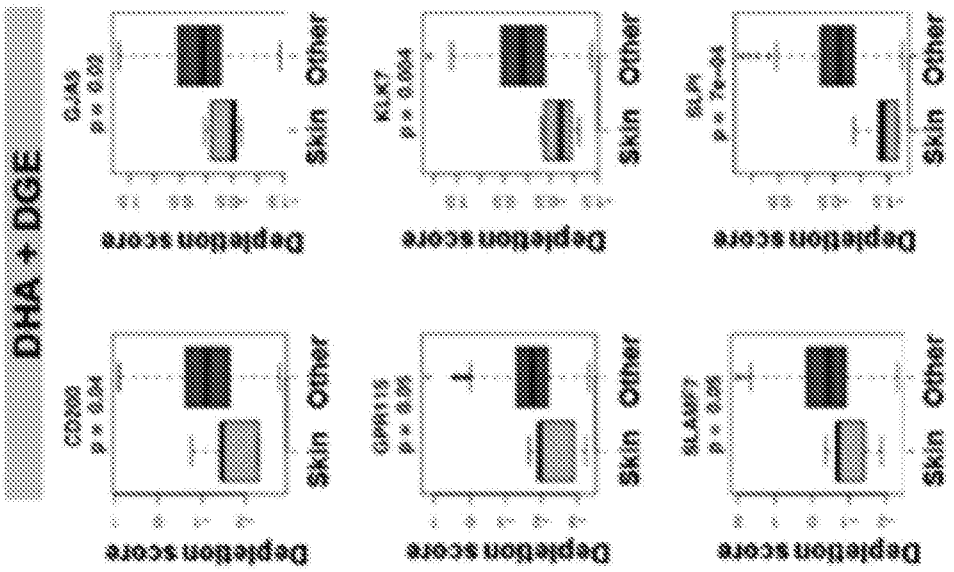
DHA + DGE
Depletion score
Skin
Other

FIG. 9C

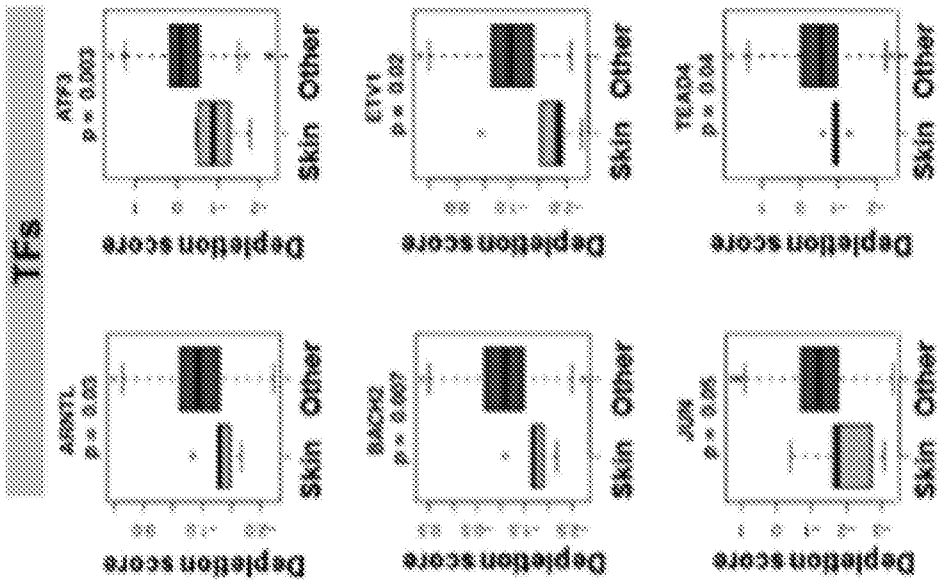
TFs
Depletion score
Skin
Other

FIG. 9E

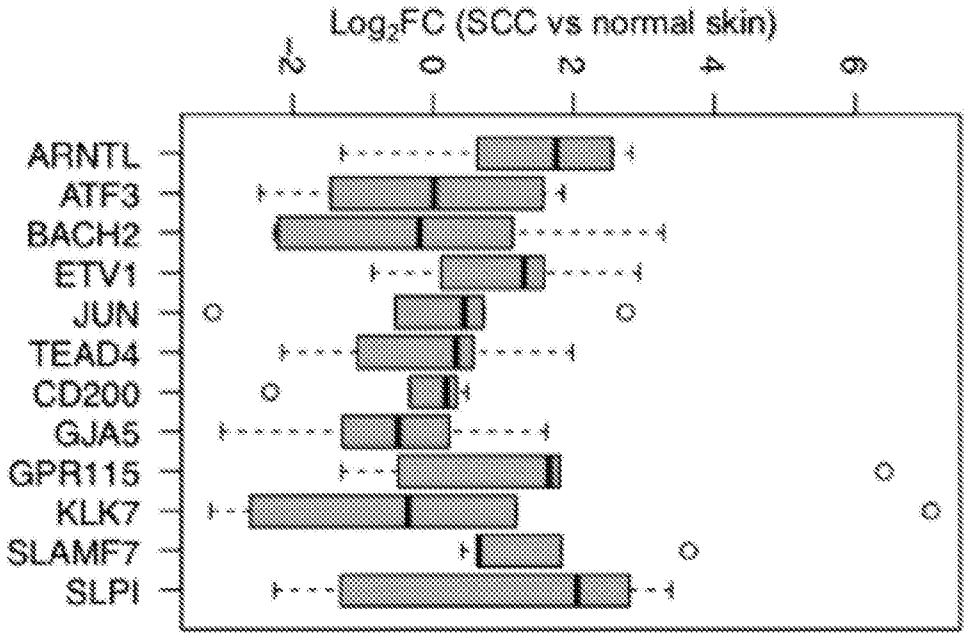
Log2FC (SCC vs normal skin)
-2
0
2
4
6
ARNTL
ATF3
BACH2
ETV1
JUN
TEAD4
CD200
GJA5
GPR115
KLK7
SLAMF7
SLPI

FIG. 10A

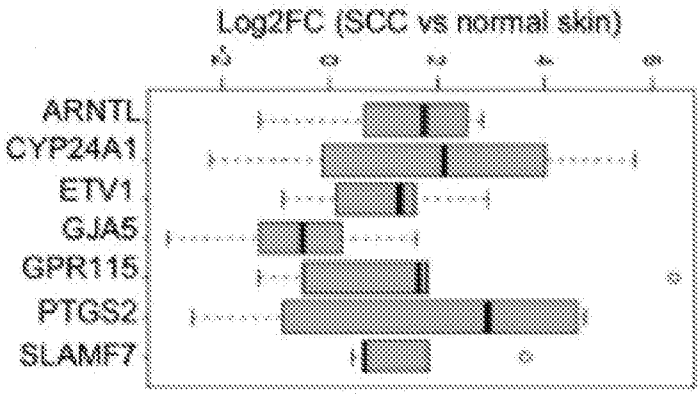

FIG. 10B

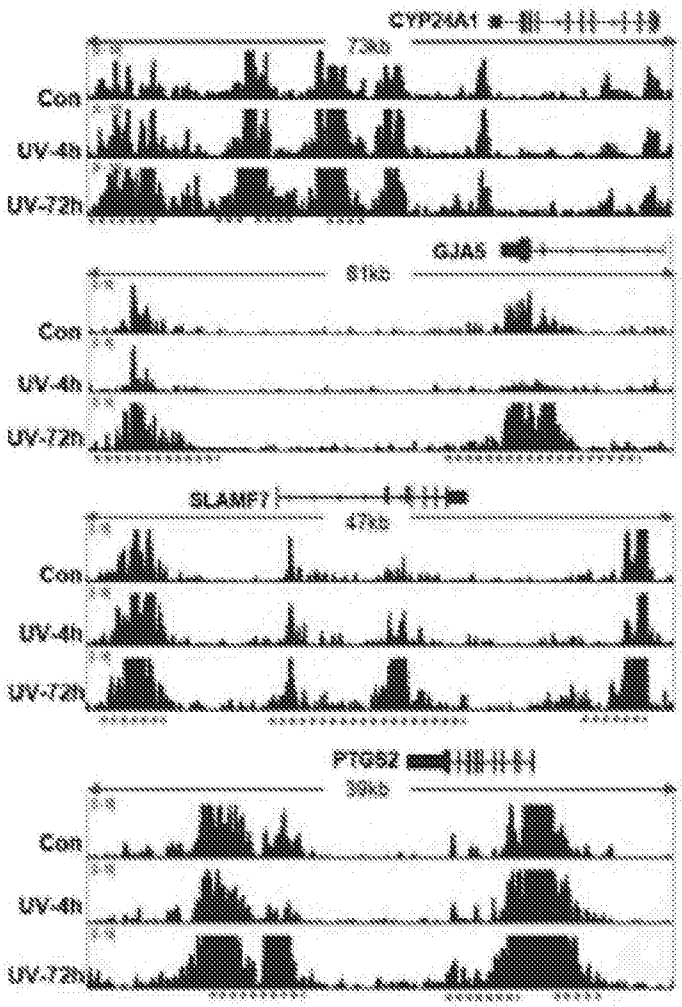

FIG. 10C

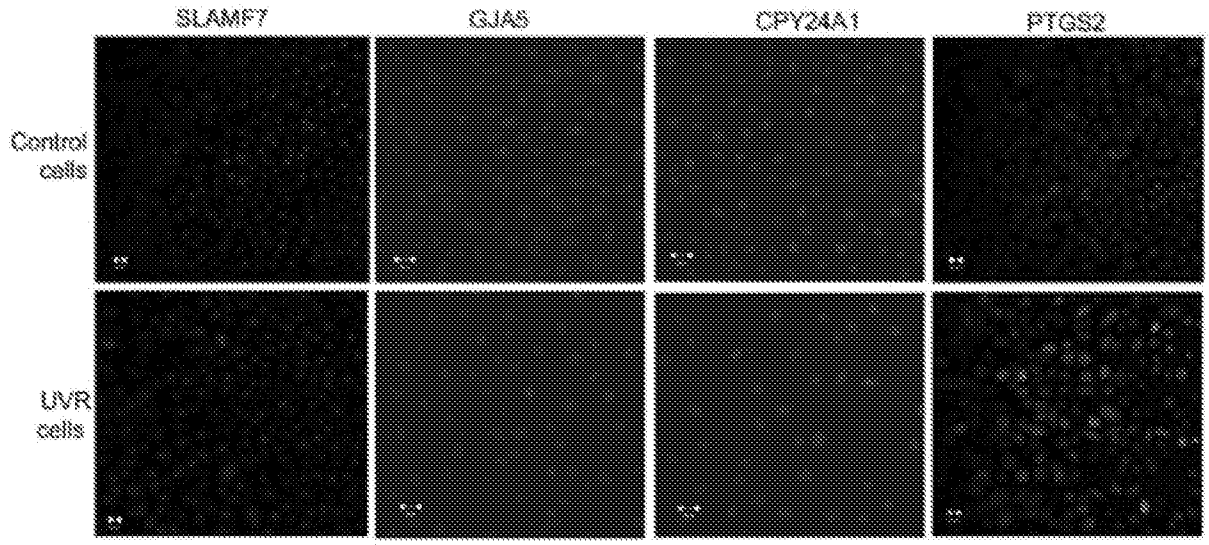

FIG. 10D

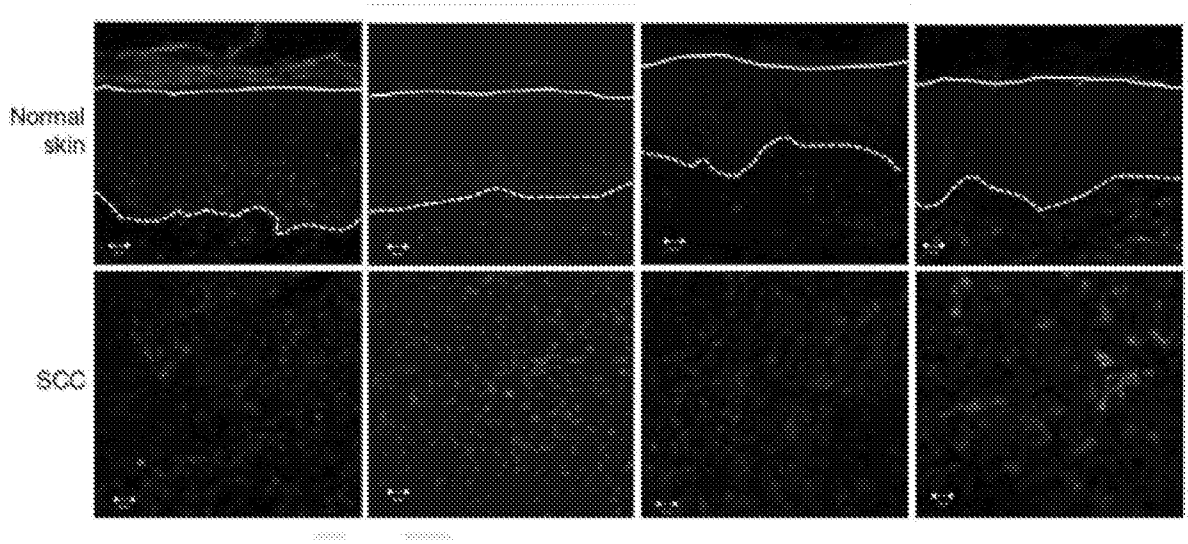

INTERNATIONAL SEARCH REPORT

International application No.
PCT/US 17/22848

A. CLASSIFICATION OF SUBJECT MATTER
IPC(8) - C12Q 1/68 (2017.01)
CPC - C12Q 1/6874 , C12Q 1/6886, C12Q 1/6881

According to International Patent Classification (IPC) or to both national classification and IPC

B. FIELDS SEARCHED

Minimum documentation searched (classification system followed by classification symbols)
See Search History Document

Documentation searched other than minimum documentation to the extent that such documents are included in the fields searched
See Search History Document

Electronic data base consulted during the international search (name of data base and, where practicable, search terms used)
See Search History Document

C. DOCUMENTS CONSIDERED TO BE RELEVANT

Category*	Citation of document, with indication, where appropriate, of the relevant passages	Relevant to claim No.
X ---------- Y	US 2013/0072572 A1 (PAPAZOGLOU et al.) 21 March 2013 (21.03.2013); para [0016], [0051], [0184], [0213]	26-28, 36 ---------- 1, 2, 5-9, 12, 13, 16, 17, 20, 22-25 and 42
Y	WO 2014/082083 A1 (CARIS SCIENCE, INC.) 30 May 2014 (30.05.2014); abstract, para [0044], [00598]	1, 2, 5-9, 12, 13, 16, 17, 20, 22-25 and 42
Y	US 2014/0045915 (SKOG etal.) 13 February 2014 (13.02.2014); Abstract, claim 48, Table 3	1, 2, 5-9, 12, 13, 16, 17, 20, 22-25 and 42

☐ Further documents are listed in the continuation of Box C. ☐ See patent family annex.

* Special categories of cited documents:
"A" document defining the general state of the art which is not considered to be of particular relevance
"E" earlier application or patent but published on or after the international filing date
"L" document which may throw doubts on priority claim(s) or which is cited to establish the publication date of another citation or other special reason (as specified)
"O" document referring to an oral disclosure, use, exhibition or other means
"P" document published prior to the international filing date but later than the priority date claimed
"T" later document published after the international filing date or priority date and not in conflict with the application but cited to understand the principle or theory underlying the invention
"X" document of particular relevance; the claimed invention cannot be considered novel or cannot be considered to involve an inventive step when the document is taken alone
"Y" document of particular relevance; the claimed invention cannot be considered to involve an inventive step when the document is combined with one or more other such documents, such combination being obvious to a person skilled in the art
"&" document member of the same patent family

Date of the actual completion of the international search	Date of mailing of the international search report
27 June 2017	19 JUL 2017
Name and mailing address of the ISA/US Mail Stop PCT, Attn: ISA/US, Commissioner for Patents P.O. Box 1450, Alexandria, Virginia 22313-1450 Facsimile No. 571-273-8300	Authorized officer: Lee W. Young PCT Helpdesk: 571-272-4300 PCT OSP: 571-272-7774

Form PCT/ISA/210 (second sheet) (January 2015)

INTERNATIONAL SEARCH REPORT

International application No.
PCT/US 17/22848

Box No. II Observations where certain claims were found unsearchable (Continuation of item 2 of first sheet)

This international search report has not been established in respect of certain claims under Article 17(2)(a) for the following reasons:

1. ☐ Claims Nos.:
because they relate to subject matter not required to be searched by this Authority, namely:

2. ☐ Claims Nos.:
because they relate to parts of the international application that do not comply with the prescribed requirements to such an extent that no meaningful international search can be carried out, specifically:

3. ☒ Claims Nos.: 29-35, 37-41, 43-45
because they are dependent claims and are not drafted in accordance with the second and third sentences of Rule 6.4(a).

Box No. III Observations where unity of invention is lacking (Continuation of item 3 of first sheet)

This International Searching Authority found multiple inventions in this international application, as follows:
This application contains the following inventions or groups of inventions which are not so linked as to form a single general inventive concept under PCT Rule 13.1. In order for all inventions to be examined, the appropriate additional examination fees must be paid.

*****Continued in Supplemental Box****

1. ☐ As all required additional search fees were timely paid by the applicant, this international search report covers all searchable claims.

2. ☐ As all searchable claims could be searched without effort justifying additional fees, this Authority did not invite payment of additional fees.

3. ☐ As only some of the required additional search fees were timely paid by the applicant, this international search report covers only those claims for which fees were paid, specifically claims Nos.:

4. ☒ No required additional search fees were timely paid by the applicant. Consequently, this international search report is restricted to the invention first mentioned in the claims; it is covered by claims Nos.:
1, 2, 5-9, 12, 13, 16, 17, 20, 22-28, 36 and 42 limited to ADAMTS14 and ANGPTL4

Remark on Protest

☐ The additional search fees were accompanied by the applicant's protest and, where applicable, the payment of a protest fee.

☐ The additional search fees were accompanied by the applicant's protest but the applicable protest fee was not paid within the time limit specified in the invitation.

☐ No protest accompanied the payment of additional search fees.

INTERNATIONAL SEARCH REPORT

International application No.
PCT/US 17/22848

Continuation of Box III: Observations where unity of invention is lacking:

Group I+, claims 1-20, 22-28, 36 and 42, directed to a method, a kit or an assay for detecting ultraviolet radiation (UVR)-induced skin damage in a subject comprising analyzing expression levels in the skin sample of UVR-induced differentially expressed genes (DEGs) listed in Table 8 or a subset thereof. The method/kit/assay will be searched to the extent that the DEGs encompasses the first two genes listed in Table 8, ADAMTS14 and ANGPTL4 (the minimal number of genes meets claim limitation "analyzing expression levels...or a subet thereof"). It is believed that claims 1, 2, 5-9, 12, 13, 16, 17, 20, 22-28, 36 and 42 encompass this first named invention, and thus these claims will be searched without fee to the extent that they encompass ADAMTS14 and ANGPTL4. Additional DEGs will be searched upon the payment of additional fees. Applicants must specify the claims that encompass any additionally elected DEGs. Applicants must further indicate, if applicable, the claims which encompass the first named invention, if different than what was indicated above for this group. Failure to clearly identify how any paid additional invention fees are to be applied to the "+" group(s) will result in only the first claimed invention to be searched. An exemplary election would be a subset of two DEGs selected from IL6, PTGS2, IL1 B, CDKN1A, BCL2L1, ICAM1, HMOX1, VAV1, PLA2G16, MMP1, HIST1H4H, CYP4F3, and CD8A (claims 1-3, 5-10, 12-14, 16-18, 20, 22-28, 36 and 42).

Group II, claims 21 and 46, directed to a method of measuring the effectiveness of a test agent in reducing ultraviolet radiation (UVR)-induced damage, or of evaluating a sunscreen formulation.

The inventions listed as Groups I+ and II do not relate to a single special technical feature under PCT Rule 13.1 because, under PCT Rule 13.2, they lack the same or corresponding special technical features for the following reasons:

Special technical features:

Group I+ inventions have the special technical feature of identifying, monitoring, diagnosing and treating skin cancer or ultraviolet radiation (UVR)-induced skin damage in a test subject, that is not required by Group II.

Group II has the special technical feature of a method of evaluating a test agent or a suncreen formulation for UV protective effect, that is not required by Group I+ inventions.

The inventions of Group I+ each include the special technical feature of specific DEGs, recited therein. Each invention requires an unique subset of DEGs, not required by any other inventions.

Common technical features:

The inventions of Group I+ and II share the common technical features of a method of detecting, identifying and monitoring UVR-induced skin damage or diagnosing skin cancer in a subject comprising obtaining a skin sample from the subject, analyzing expression levels in the skin sample of UVR-induced DEGs, and comparing expression levels of the UVR-induced DEGs, or a subset thereof, from a test skin sample from the subject, with expression levels of the same genes in a reference skin sample and/or a control skin sample, wherein, when the expression levels of the UVR-induced DEGs in the skin sample differs from the level of each of the UVR-induced DEGs in the control sample, the subject is identified as likely being afflicted with UVR-induced skin damage and /or is diagnosed with skin cancer as indicated by the presence or absence of squamous cell carcinoma or precancerous skin lesion cells.

The inventions of Group I+ share the common technical features of a kit for performing said method comprising: a set of primers or probes that specifically bind to UVR-induced differentially expressed genes (DEGs), packaged together with instructions for its use.

The inventions of Group I+ share the common technical features of administering a treatment for UVR-induced skin damage to the diagnosed subject if the levels differ.

The inventions of Group I+ share the common technical features of an assay comprising a system for performing the method.

However, these shared technical features do not represent a contribution over prior art, because these shared technical features are made obvious by US 2013/0072572 A1 to Papazoglou et al. (hereinafter Papazoglou), in view of US 2015/0376717 A1 to The University of North Carolina at Chapel Hill (hereinafter UNC).

Papazoglou teaches a method of identifying or monitoring ultraviolet radiation (UVR)-induced skin damage in a test subject (para [0051] -Accordingly, the present invention provides methods for the examination of skin cells and skin tissues, collectively known as skin samples, for the diagnosis or prognosis of UVR-induced skin damage), said method comprising the steps of:
a) obtaining a skin sample from the subject (para [0051] -The method comprises obtaining a skin sample from a subject),
a) analyzing expression level in a biological sample obtained from the subject of UVR-induced differentially expressed gene (DEG) (para [0051] -measuring the level of Syk kinase in the skin sample, and comparing the level of Syk kinase in the sample to a control sample.);
b) comparing the expression profile level of the UVR-induced biomarker in the biological sample with a predetermined reference standard for the gene (para [0051] -measuring the level of Syk kinase in the skin sample, and comparing the level of Syk kinase in the sample to a control sample. Increased expression of Syk kinase in the skin sample relative to a control sample identifies the subject that the sample was obtained from as being afflicted with or at risk of developing UVR-induced skin damage); and
c) identifying or monitoring UVR-induced skin damage in the test subject based on the comparison in b) (para [0198] -As noted, it is contemplated that the biomarkers of the invention will find utility as immunogens, e.g., in immunohistochemistry and in ELISA assays. One evident utility of the encoded antigens and corresponding antibodies is in immunoassays for the detection of biomarker proteins, as needed in diagnosis and prognostic monitoring.), however Papazoglou fails to teach wherein the skin damage is skin cancer and further fails to teach wherein the DEG is more than one DEGs.

*****Continuation in Supplemental Box*****

Continuation of Previous Page:

UNC teaches identifying multiple differentially expressed genes in skin samples to diagnose melanoma (para [0017] In particular non-limiting embodiments, the present invention provides a method for detecting melanoma in a tissue sample which comprises: (a) measuring a level of methylation of one or more regulatory elements differentially methylated in melanoma and benign nevi; and (b) determining whether melanoma is present or absent in the tissue sample...There are many sources for the samples, including but not limited to...a skin biopsy.). UNC further teaches wherein a DEG indicative of melanoma is KLK10 (para [0018] In particular non-limiting embodiments, the present invention provides that the differentially methylatated regulatory elements are elements associated with immune response/inflammatory pathway genes, hormonal regulation genes, or cell growth/cell adhesion/apoptosis genes... In another non-limiting embodiment, hypomethylation of the regulatory elements associated with a gene encoding...KLK10... is indicative of melanoma.). In light of the fact that UNC teaches wherein KLK10 is a known marker for identifying skin damage, and "DNA methylation is an epigenetic chemical modification that does not alter the sequence code, but can be heritable, and is involved in the regulation of gene expression" (para [0015]), it would have been obvious to an artisan of ordinary skill in the art to utilize the method taught by Papazoglou to detect modifications in KLK10 as well as Syk expression in patients exposed to ultraviolet radiation in order to detect UVR induced skin damage including melanoma.

Papazoglou further teaches a kit for performing said method comprising: a set of primers or probes that specifically bind to a UVR-induced DEG (para [0217] "Such methods typically use pairs of oligonucleotide primers that are specific for the biomarker of interest"; [0334] "the kit comprises compositions required for the detection of Syk kinase expression, function, or activity in a skin sample invention and an instructional material which describes, for instance, the method for detecting Syk kinase expression"), packaged together with instructions for its use (para [0132] "The instructional material of the kit may, for example, be affixed to a container that contains the compound and/or composition of the invention"), and an assay comprising a system for performing the method (para [0016] "the measuring of the Syk kinase comprises an immunoassay for assessing the level of the Syk kinase in the sample").

Papazoglou further teaches treating the subject by administering a treatment for UVR-induced skin damage to the diagnosed subject if the levels differ (para [0023] "method of treating a disease or disorder associated with a change of Syk kinase expression in the skin in a mammal. The method comprises the step of topically administering to the skin of the mammal a pharmaceutical composition").

As the technical features were known in the art at the time of the invention, they cannot be considered special technical features that would otherwise unify the groups.

Therefore, Group I+ and II inventions lack unity under PCT Rule 13 because they do not share the same or corresponding special technical feature.

NOTE, continuation of number 4 above: claims 29-35, 37-41 and 43-45 are held unsearchable because they are dependent claims and are not drafted in accordance with the second and third sentences of Rule 6.4(a).